

# **NUMERICAL MODELLING OF RAILWAY EMBANKMENT**

A DISSERTATION  
SUBMITTED IN PARTIAL FULFILLMENT OF THE REQUIREMENTS  
FOR THE AWARD OF THE DEGREE  
OF

MASTER OF TECHNOLOGY  
IN  
**GEOTECHNICAL ENGINEERING**

Submitted by:  
**LAV KUSH PRASAD**  
**(2K20/GTE/12)**

Under the supervision of

**Prof. ANIL KUMAR SAHU**



**DEPARTMENT OF CIVIL ENGINEERING**  
**DELHI TECHNOLOGICAL UNIVERSITY**  
(Formerly Delhi College of Engineering)  
Bawana Road, Delhi-110042

MAY, 2022

DELHI TECHNOLOGICAL UNIVERSITY  
(Formerly Delhi College of Engineering)  
Bawana Road, Delhi-110042

**CANDIDATE'S DECLARATION**

I, Lav Kush Prasad (2K20/GTE/12) of M.Tech (Geotechnical Engineering), hereby declare that the Project Dissertation titled "NUMERICAL MODELLING OF RAILWAY EMBANKMENT". Which is submitted by me to the Department of Civil Engineering, Delhi Technological University, Delhi is submitted in partial fulfillment of the requirement for the award of the degree of Master of Technology, is original and not copied from any source without proper citation. This work has not previously formed the basis for the award of any Degree, Diploma Associateship, Fellowship or other similar title or recognition.

Place: Delhi  
Date:

(LAV KUSH PRASAD)  
2K20/GTE/12

**CIVIL ENGINEERING DEPARTMENT  
DELHI TECHNOLOGICAL UNIVERSITY  
(Formerly Delhi College of Engineering)  
Bawana Road, Delhi -110042**

**CERTIFICATE**

I hereby certify that the Project Dissertation entitled "**NUMERICAL MODELLING OF RAILWAY EMBANKMENT**". Which is submitted by Lav Kush Prasad (2K20/GTE/12) of M.Tech (GeotechnicalEngineering), Delhi Technological University, Delhi submitted in partial fulfillment of the requirement for the award of Master of Technology, is a record of the project work carried out by the student under my supervision. To the best of my knowledge, this work has not been submitted in part or full for any Degree or Diploma to this University or elsewhere.

**Place: Delhi**  
**Date:**

**(Prof. ANIL KUMAR SAHU)**  
**SUPERVISOR**  
**DEPARTMENT OF CIVIL ENGINEERING**  
**DELHI TECHNOLOGICAL UNIVERSITY**  
**Bawana Road, Delhi -110042**

## **ACKNOWLEDGEMENT**

As I write this acknowledgement, I must clarify that this is not just a formal acknowledgement but also a sincere note of thanks and regard from my side. I have taken efforts in this Project Dissertation. However, it would not have been possible without the kind support and help of many individuals and organizations. I would like to extend my sincere thanks to all of them. I express my sincere thanks to the University Management. My sincere thanks also go to Vice Chancellor **Prof. Jai Prakash Saini** and Head of Department **Prof. V. K. Minocha**. I am highly indebted to my supervisor **Prof. Anil Kumar Sahu** for his guidance and constant supervision as well as for providing necessary information regarding the project & also for his support in completing the Project Dissertation. I would like to express my special gratitude and thanks to **Prof. A. Trivedi, Prof. A. K. Shrivastava, Prof. A. K. Gupta, Prof. Kongan Aryan, Prof. Raju Sarkar**, Department of Civil Engineering and all the Faculty member of Civil Engineering Delhi Technological University for guiding throughout this project. My thanks and appreciations also go to my colleague in developing the project and people who have willingly helped me out with their abilities. In the end, I thank god almighty and my parents for bestowing their blessings and grace in completion of the Project Dissertation.

**LAV KUSH PRASAD**  
**(2K20/GTE/12)**  
DEPARTMENT OF CIVIL ENGINEERING  
DELHI TECHNOLOGICAL UNIVERSITY

## **ABSTRACT**

Over the past few decades, the increasing demands of railways operations in the form of heavy loading and high speed have been noticed. Due to this, there have been an increase in overall stresses throughout the railway substructure. Railway formation and ballast deform progressive under heavy axle cyclic loading, therefore the rail track needs proper design of ballast and formation bed to achieve the desire stability for the safe and sound serviceability of the track. For the overall stability of the track on soft formation, the ground is improved by different techniques prior to the construction on that, in order to avoid the failure and differential settlement during the designed trains operation.

The numerical analyses illustrate that the total deformation and bearing capacity of the railway tracks mostly depend on the changes in the friction angle and cohesion of the selected soils of the subgrade. To avoid failure in the formation of track under the design loads, the proper selection of types of soils, its layer thickness, well compaction during construction and provision of proper track drainage system are extremely important. For the construction of new railway tracks the soils having greater values of friction angle, cohesion and elastic stiffness with the well graded ballast cushion under the sleepers of designed side slopes can be used to reduce the maintenance cost, considerably increase the life time of the components of the tracks and ultimately give better performance of the tracks.

**Keywords: railway track, ballast, subgrade, numerical modelling, drainage, track maintenance, settlement.**

## CONTENTS

<b>Candidate's Declaration</b>	<b>ii</b>
<b>Certificate</b>	<b>iii</b>
<b>Acknowledgment</b>	<b>iv</b>
<b>Abstract</b>	<b>v</b>
<b>Contents</b>	<b>vi</b>
<b>List of Figures</b>	<b>vii</b>
<b>List of Tables</b>	<b>x</b>
<b>List of Symbols And Abbreviations</b>	<b>xi</b>
<b>CHAPTER 1 INTRODUCTION</b>	<b>1</b>
1.1 Components of Railway Geotechnics	2
1.2 Geocell	4
1.3 Objectives	5
<b>CHAPTER 2 LITERATURE REVIEW</b>	<b>6</b>
<b>CHAPTER 3 MATERIALS AND METHODS</b>	<b>12</b>
3.1 Finite Element Railway Substructure Geometry	13
3.2 Finite Element Material Properties	19
3.3 Finite Element Mesh and Boundary Conditions	20
3.4 Finite Element Mesh Convergence and Model Validation	24
3.5 Load Calculation	26
3.6 Finite Element Loading	26
3.7 Finite Element Problem Size	30
<b>CHAPTER 4 RESULTS AND DISCUSSION</b>	<b>32</b>
<b>CHAPTER 5 CONCLUSION</b>	<b>55</b>
5.1 Conclusions	55
5.2 Future Scope of the Project	55
<b>REFERENCES</b>	<b>56</b>

## **LIST OF FIGURES**

Figure 1.1	Cross section view of typical ballast track ( Alabbasi 2015)	1
Figure 1.2	Types of Rails (Mundrey 2010)	2
Figure 1.3	Geocell, when shipped (top) and outstretched (bottom) (Koerner, 2005)	5
Figure 3.1	Basic Layout of PLAXIS 2D	12
Figure 3.2	I.R.S 52kg/m Rail Section – Key To Dimension Table (Mundrey 2005)	13
Figure 3.3	Cross Section of PCS-12 Sleeper (Agarwal 2017)	14
Figure 3.4	Geometrical representation of 2D Model Layout	15
Figure 3.5	Geometrical representation of 2-D Model with Unreinforced Ballast	15
Figure 3.6	Geometrical representation of 2-D Model with Geocell Confinement Width 2.0m	16
Figure 3.7	Geometrical representation of 2-D Model with Geocell Confinement Width 2.3m	16
Figure 3.8	Geometrical representation of 2-D Model with Geocell Confinement Width 2.6m	17
Figure 3.9	Geometrical representation of 2-D Model with Geocell Confinement Width 2.9m	17
Figure 3.10	Geometrical representation of 2-D Model with Geocell Confinement Width 3.2m	18
Figure 3.11	Geometrical representation of 2-D Model with Geocell Confinement Width 3.5m	18
Figure 3.12	Geometrical representation of 2-D Model with Geocell Confinement Width 3.8m	19
Figure 3.13	2-D Meshed Model with Unreinforced Ballast	21
Figure 3.14	2-D Meshed Model with Geocell Confined Ballast of 2.0 m	21
Figure 3.15	2D Meshed Model with Geocell Confined Ballast of 2.9 m	22
Figure 3.16	2D Meshed Model with Geocell Confined Ballast of 3.8 m	22

Figure 3.17	Number of stress points generated by very fine mesh in Embankment	23
Figure 3.18	Speed vs Speed Factor Chart (Mundrey 2005)	27
Figure 3.19	Contact area between Wheel and Rail Track (Mundrey 2005)	28
Figure 3.20	Contact between Wheel and Rail Track	29
Figure 4.1	Subgrade Stress Distribution in 2-D Model with Unreinforced Ballast	32
Figure 4.2	Subgrade Stress Distribution in 2-D Model with Geocell Confinement Width 2.0m	33
Figure 4.3	Subgrade Stress Distribution in 2-D Model with Geocell Confinement Width 2.3m	33
Figure 4.4	Subgrade Stress Distribution in 2-D Model with Geocell Confinement Width 2.6m	34
Figure 4.5	Subgrade Stress Distribution in 2-D Model with Geocell Confinement Width 2.9m	34
Figure 4.6	Subgrade Stress Distribution in 2-D Model with Geocell Confinement Width 3.2m	35
Figure 4.7	Subgrade Stress Distribution in 2-D Model with Geocell Confinement Width 3.5m	35
Figure 4.8	Subgrade Stress Distribution in 2-D Model with Geocell Confinement Width 3.8m	36
Figure 4.9	Subgrade Horizontal Displacement in 2-D Model with Unreinforced Ballast	36
Figure 4.10	Subgrade Horizontal Displacement in 2-D Model with Geocell Confinement Width 2.0m	37
Figure 4.11	Subgrade Horizontal Displacement in 2-D Model with Geocell Confinement Width 2.3m	37
Figure 4.12	Subgrade Horizontal Displacement in 2-D Model with Geocell Confinement Width 2.6m	38
Figure 4.13	Subgrade Horizontal Displacement in 2-D Model with Geocell Confinement Width 2.9m	38
Figure 4.14	Subgrade Horizontal Displacement in 2-D Model with Geocell Confinement Width 3.2m	39
Figure 4.15	Subgrade Horizontal Displacement in 2-D Model with Geocell Confinement Width 3.5m	39
Figure 4.16	Subgrade Horizontal Displacement in 2-D Model with Geocell Confinement width 3.8m	40
Figure 4.17	Subgrade Total Displacement in 2-D Model with Unreinforced Ballast	40
Figure 4.18	Subgrade Total Displacement in 2-D Model with Geocell Confinement Width 2.0m	41
Figure 4.19	Subgrade Total Displacement in 2-D Model with Geocell Confinement Width 2.3m	41
Figure 4.20	Subgrade Total Displacement in 2-D Model with Geocell Confinement Width 2.6m	42



Figure 4.21	Subgrade Total Displacement in 2-D Model with Geocell Confinement Width 2.9m	42
Figure 4.22	Subgrade Total Displacement in 2-D Model with Geocell Confinement Width 3.2m	43
Figure 4.23	Subgrade Total Displacement in 2-D Model with Geocell Confinement Width 3.5m	43
Figure 4.24	Subgrade Total Displacement in 2-D Model with Geocell Confinement Width 3.8m	44
Figure 4.25	Subgrade Mean Stresses in 2-D Model with Unreinforced Ballast	44
Figure 4.26	Subgrade Mean Stresses in 2-D Model with Geocell Confinement Width 2.0m	45
Figure 4.27	Subgrade Mean Stresses in 2-D Model with Geocell Confinement Width 2.3m	45
Figure 4.28	Subgrade Mean Stresses in 2-D Model with Geocell Confinement Width 2.6m	46
Figure 4.29	Subgrade Mean Stresses in 2-D Model with Geocell Confinement Width 2.9m	46
Figure 4.30	Subgrade Mean Stresses in 2-D Model with Geocell Confinement Width 3.2m	47
Figure 4.31	Subgrade Mean Stresses in 2-D Model with Geocell Confinement Width 3.5m	47
Figure 4.32	Subgrade Mean Stresses in 2-D Model with Geocell Confinement Width 3.8 m	48
Figure 4.33	Subgrade Total Stresses in 2-D Model with Unreinforced Ballast	48
Figure 4.34	Subgrade Total Stresses in 2-D Model with Geocell Confinement Width 2.0m	49
Figure 4.35	Subgrade Total Stresses in 2-D Model with Geocell Confinement Width 2.3m	49
Figure 4.36	Subgrade Total Stresses in 2-D Model with Geocell Confinement Width 2.6m	50
Figure 4.37	Subgrade Total Stresses in 2-D Model with Geocell Confinement Width 2.9m	50
Figure 4.38	Subgrade Total Stresses in 2-D Model with Geocell Confinement Width 3.2m	51
Figure 4.39	Subgrade Total Stresses in 2-D Model with Geocell Confinement Width 3.5m	51
Figure 4.40	Subgrade Total Stresses in 2-D Model with Geocell Confinement Width 3.8m	52
Figure 4.41	Vertical Settlement vs Geocell Layer confinement.	52
Figure 4.42	Horizontal Settlement vs Geocell Layer confinement.	53
Figure 4.43	Total Settlement vs Geocell Layer confinement.	53
Figure 4.44	Comparison of Subgrade Stresses over the length across the Ballast for varying Geocell Confinement	54

---

## **LIST OF TABLES**

Table 3.1	Dimension Table (Mundrey 2005)	13
Table 3.2	FE Material Properties (Leshchinsky et al. 2013 ; Lal et al. 2016 ; Kumar and Sambasivarao 2014)	20
Table 3.3	FE Subgrade Properties	20
Table 3.4	Mesh Information	24
Table 4.1	Result Comparisons	54

## **LIST OF SYMBOLS AND ABBREVIATIONS**

FE	Finite Element
kg	Kilogram
km	Kilometre
kN	Kilonewton
M	Metre
MPa	Megapascal
NPA	Novel Polymeric Alloy
Pa	Pascal
psi	Pounds per square inch
PCS	Prestressed Concrete Sleeper
sec	Seconds
SF	Speed Factor

## CHAPTER 1.

### INTRODUCTION

Railways are an important part of a country's transportation infrastructure and plays a significant role in keeping the economy strong. Indian Railways is presently preparing to rebuild and enhance its infrastructure in order to meet future traffic demands. The railway network has been expanded by building new tracks, as well as increased transit efficiency by running heavier, longer, and faster trains. The track-foundation-soil system has been acknowledged as one of the key factors in bringing about these modifications by Indian railroads.

The basic components of ballasted track structures are shown in Figure 1. These may be classified into two groups: superstructure and substructure. Rails, the fastening system, and sleepers are all part of the superstructure (ties). Subgrade, subballast, and ballast are all parts of the substructure. The sleeper ballast interface separates the superstructure and substructure.

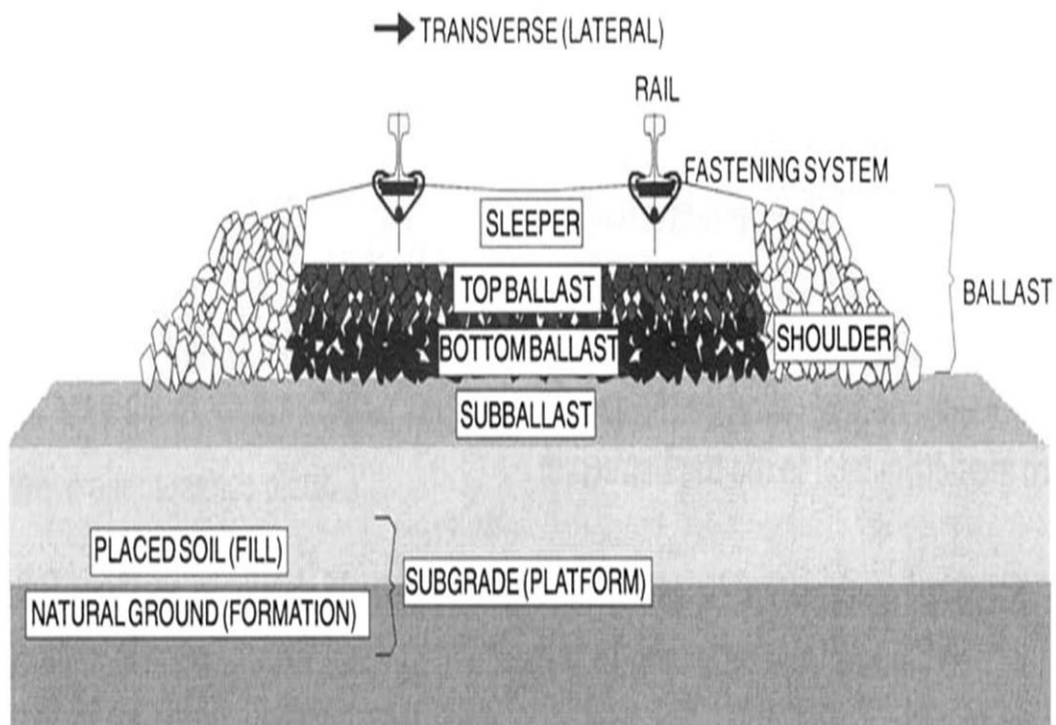


Figure 1.1 Cross section view of typical ballast track ( Alabbasi 2015)

Study of railway geotechnics includes various methods of improving the parametric properties of its components.

## 1.1. COMPONENTS OF RAILWAY GEOTECHNICS

Various components of railway geotechnics are –

- 1.1.1. Rail
- 1.1.2. Sleeper
- 1.1.3. Ballast
- 1.1.4. Subgrade

### 1.1.1. Rail

Rail is that component of the Rail transport system which is in direct contact with the train wheels. It consists of Head, Web and Foot. Double-headed, bull-headed and flat-footed are the type of rails, but the performance of flat-footed rail is much better than the others. Strength of rail section is represented by the modulus of the section. Figure 1.3 shows the type of rails.

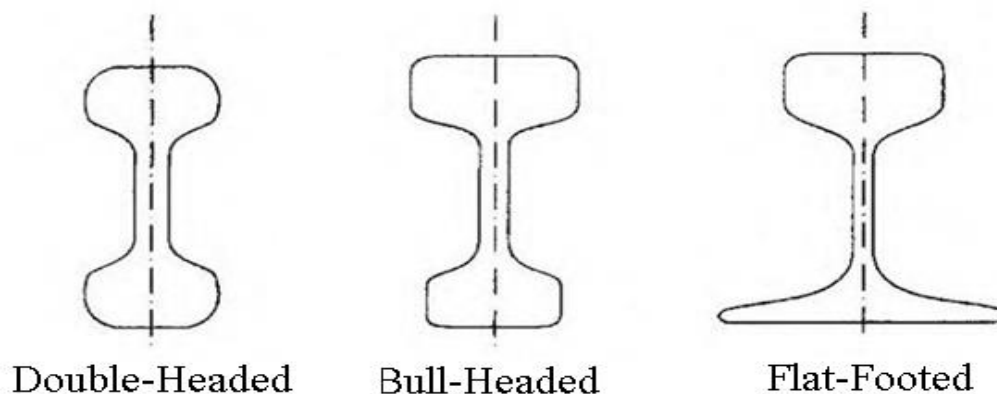


Figure 1.2 Types of Rails (Mundrey 2010)

Functions of Rail: -

- Provides hard and unyielding surface to rolling wheel.
- Provides a smooth surface (to keep the friction between the rails and wheels minimum).
- Act as a beam and transmit the wheel loads to the sleepers.

### 1.1.2. Sleeper

Sleeper is the component which lies in between the rail and ballast. Following are the materials used for make different type of sleeper used in India Railway: -

- Wooden
- Cast iron
- Concrete
- Steel

Most commonly used, in modern Indian railway, are Concrete type.

Functions of Sleeper are as following: -

- Transferring the load from rails to ballast uniformly.
- Acts as an elastic medium which absorbs blows and vibration caused due to moving train loads.
- Act as rigid support to rails.

The number of sleepers per unit rail length is defined by term sleeper density.

### 1.1.3. Ballast

Ballast is the material, granular in nature, placed above subgrade and is that layer which is in direct contact of sleeper ties. It is angular big size granular material obtained by crushing of rocks like basalt and granite. The thickness of ballast layer should be kept at least 200mm

Different types of ballast used in India are –

- Broken Stone
- Gravel
- Kankar
- Brick Ballast etc.

Functions of Ballast –

- Supports the sleepers.
- Transmits the train stresses over the subgrade uniformly.
- Maintaining proper drainage in tracks.
- Provide elasticity to the track.
- Used in boxing the sleeper for the lateral stability

#### 1.1.4. Subgrade

Subgrade acts as a platform on which rail substructure lies. Subgrade can be natural soil or rock or compacted soil fill. Trackbed, Rail Foundation are other terms used for it. The primary function of the subgrade is to provide uniform and adequate support to the rail track system. Sometimes natural soil as subgrade is not adequate in that case either it is replaced by stiff soil. In some cases, reinforcement of ballast or subgrade is done in such a way that subgrade stress is decreased.

In present times, India is developing at a rapid rate. Along with India, Indian Railway is also evolving at a higher growth rate than ever. Development of Indian Railway includes traffic management of trains, infrastructural development of the railway station and the most important of all average speed of trains. Various high-speed train projects are under construction, and also the new railway track system components which are adequate for the stresses of the high-speed train are being constructed. One of the latest additions to components is Subgrade which results in the conception of another division Railway Geotechnics. Railway Geotechnics is a fusion of Railway Engineering and Geotechnical Engineering.

In many cases during the laying of new track system, Engineers faces the situation where the subgrade below the ballast is weak soil like soft clay. Soil improvement by replacement it with stiff and stable soil economic up to certain depth after which excavation is not a cost-effective option. In this type of situations, another option is to reinforce the soil or ballast with geosynthetics.

## 1.2. GEOCELL

Geocells are 3-D honeycombed structures, cellular in nature that result in a confining system when compacted soil is filled in its cells. They are also known as Cellular Confinement Systems. Polymeric materials cut into strips and joined together using ultrasonic welding in series result in Geocell. The stiff walls of a flexible 3D cellular mattress are formed by these geocell strips when expanded. Filling it with any material, the cell- material interaction occurs resulting in a new entity.

Functions of Geocell –

- Cellular confinement provided by it results in a reduction of soil particles lateral movements.
- It forms a stiffened entity, distributing loads over a larger area.

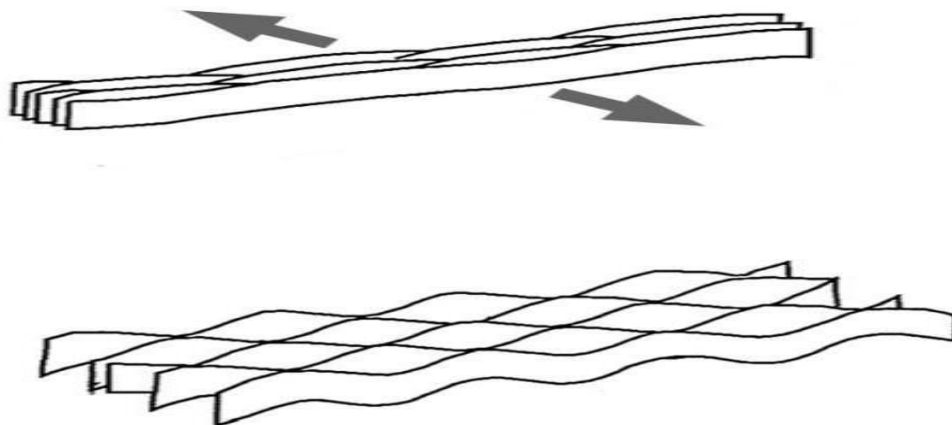


Figure 1.3 Geocell, when shipped (top) and outstretched (bottom) (Koerner, 2005)

Geocell is generally used in slope stability and earth retaining applications. With an increase in technology, advanced polymer manufactured using materials Novel Polymeric Alloy (NPA) is used to manufacture geocell, this geocell due to long life, higher stiffness and creep resistance are used in road and rail load support.

### 1.3. OBJECTIVES

Based on the literature survey in the field of railway geotechnics and geosynthetic reinforcements, the following objectives are to be performed –

- To perform stress analyses of railway subgrade with geocell confined ballast by analysing 2-D finite element model using Plaxis 2D.
- To perform settlement analyses of railway subgrade with geocell confined ballast by analysing 2-D finite element model using Plaxis 2D.
- To enhance the strength of embankment by using Geocell..
- To determine the optimum geocell confinement width.
- To study the behaviour of geocell in railway geotechnique.

In order to fulfil the objectives, the literatures have been reviewed, further which is presented in the succeeding chapters.



## **CHAPTER 2.**

### **LITERATURE REVIEW**

In the present chapter, literature has been reviewed with respect to the following aspects–

- 1) Numerical modelling on railway embankment.
- 2) Static & dynamic analysis of some components of railway embankment.
- 3) The confinement of ballast and subgrade by geocell or similar materials

Heath (1972) observed the British Railway devised a strategy based on research that tries to defend against excessive plastic deformation by imposing a stress threshold. Large plastic deformations in the subsurface occur when stresses in the subsoil exceed the threshold value, while minor cumulative deformations occur when stressors are below the threshold value.

Cowland et al. (1993) used several equipment, such as surface settlement markers, to monitor and observe the performance of a geocell' mattress foundation. The geocell was made of high-density polyethylene geogrids and is triangular in shape. The monitoring embankment was made of soft clay and was completely equipped with these equipment. The conclusion drawn from this investigation is that the geocell mattress acts as a foundation (raft) for the embankment.

Yetimoglu et al. (1994) modelled a rectangular foundation on geogrid reinforced sand using both computational and physical methods. A bearing capacity setup consisting of a 70cm70cm100cm steel tank in which sand is placed and load is applied using a hydraulic pump was created for physical modelling, and a finite element method DASCAR was utilised for numerical modelling. Geogrid reinforcement, footing, and assembly of triangular and quadrilateral parts for sand, all of which were axisymmetric, were represented by a series of discrete shell elements. Uniaxial geogrid was employed to reinforce the structure. The results of both analyses were nearly identical, indicating that reinforced soil increased bearing capacity while reducing settlement corresponding to a load. He also discovered that increasing the reinforced layer in sand improved soil properties, which was inversely proportional to vertical spacing between the layers.

Rajagopal et al. (1998) analysed the effect of geocell confinement on natural granular soil strength and stiffness. As part of the study, several triaxial compression tests were done. The confinement geocells were made from a variety of woven and nonwoven geotextiles. The model geocells were created using a variety of geosynthetics and various mesh elements. Geocell-sand

composites are 100 mm diameter and 200 mm thick. In a triaxial test apparatus, various confining pressures were applied. The results that geocell confinement adds apparent cohesive strength to cohesionless soils brought to this conclusion. This apparent strength is determined by the tensile modulus of the geosynthetics used to make the geocell.

Chaney et al. (2000) experimentally analyzed the modulus of elasticity of geogrid-reinforced sand in an experimental research. On sand reinforced structures, plate load tests were performed at various depths. Deformation per unit pressure reduces in reinforced soil, according to the deformation versus applied pressure graphs. In addition, the data analysis of test results reveals the phenomena of elastic modulus increment with the addition of geogrid reinforcement.

Han and Gabr (2002) had compared the unreinforced pile-supported structure and the reinforced pile-supported structure. A non-linear hyperbolic elastic model was numerically modelled using FLAC. FLAC is a continuum model that employs an explicit finite difference code for big displacement modelling. The presence of geosynthetics in the fill improves the stress concentration ratio, reduces the soil yield above the pile head, and reduces the chances of differential settlement because geosynthetic reinforced soil is rigid in an ideal case. In addition, when the tensile strength of the geosynthetics increases up to a limit of 4000kN/m, the settlement decreases.

Indraratna et al. (2006) demonstrated two different techniques of stabilising railroad bed. One was to reinforce ballast by geocomposites and others to reinforce the soft soil by prefabricated vertical drains. Purpose of ballast is to distribute the load uniformly from sleepers, damping of dynamic loads and providing free drainage condition. Ballast fails when it degrades and settles more. To reduce degradation, a uniformity coefficient of 2.2 for ballast material was recommended. For Settlement, geotextiles, geogrid and geocomposites were used, and modelling was done using PLAXIS, which is a finite element software and results got better in the same order. Also, the optimum depth for placing geosynthetics was 150mm. For improving soil PVDs were used. Short PVDs (5m-8m) were enough to release the pore pressure stiffness the foundations up to the depth of some metres.

In other research, Indraratna et al. (2006) conducted a large scale triaxial test to study the behaviour of ballast due to the application of static and dynamic loads. Effect of geosynthetics on the performance of ballast under similar loading condition was also investigated. A prismoid triaxial apparatus of large scale i.e. 800mm in length, 600mm width and 600mm in height was used for simulation of the real situation of railway track, and the load was provided with the help of servo-hydraulic actuator (cyclic vertical load). Fresh and Recycled ballast (dry and wet) was used, and for reinforcement purpose geotextile, geogrid and geocomposites were used. Results obtained after 500000 load cycles show a

decrease in a settlement in reinforced soil. Least settlement was seen in case of geogrid. A similar pattern was followed in the case of lateral and vertical strain. Also, recycled ballast consisting of geocomposites results in a reduction in the breakage index as compared to the fresh unreinforced ballast.

Zhou and Wen (2006) conducted a laboratory test for the analysis of the effect layer of geosynthetic materials placed in a sand cushion, creating a composite layer over foundation composed of soft soil. All in-situ conditions of the embankment were simulated in the laboratory test. From the results, an observation was made that provision of a geosynthetic material layer in embankment increase the overall bearing capacity and reduces the settlement of soft under the soil.

Lackenby et al. (2007) performed cyclic triaxial tests for the determination of the effect of confining pressure and deviator stress on deformation of ballast (permanent and resilient) and degradation. For having actual load condition, large scale triaxial apparatus was incorporated. Initially, the static load was applied, but after some time, the dynamic load was applied to replicate the high-speed load. From the test results, graphs were plotted between axial strain vs confining stress and BBI vs confining stress and conclusion was made that as confining pressure increase, axial strain decreases. Also confining pressure plays an essential role in ballast degradation.

Atalar et al. (2009) observed the effect of soil-geogrid composite on the young's modulus of elasticity of soil which is granular in nature with the help of cyclic plate load test. Elastic Modulus values were determined for the various arrangement of geogrid reinforcements. Three tests were conducted with a different number of reinforced layers. Reinforcement of soil was done using Bi-axial polymer geogrid (polypropylene). From the test, results conclusion was made that soil reinforced with geogrid shows improvement in various properties of soil. Out of which stiffness plays important role in predicting the strength of the soil. As stiffness is increased the settlement decreases. Increment in stiffness also means modulus of elasticity is increased. Modulus of elasticity improves from 9% to 54% increases with the increase in the reinforced layer. For determination of elastic modulus, cyclic plate load test equation is used.

Ziaie (2011) performed a laboratorial study of the outcomes of geogrid and geosynthetic reinforcement on the thickness of sub-base of the two-layer soil system. Bearing ratio test in four conditions- unreinforced, reinforced with sub base thickness 40,55 and 70mm were performed. Two layers of soil are of sand (top) and clay (bottom). Soil classification was done according to the Unified Soil Classification system. Series of bearing ratio tests were conducted on oven-dried samples with the required amount of water content. Testing was done according to ASTM D1883-05. Results show that improvement in geogrid is more than geosynthetic reinforced and layer 40mm shows most the improvement while in 70mm layer improvement was negligible. It was

concluded that less is the thickness of subbase more is the improvement, which benefits the requirement of decrease thickness of sub-base.

Leshchinsky and Ling (2013) suggests that in various case of railway geotechnics where ballast is inadequate for stress to be applied and improvement of below soil is expensive, in these cases geocell reinforcement of ballast should be done, in which ballast is confined in geocell which result in mattressing effect. For numerical modelling, approach has been used and for that purpose ABAQUS has been used. Ballast was modelled in such way that its obeyed Drucker Prager yield criterion. Geocell was modelled as elastic materials. FE mesh for ballast is represented as C3D4R, rails as C3D8R and soil as C3D8R. He further has done the numerical analysis on two basis- varying stiffness of geocell and varying stiffness of soil, comparing the subgrade stress. The conclusion made from results of Abaqus were Confinement of ballast decrease the vertical deformation and settlement because of the mattressing effect in which geocell redistributes the stress in more uniform way. Also, peak stresses in very weak clay are reduced. Lateral deformation at ballast level is decreased. While modelling was done without taking time-dependent soil behaviour.

Kumar (2014) conducted a numerical analysis of statically and dynamically loaded pre-stressed concrete sleepers using ANSYS. For a better understanding of the dynamic effect on the sleeper comparison of finite element model with ballast and without ballast were compared. Dynamic analyses were done for the two conditions, free-free condition and in-situ condition and observation were made that in case free-free condition natural frequency was much lower than in case of the in-situ condition.

Leshchinsky et al. (2015) conducted a number of triaxial compression test for the determination of mechanical property of sand (GP) mix with a microgrid. Use of microgrid grids results in an economic reinforced layer. Sand used was subangular and poorly graded while microgrid reinforcements have a composition of non-ceasing charcoal flexible fibreglass material. Microgrids of different aspect ratio and dimensions were used and orientation at which it was placed was random. A series of CD Triaxial Test were conducted, and from results, an increase in the angle of friction and modulus of elasticity was interpreted and were represented by strength improvement factor and stiffness improvement factor. It was also observed the reinforcement of greater aspect ratio at lesser concentration gives a better result than a higher concentration of reinforcement in soil. From the result, it was concluded that microgrid is cost effective method but may be sufficient for only shallow ground improvements.

Nikraz et al. (2015) used a method to calculate the load bearing behaviour of strip footing by software Abaqus/CAE. The elastoplastic Drucker-Prager model was used to represent soil behaviour in this software, and the footing and soil were assumed to be isotropic and linear elastic. Drucker-Prager model uses properties

like density, Poisson's ratio, modulus of elasticity, cohesive strength, angle of friction ( $\Phi$ ) and dilation angle. Axi-symmetric approach was used to design the model. From the results of ABAQUS, it was concluded that for FEM analysis, the values of bearing capacity when dilation angle is considered is 13% higher than when dilation angle is considered and Terzaghi results and in between them. The model described in this paper is for short term stability of footing.

Van Dyk et al. (2015) evaluated the effectiveness of various methods of defining dynamic wheel load design factor to consider the dynamic effect while doing static analysis. Various evaluated were Talbot, Indian Railways, German Railways, British Railways etc. The conclusion from the study was made that higher no of elements considered while determining the dynamic factor better would be the dynamic representation dynamic load effect.

Das (2016) has reviewed different publishing and various case studies of different layers of ballast reinforced with geogrid on soft soil subgrade. Various reinforcement mechanism, the performance of geogrid reinforced ballast, the basis for selection of optimum geogrid, the influence of its stiffness etc. were assessed. The conclusion from the assessment was made that reinforcement of railroad bed with geogrid reduces the rate of permanent settlement. With an increase in stiffness of geogrid vertical settlement decreases up to an extent beyond this effect of stiffness reduces. Also, the optimum size of the aperture of geogrid is  $1.4 \times$  (Nominal Size of Ballast) being used.

Lal et al. (2016) conducted a review of rail-wheel contact stresses using software Ansys 15.0 and Creo-parametric 2.0. For the modelling of rail International Union of Railways, guidelines were followed and, Indian guidelines for weight per unit length were obeyed. Results from the whole analysis showed that design is safe, and all stresses were within permissible range.

Esmaili et al. (2017) observed the consequences of geogrid reinforcement on bearing strength and vertical deformation of high speed railway embankment. In this research, both physical and numerical model were made and results were compared. Physical models were made to actual scale for different embankment heights (5m, 10m, 15m, 20m), for each height 5 models were made one without reinforcement and other four with the different number of the reinforcement layer. Numerical modelling was done using software PLAXIS and models similar to physical ones were simulated. Results revealed that an optimum number of reinforced layers for different embankment height were different beyond which further increase in reinforcement layer does improve the soil. Also, the effect of geogrid tensile strength reduces with the decrease in embankment height and by improving soil characteristics.

Min Son (2019) performed on Numerical Study on scale effect of repetitive Plate Loading Tests are used to determine the elastic modulus of a target structure which is subjected to dynamic loading. These tests are usually used on railway

roadbeds. The strain modulus decreased as the loading-plate size decreased. On the basis of subgrade condition, the ratio of the elastic modulus to the strain modulus was 1.13 for gravel and fine gravel, 1.21 for sand, and 1.00 for sandy and cohesive soil.

Yahia Alabbasi (2019) investigated on Conventional ballasted tracks. The mechanical behaviour of railroad ballast has been studied and estimated using a numerical approach. Numerical approaches such as FEM and DEM have been widely employed to simulate ballast behaviour with the advancement of computer resources. The majority of studies used a smaller number of load cycles to model the behaviour of railroad ballast under pure continuous sinusoidal loadings.

Arthur de Oliveira Lima (2021) analysed on Track Modulus assessment of engineered interspersed concrete sleepers in railway track. On the basis of measurement of sleepers both timber sleepers & EIC sleepers presented a similar track response and the variance in performance for the two sleeper types cannot be clearly distinguished with track-displacement or modulus results. On outcome of theoretical analysis is the interspersed standard concrete sleepers placed within a timber-sleeper track can experience a load up to 5 times greater than the load supported by adjacent timber sleepers.

Amninder Singh Nayyar (2021) observed by numerical analysis of railway substructure with geocell-reinforced ballast and concluded that the geocell reinforcement improves stress distribution. Geocell confined ballast portion behaves as a stress absorbing pad due to its high-stress tolerance, which results in absorption and distribution of stresses over a wider area. Additionally, while keeping other conditions and variables constant, with the increase in width of geocell confinement, the magnitude of subgrade stresses decreases.

After literature review, following research gaps are observed –

- 1) The study on the confinement width of geocell is meagre.
- 2) Effect of geocell on settlement of Subgrade.
- 3) Effect of fineness of mesh generated for finite element model is underestimated.

To fulfil the observed research gap, an attempt has been made to work in this direction. Keeping the objectives in mind the study on numerical modelling on railway geotechnics on various aspects are presented in the following chapters.

## CHAPTER 3.

### MATERIALS AND METHODS

As discussed in the objective for the analyses of subgrade stress, 2-D model of the rail track system were designed and simulations were carried out using finite element software PLAXIS 2D.

PLAXIS 2D is, finite element (FEM) software firstly launched in 1982, used to create simulation models of various real-world problems like strength and toughness analysis of electronics or machine components, stress distribution in building, railway structure or soil etc.

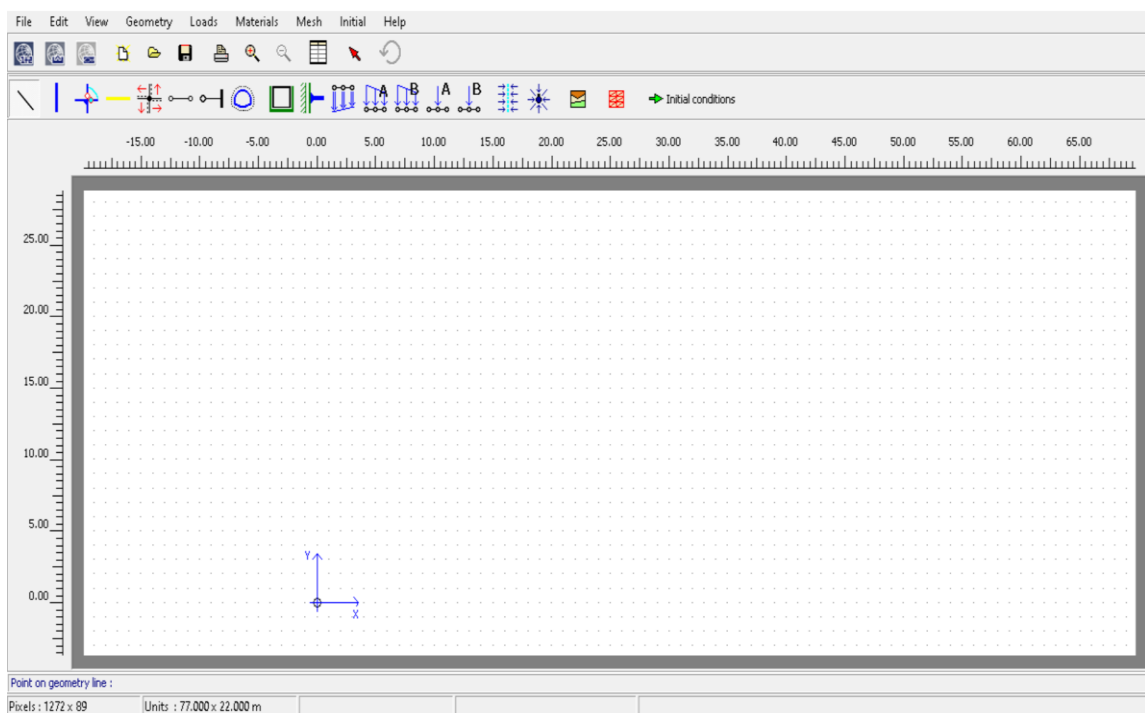


Figure 3.1 Basic Layout of PLAXIS 2D

Version of PLAXIS 2D used for conducting whole simulation and stress analyses of the embankment is 8.6.

In the whole analysis, eight models were simulated including unreinforced and geocell confined ballast in 2-D analysis.

### 3.1 FINITE ELEMENT RAILWAY SUBSTRUCTURE GEOMETRY

All the models were designed in PLAXIS 2D and are in accordance with Indian Railway standards. 52kg/m Rail section is considered for the analysis and its cross-section is shown in Figure 3.2 as per I.R.S. and dimensions of 52Kg/m Rails are mentioned in Table 3.1

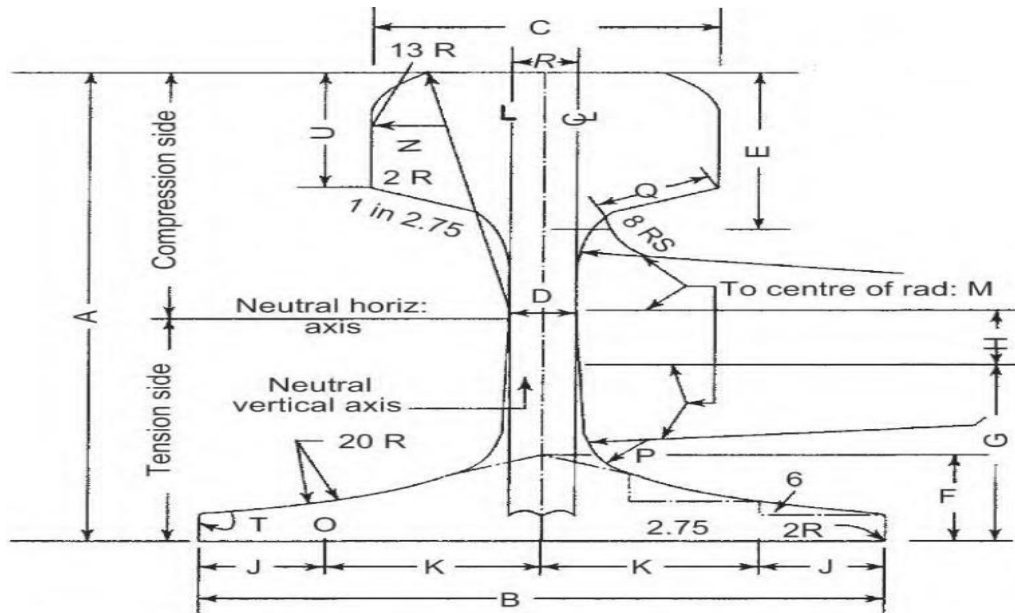


Figure 3.2 I.R.S 52kg/m Rail Section – Key To Dimension Table (Mundrey 2005)

Table 3.1 Dimension Table (Mundrey 2005)

Rail Section	Weight per metre	A	B	C	D	E	F	G	H	J	K
	Kg	mm	mm	mm	mm	mm	mm	mm	mm	mm	mm
52kg	51.89	156	136	67	15.5	51	29	60	19	24	44
Rail Section	Weight per metre	L	M	N	O	P	Q	R	S	T	U
	Kg	mm	mm	mm	mm	mm	mm	mm	mm	mm	mm
	52kg	51.89	305	381	80	13	13	17.5	18	22.5	5

For modelling, sleeper considered was PCS-12 which made of prestressed concrete and M+5 is taken as sleeper density for the analysis.



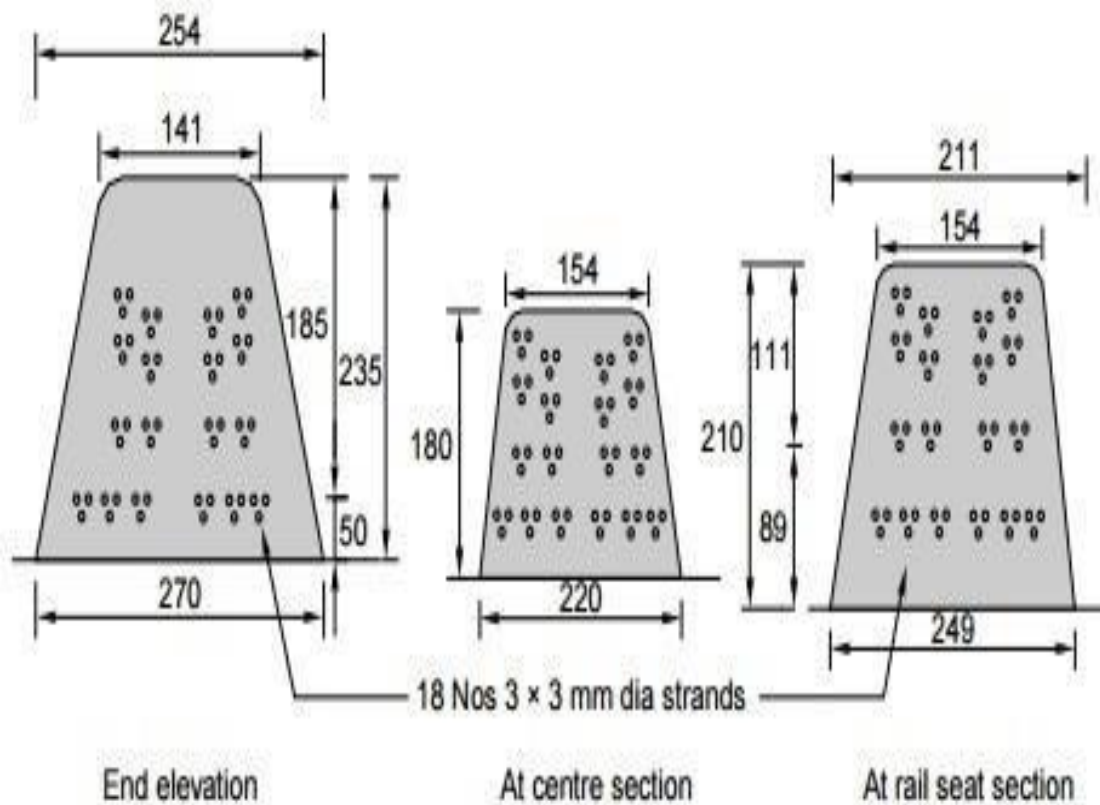


Figure 3.3 Cross Section of PCS-12 Sleeper (Agarwal 2017)

Width of ballast at base level is  $4.6\text{ m}$ , and at the crest, the level is  $3.4\text{ m}$  with a side slope of  $1.5:1$ .  $350\text{ mm}$  of the ballast layer was provided. In the case of reinforced ballast, geocell confinement was done at the centre of the ballast layer. Height of Geocell is  $0.1\text{ m}$ , and its width varies from  $2\text{ m}$  to  $3.8\text{ m}$ . Width of Clay subgrade layer at base level is  $9.1\text{ m}$ , and at the crest level is  $7.40\text{ m}$  with a side slope of  $1.5:1$ .  $350\text{ mm}$  of the ballast layer was provided. Width and depth of soil subgrade consider for the model is  $9.10\text{ m}$  and  $4.0\text{ m}$  respectively. Geometrical representation of 2-D Model analysed are shown in Figure 3.4 to Figure 3.12 where Figure 3.4 and 3.5 is a geometrical representation of the 2-D model layout and geometrical representation of 2-D model with unreinforced ballast and rest figures are a geometrical representation of the 2-D model with different geocell confinement width.

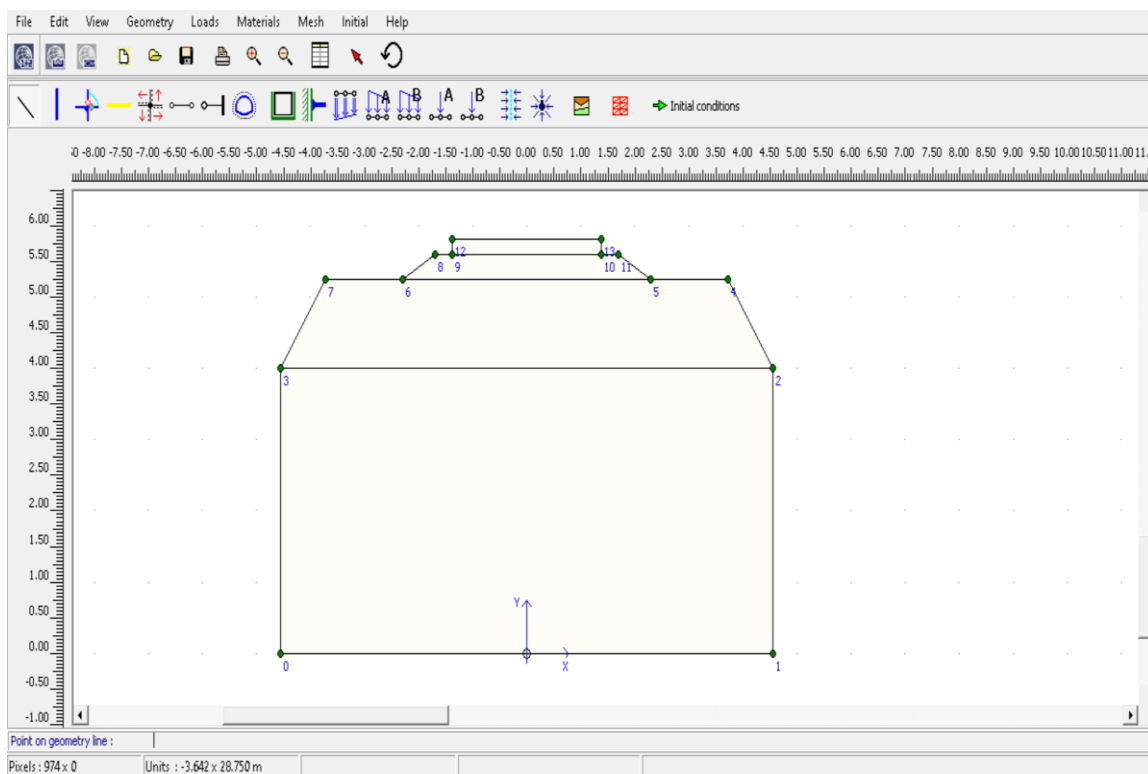


Figure 3.4 Geometrical representation of 2D Model Layout.

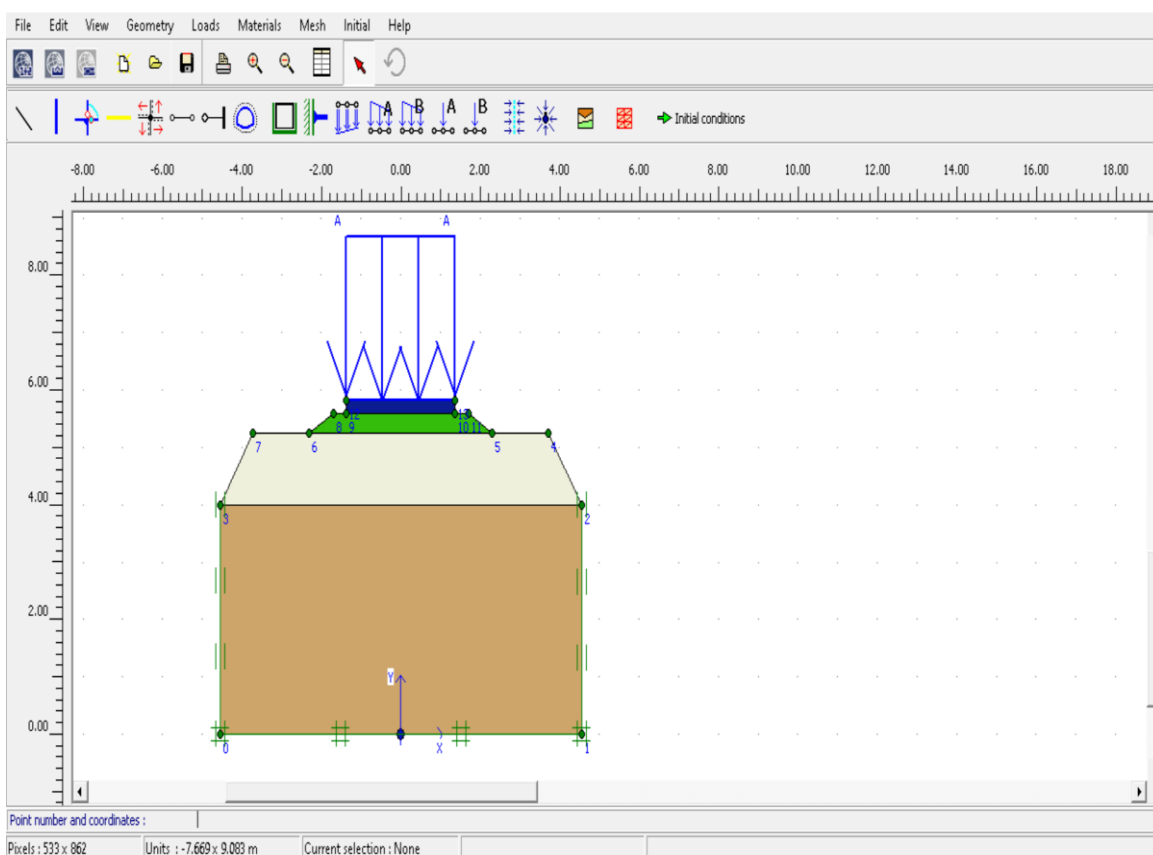


Figure 3.5 Geometrical representation of 2D Model with Unreinforced Ballast.

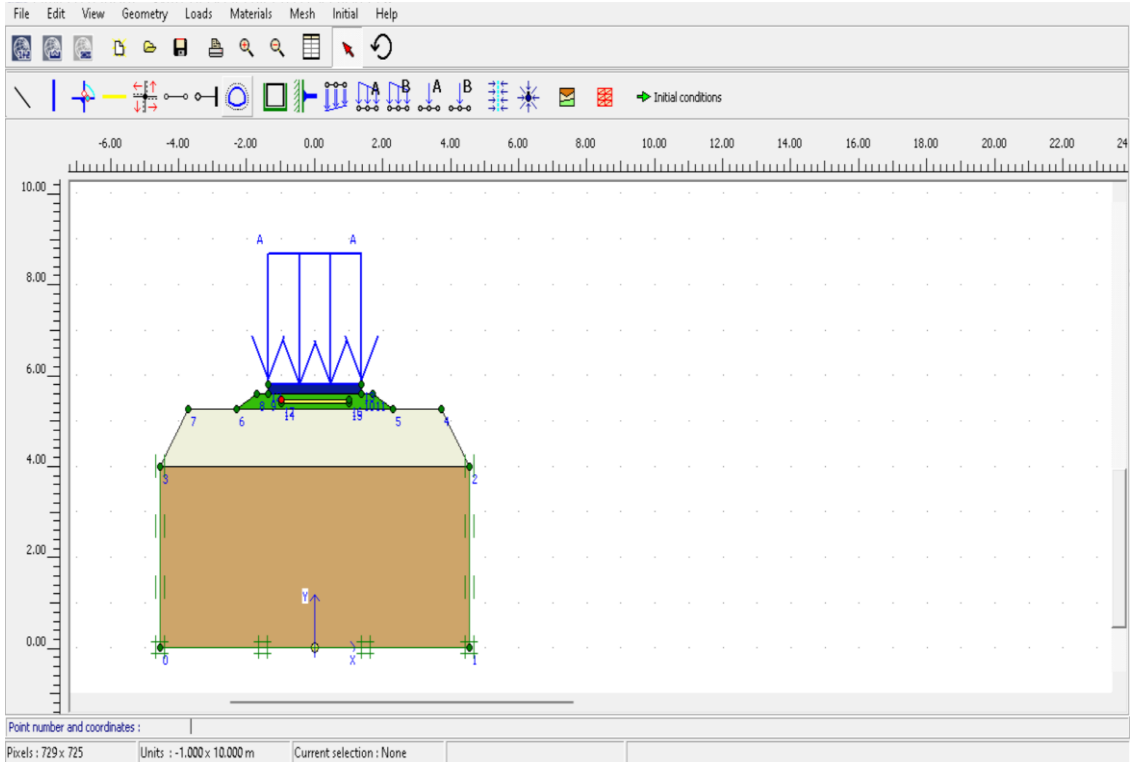


Figure 3.6 Geometrical representation of 2D Model with Geocell Confinement Width 2.00 m

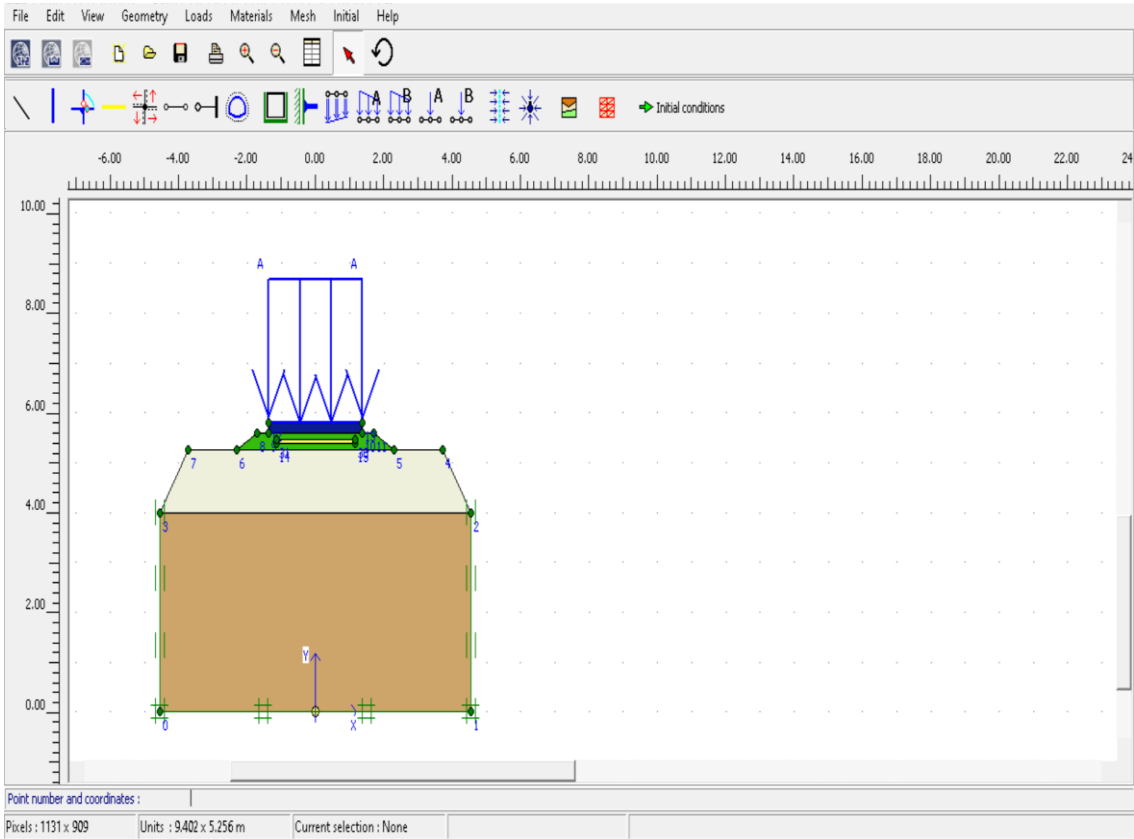


Figure 3.7 Geometrical representation of 2D Model with Geocell Confinement Width 2.3 m.

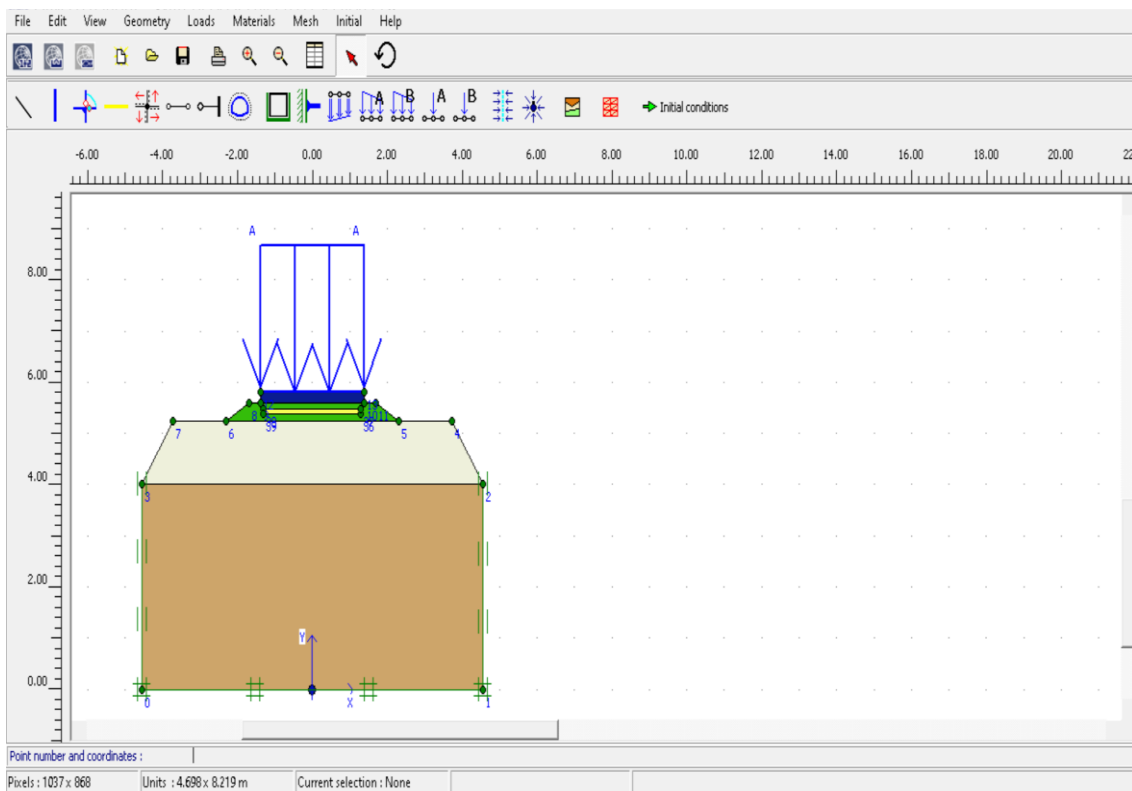


Figure 3.8 Geometrical representation of 2D Model with Geocell Confinement Width 2.6m

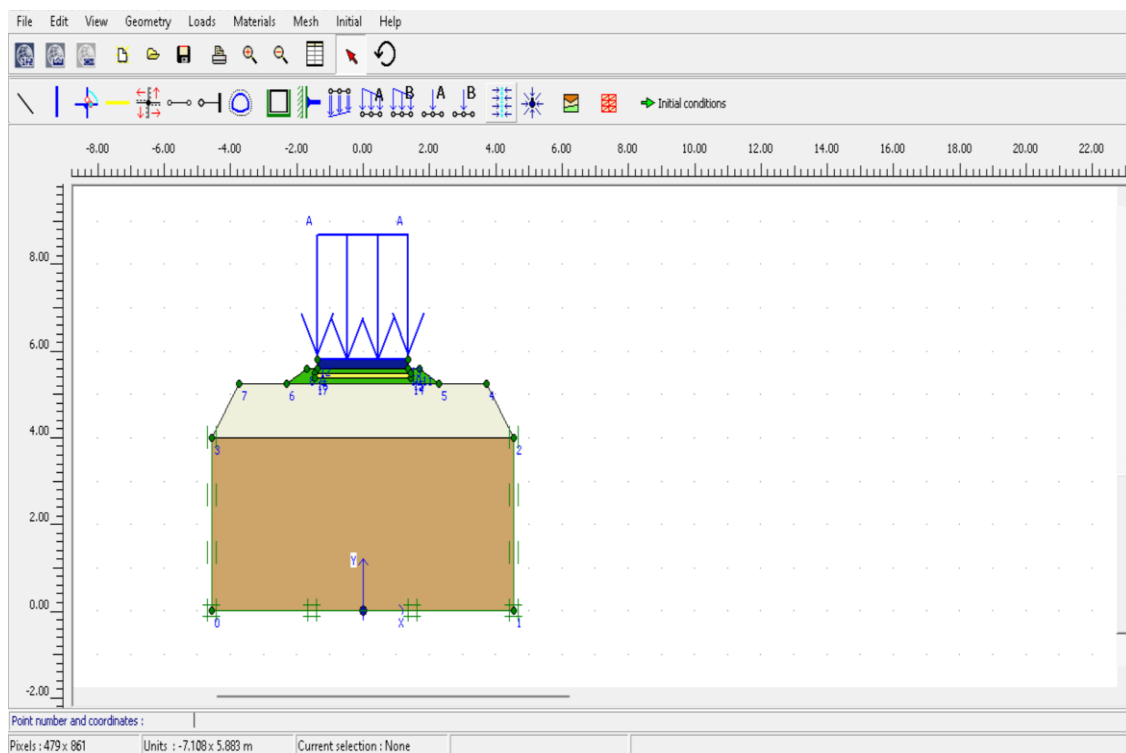


Figure 3.9 Geometrical representation of 2D Model with Geocell Confinement Width 2.

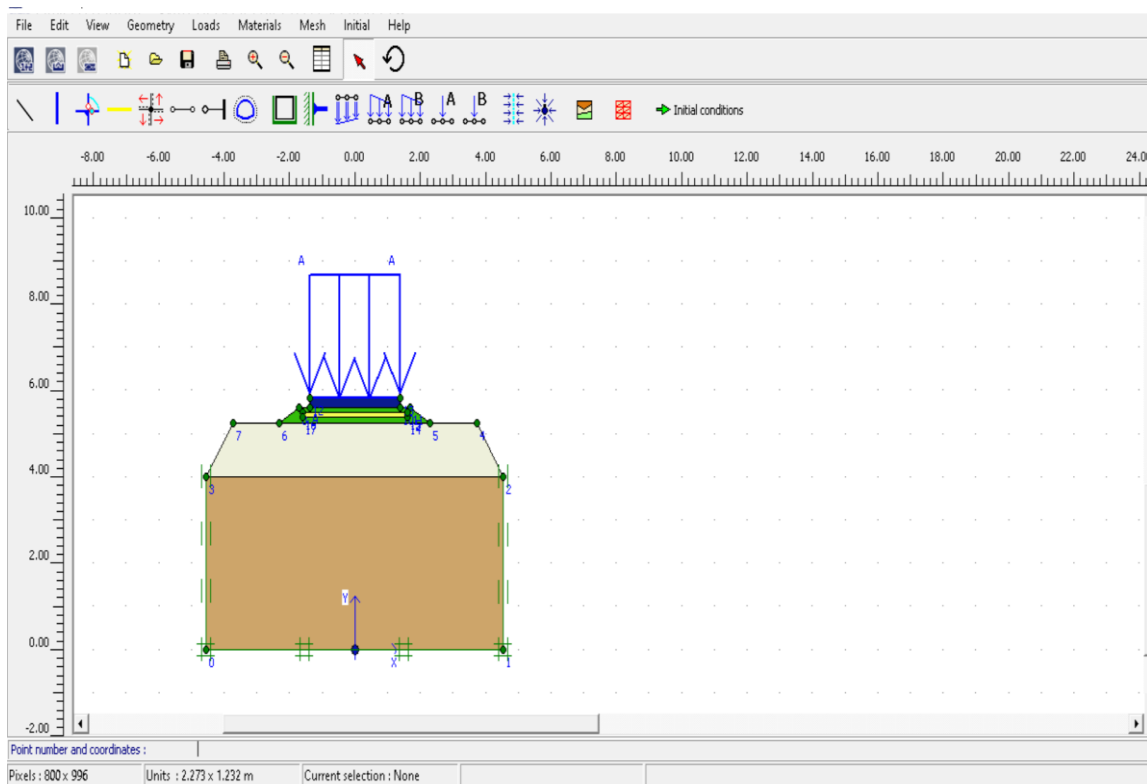


Figure 3.10 Geometrical representation of 2D Model with Geocell Confinement Width 3.2m

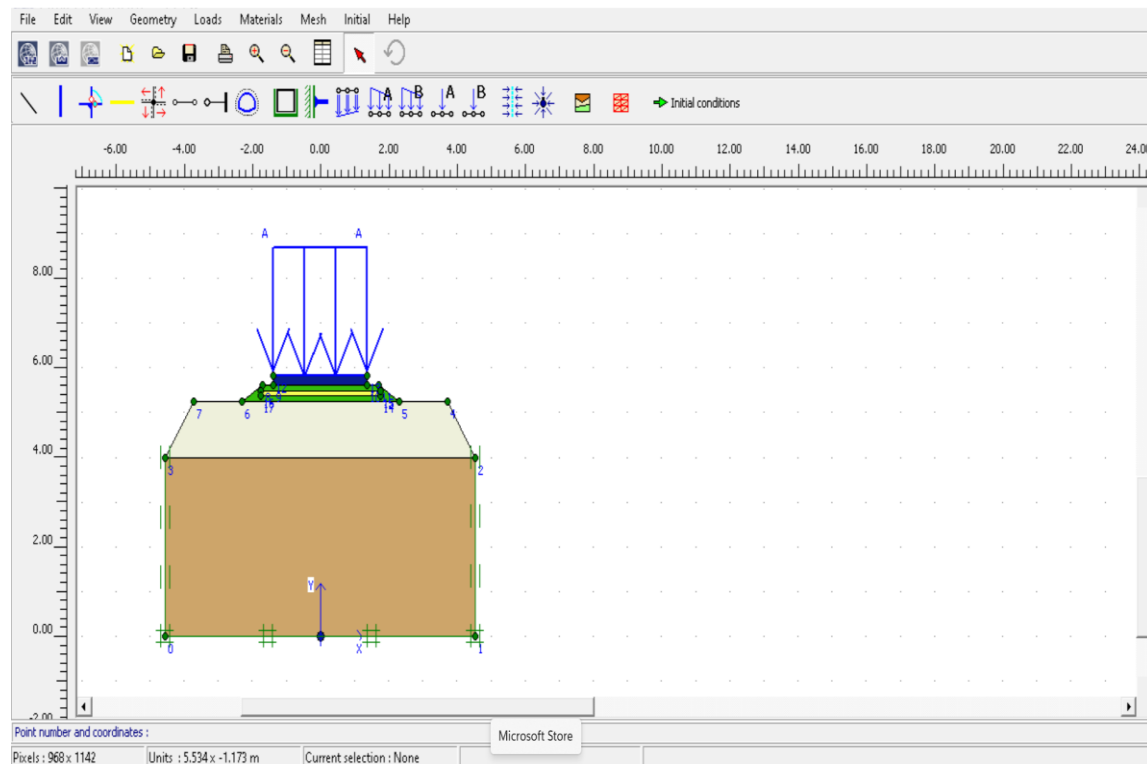


Figure 3.11 Geometrical representation of 2D Model with Geocell Confinement Width 3.5m

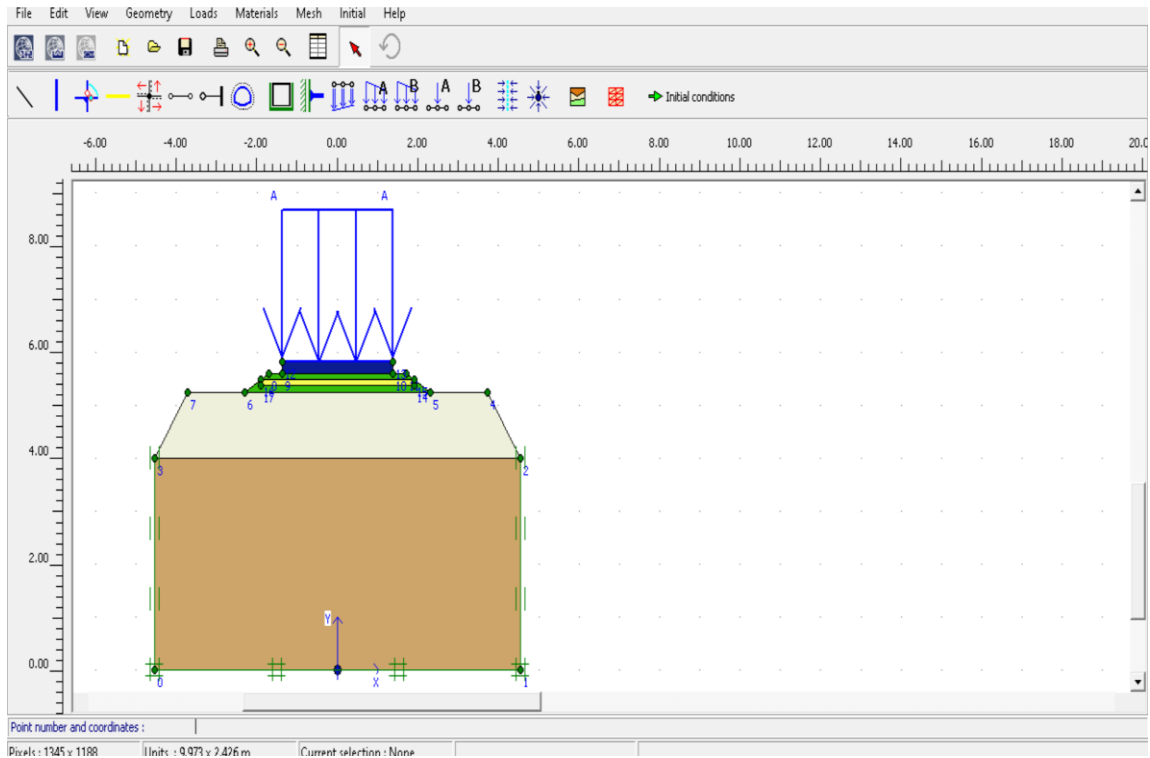


Figure 3.12 Geometrical representation of 2D Model with Geocell Confinement Width 3.8m

### 3.2 FINITE ELEMENT MATERIAL PROPERTIES

For modelling, subgrade was taken as soft clay and low strength aggregate was taken as ballast. The rail and sleepers were taken in accordance with Indian Rail Standard. Geocell considered in all models was made of Novel Polymeric Alloy (NPA) rather than standard material because it had greater stiffness and creep resistance in comparison to standard materials like polyethylene (Leshchinsky et al. 2013). During analysis rail, sleepers, geocell and subgrade had been simulated as an elastic material. While ballast and sub-ballast had been simulated as elasto-plastic material where plastic properties were given in accordance to Mohr-Coulomb Criterion with very little cohesion of  $1kPa$  (as per Leshchinsky et al. 2013), for enabling of the simulation process. Subgrade was considered as elastic in order to decrease the computational cost. Material properties used for defining different component of numerical models are given in Table 3.2 and Table 3.3.

Table 3.2 Finite Element Material Properties (Leshchinsky et al. 2013; Lal et al. 2016; Kumar and Sambasivarao 2014)

MATERIAL	Mass Density $\rho$ ( $kg/m^3$ )	Elastic Modulus $E(MPa)$	Poisson's Ratio $\mu$	Internal Angle of Friction $\varphi$ ( $^\circ$ )	Angle of Dilation $\psi$ ( $^\circ$ )
Geocell	1500	2070	0.35	-	-
Sleeper	2400	30000	0.300	-	-
Ballast	1520	2	0.350	45	15

Table 3.3 Finite Element Subgrade Properties

Material	Mass Density $\rho$ ( $kg/m^3$ )	Elastic Modulus $E(MPa)$	Poisson's Ratio $\mu$	Internal Angle of Friction $\varphi$ ( $^\circ$ )	Cohesion (kPa)
Subgrade I	1600	2	0.15	30	10
Subgrade II	1600	2	0.15	14.015	20.67

### 3.3 FINITE ELEMENT MESH AND BOUNDARY CONDITIONS

Meshing is a procedure of dividing a part of the finite element model into very small fragments. Mesh may be rectangular, triangular and square in shape. For finite element analysis, the meshing of parts is required, as shown in Figure 3.13 and Figure 3.14 in the case of the 2-D model. Figure 3.13 shows a meshed model with unreinforced ballast and Figure 3.14 gives a representation of the meshed model with geocell confined ballast. In the 2-D model, Fine Triangular ballast mesh is selected for the interlocking effect of granular ballast materials (Leshchinsky et al. 2013). For rail and geocell element type CPE4R for meshing was used. Railway Embankment was modelled finely. Interaction between different parts was taken in such a way that there was no sliding. The whole model was a constraint in the x-direction to prevent lateral displacement. Also, the base of subgrade was a constraint in the whole direction.

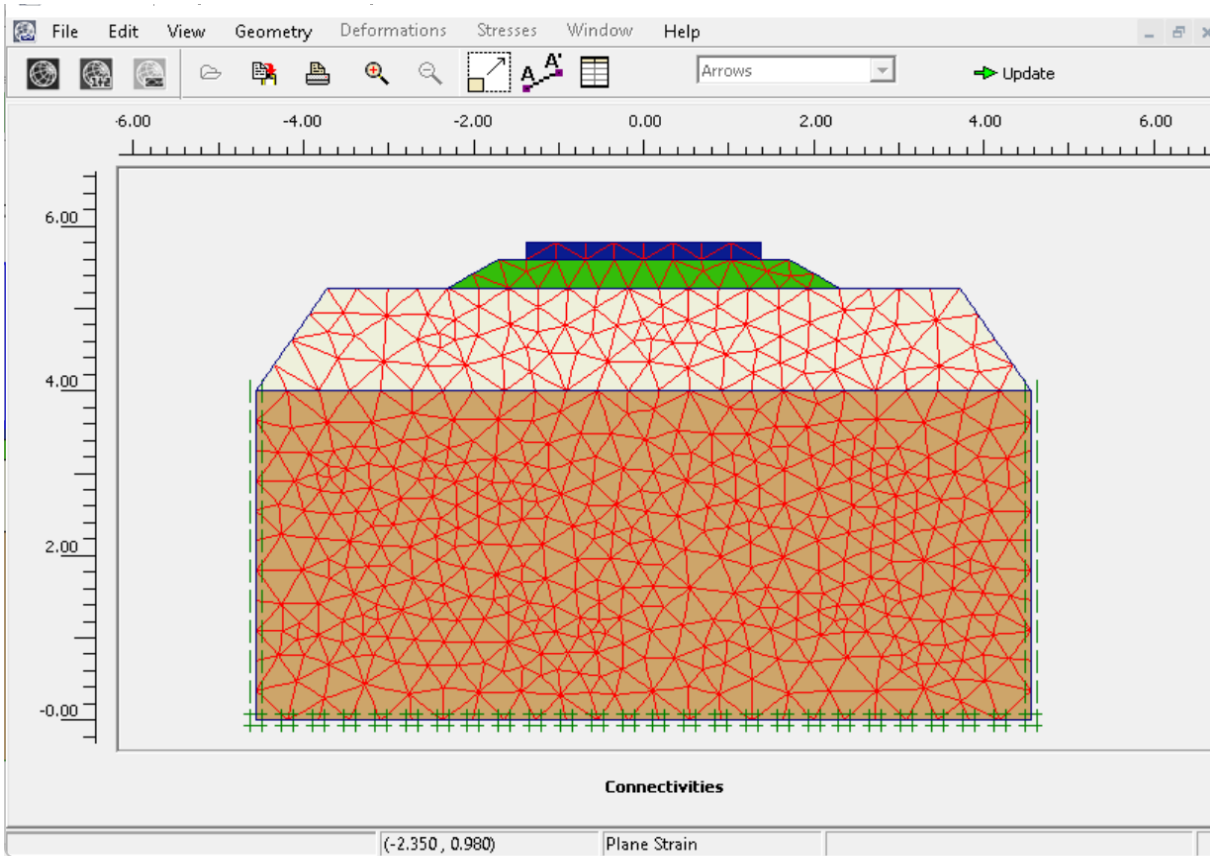


Figure 3.13 2D Meshed Model with Unreinforced Ballast

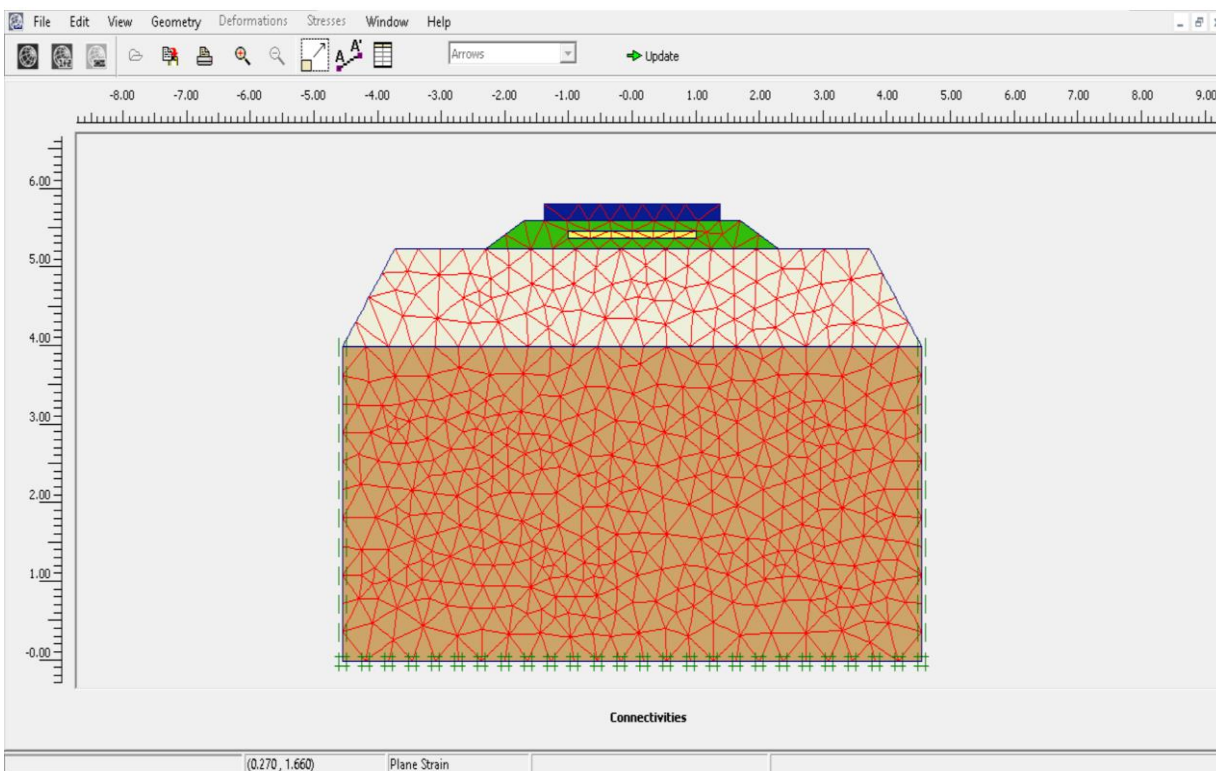


Figure 3.14 2D Meshed Model with Geocell Confined Ballast of 2.0 m



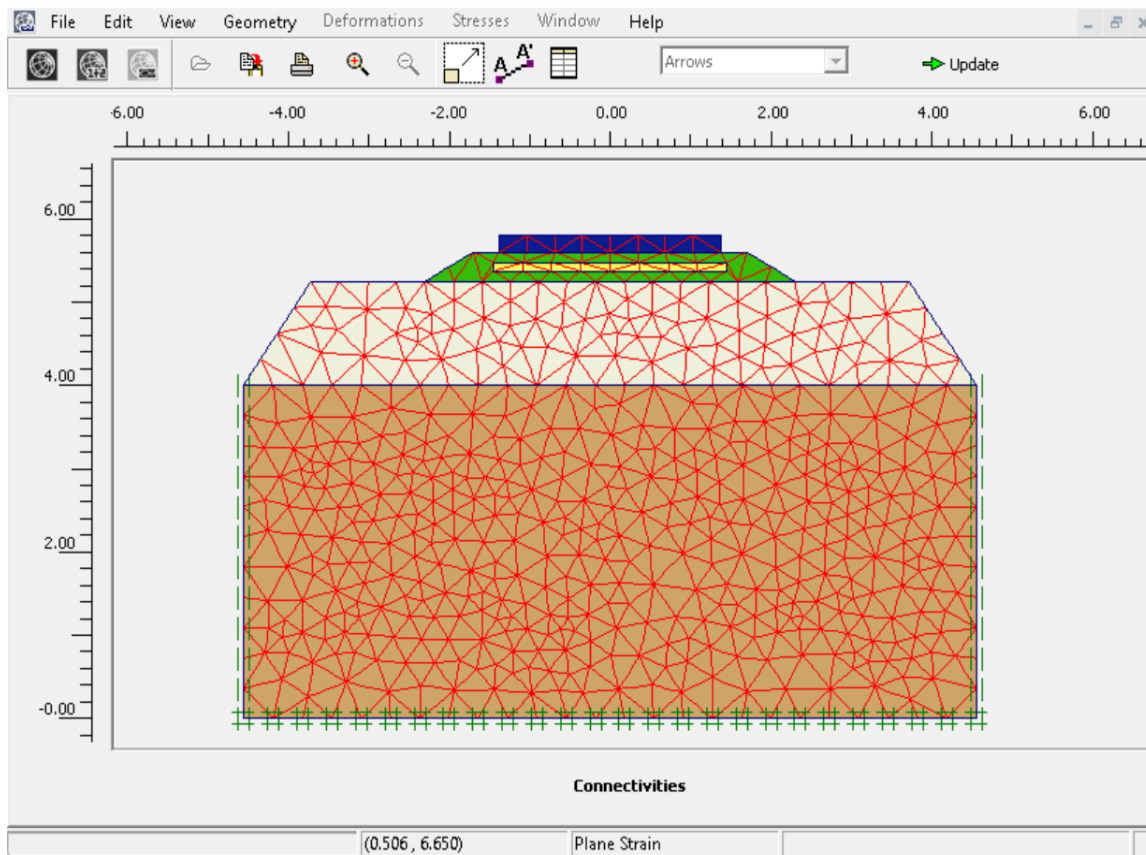


Figure 3.15 2D Meshed Model with Geocell Confined Ballast of 2.9 m

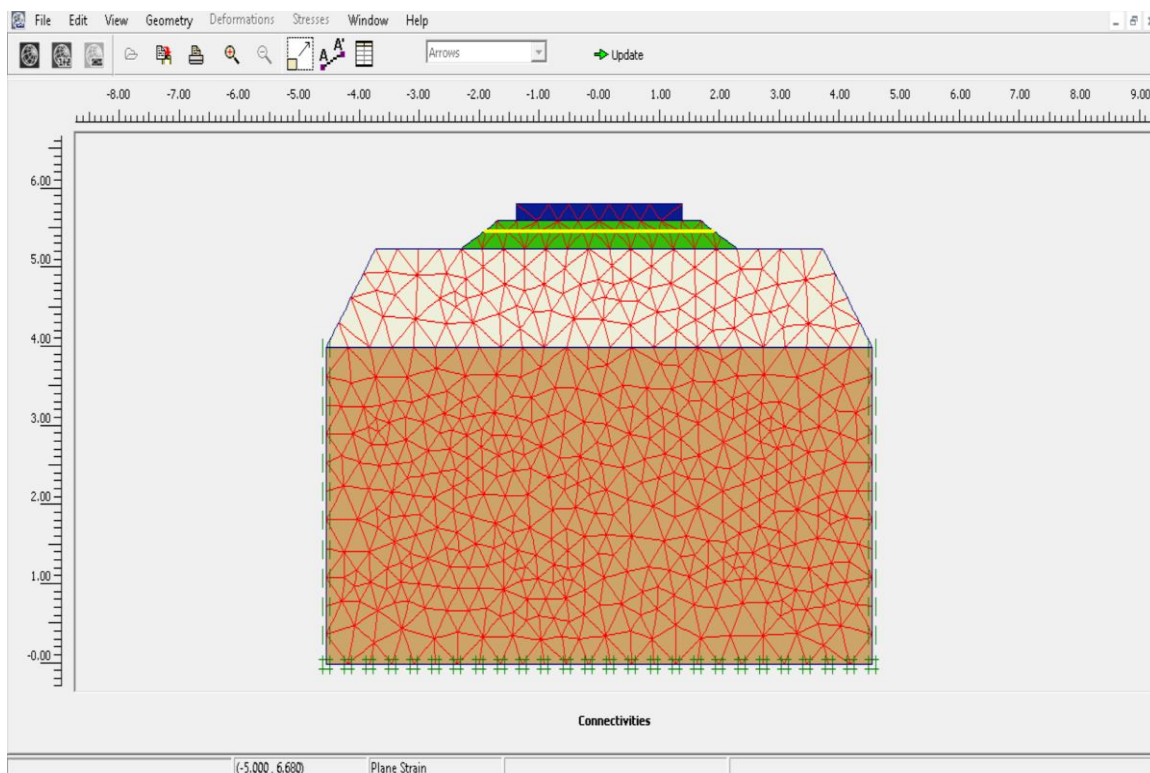


Figure 3.16 2D Meshed Model with Geocell Confined Ballast of 3.8 m

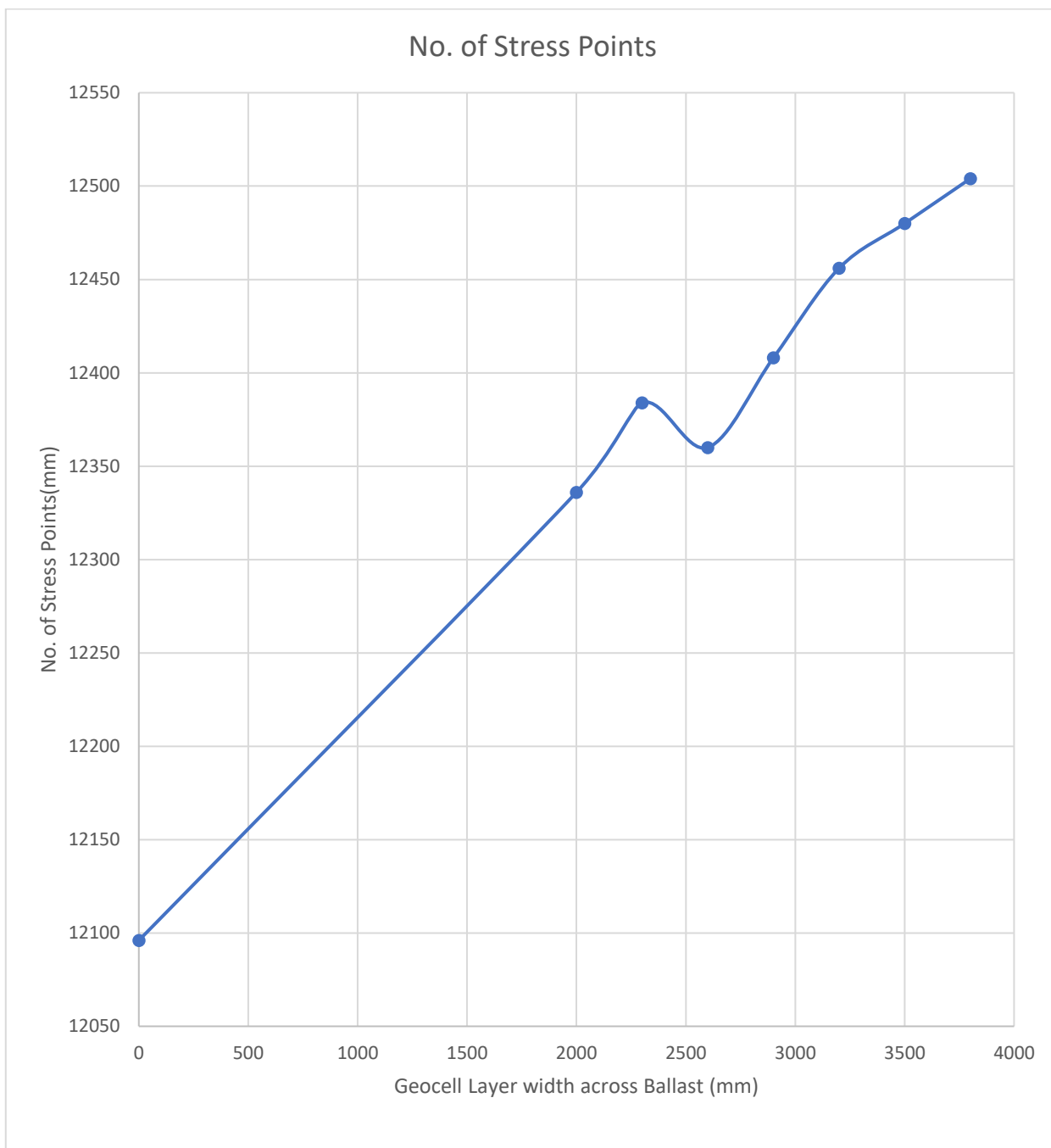


Figure 3.17 Number of stress points generated by very fine mesh in Embankment

Number of Stress points generated for various cases of models for reinforced and varying geocell width across Ballast are shown in graphical view.

### 3.4 FINITE ELEMENT MESH CONVERGENCE AND MODEL VALIDATION

Meshing is the essence of finite element analysis. Compatibility of whole Finite Element model depends upon element type and size of the mesh. Mesh convergence is the procedure in which it is verified that any change size of mesh does not result in drastic changes in the results. For this purpose, a model was analysed for different mesh properties as given in

Table 3.4 and plot between the Geocell layer width across ballast and relative mesh density was plotted as shown in Figure 3.17.

Table 3.4 Mesh Information of Unreinforced Embankment

General info

<b>Project</b> Filename : Directory : C:\Users\lavku\AppData\Local\ Title :	<b>General options</b> Model : Plane Strain Elements : 15-Noded
<b>Comments</b> <div style="border: 1px solid black; height: 40px; width: 100%;"></div>	<b>Mesh</b> Number of elements : 1009 Number of nodes : 8231 Number of stress points : 12108 Average element size : $228.91 \times 10^{-3}$ m

OK

From both Figure 3.13 and 3.14, mesh size of very fine was selected for all analyses throughout the project as it gives better result in comparison to the finer meshes and give betterre results in comparison to coarser meshes.

For the validation of analysis, a particular of amount of load was applied on a portion of model shown in Figure 3.15 instead of the whole model and stresses were determined.

Also, the same problem is solved using Boussinesq's solution for the circularly loaded area.

$$\sigma_y = q \times \left[ 1 - \frac{y^3}{(b^2 + y^2)^{3/2}} \right] \quad (3.1)$$

where,

$\sigma_y$  = Vertical Stresses at depth '  $y$  ' (Pa)

$q$  = Load applied per unit area (Pa)

$b$  = Radius of circular loaded area (m)

$y$  = Depth at which stress are to be calculated (m)

In validation model,

$$q = 100000 \text{ Pa}$$

$$b = 0.3 \text{ m}$$

$$y = 0.35 \text{ m}$$

Using Equation (3.1),

$$\sigma_y = 10000 \times \left[ 1 - \frac{0.35^3}{(0.3)^2 + 0.35^2} \right]$$

$$\sigma_y = 56231 \text{ Pa}$$

### 3.5 LOAD CALCULATION

The wheel load for the broad gauge is limited to 110.25KN per wheel (Mundrey 2005).

#### Load Calculations

For 8 wheels per 2 rail length.

As per I.R.S., One rail length = 13 m

Sleeper density =  $M+5$

$$=13+5$$

$$=18 \text{ Sleepers per rail length}$$

Total Load on one rail length(13 m track) =  $110.25*8 = 882 \text{ KN}$

$$\text{Total Load on one rail} = \frac{882}{2} = 441 \text{ kN}$$

$$\text{Load per sleeper} = \frac{882 \text{ KN}}{\text{No. of sleepers per rail length (i.e. } M+5)}$$

$$= \frac{882 \text{ kN}}{(13+5)}$$

$$= 49 \text{ KN/Sleeper}$$

$$\text{Load intensity} = \frac{49 \text{ kN}}{\text{Area}}$$

$$= \frac{49}{(0.18*1.3750)}$$

$$= 98.99 \text{ kN/m}^2$$

Maximum Load on Sleeper =  $2 * 98.98 = 197.98 \text{ kN per sleeper}$

### 3.6 FINITE ELEMENT LOADING

The wheel load for the broad gauge is limited to 110.25KN per wheel (Mundrey 2005).

As train moves instead of static, condition becomes quasi-static. To account the effect of train speed, speed factor (SF) was introduced (Mundrey 2005) and its value was determined from Figure 3.27.

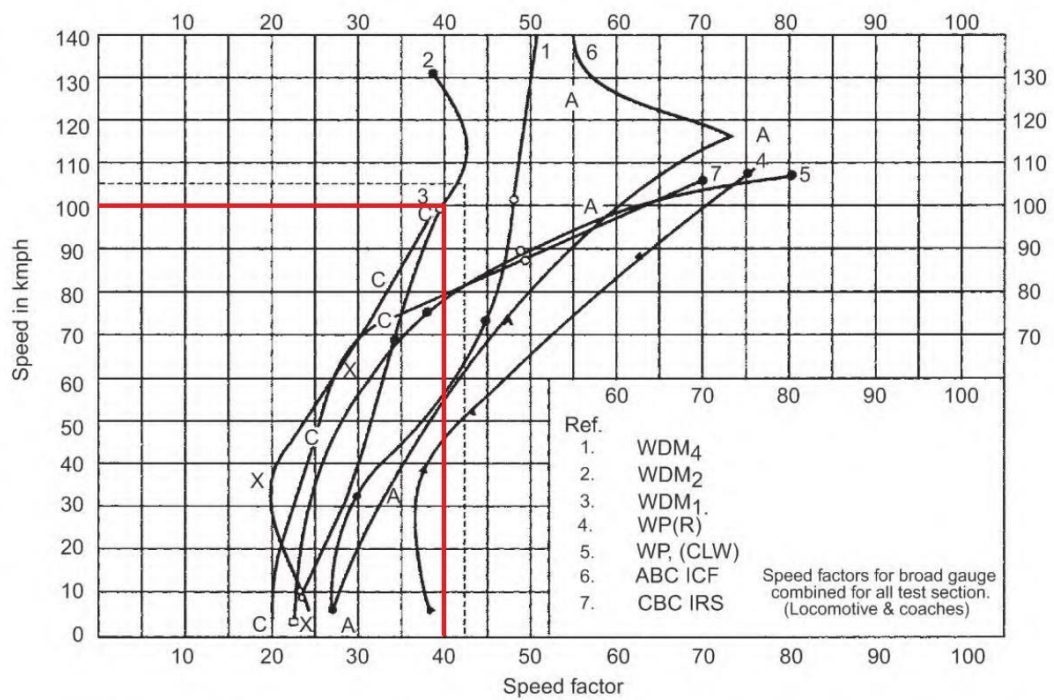


Figure 3.18 Speed vs Speed Factor Chart (Mundrey 2005)

Also to account the dynamic effect of rail load while analysing the models, dynamic factor was considered as following:-

$$P_d = \phi P_s \quad (\text{Van Dyk et al. 2015}) \quad (3.2)$$

where  $P_d$  = Dynamic Wheel Load

$P_s$  = Static Wheel Load

$\Phi$  = Dynamic Wheel Load Factor

$$\phi = 1 + \frac{v}{3 \times \sqrt{U}} \quad (\text{Srinivasan 1969}) \quad (3.3)$$

where  $\Phi$  = Dynamic Wheel Load Factor

$V$  = Speed of Train (mile/h)

$U$  = Track Modulus (psi)

To take the rail load considered on the conservative side, both above-mentioned factors were considered.

$$P = SF \times \phi \times P_s \quad (3.4)$$

Where P – Factored Load

SF – Speed Factor

$\Phi$  – Dynamic Wheel Load Factor

Assuming,  $v = 100 \text{ km/h} = 62.13 \text{ mile/h}$

$U = 6000 \text{ psi}$  (Van Dyk et al. 2015)

$P_s = 11.25 \text{ tonnes}$

From Equation (3.3), 
$$\phi = 1 + \frac{62.13}{3 \times \sqrt{6000}}$$

$$\phi = 1.267$$

From Figure 3.25  $S.F = 1.4$

From Equation (3.4), 
$$P = 1.4 \times 1.267 \times 11.025$$

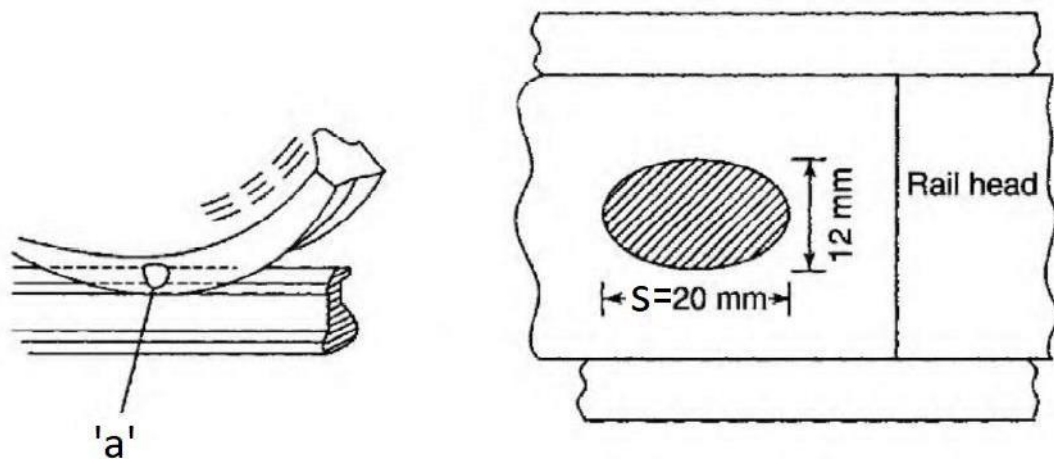
$$P \approx 195.5 \text{ kN}$$

Design Load for numerical modelling:

Considering the design load as Maximum load i.e. 198.98kN (as it will be safe for lesser value of load).

Load is distributed in two points =  $197.97 \text{ kN}/2 = 98.98 \text{ kN}$ .

Figure 3.19 Contact area between Wheel and Rail Track (Mundrey 2005)



$$\begin{aligned}
 \text{Contact Pressure due to Rail Load} &= \frac{P}{a} & (3.5) \\
 &= \frac{198800}{1.88 \times 10^{-4}} \\
 &= 1.0574 \times 10^9 \text{ kN/m}^2
 \end{aligned}$$

For determining the duration of load application: -

$$v = r\omega \quad (3.6)$$

$$\theta = \frac{s}{r} \quad (3.7)$$

$$\omega = \frac{\theta}{t} \quad (3.8)$$

where,

$r$  – radius of wheel (m) = 0.420m

$\omega$  – angular velocity of the wheel ( $\text{sec}^{-1}$ )

$v$  – velocity of the wheel (m/sec)

$\theta$  – central angle subtended by 's' length

$s$  – length of contact between wheel and rail track

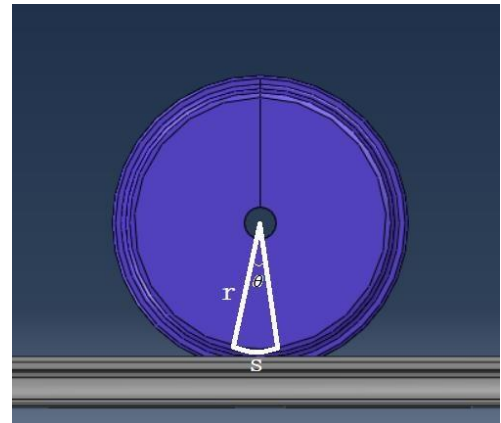


Figure 3.20 Contact between Wheel and Rail Track

With the reference of Figure 3.20 following calculation were done:

From Equation (3.6),

$$\frac{100 \times 5}{18} = .42 \times \omega$$

$$\omega = 66.13 \text{ sec}^{-1}$$

From Equation (3.7),

$$\theta = \frac{0.020}{0.420}$$

$$\theta = 0.0463 \text{ radians}$$



From Equation (3.8),

$$66.13 = \frac{0.0463}{t}$$

$$t = 7 \times 10^{-4} \text{s.}$$

### 3.7 FINITE ELEMENT PROBLEM SIZE

1) 2-D Model Problem (Unreinforced)	
Number of Elements	1009
Number of Nodes	8231
Total Number of Variables in the Model	12108
2) 2-D Model Problem (Geocell Confinement Width – 2.0m)	
Number of Elements	1028
Number of Nodes	8381
Total Number of Variables in the Model	12336
3) 2-D Model Problem (Geocell Confinement Width – 2.3m)	
Number of Elements	1032
Number of Nodes	8413
Total Number of Variables in the Model	12384
4) 2-D Model Problem (Geocell Confinement Width – 2.6m)	
Number of Elements	1030
Number of Nodes	8397
Total Number of Variables in the Model	12360

## 5) 2-D Model Problem (Geocell Confinement Width – 2.9m)

Number of Elements	1034
--------------------	------

Number of Nodes	8429
-----------------	------

Total Number of Variables in the Model	12408
--	-------

## 6) 2-D Model Problem (Geocell Confinement Width – 3.2m)

Number of Elements	1038
--------------------	------

Number of Nodes	8461
-----------------	------

Total Number of Variables in the Model	12456
--	-------

## 7) 2-D Model Problem (Geocell Confinement Width – 3.5m)

Number of Elements	1040
--------------------	------

Number of Nodes	8477
-----------------	------

Total Number of Variables in the Model	12480
--	-------

## 8) 2-D Model Problem (Geocell Confinement Width – 3.8m)

Number of Elements	1042
--------------------	------

Number of Nodes	8497
-----------------	------

Total Number of Variables in the Model	12504
--	-------

## CHAPTER 4.

### RESULTS AND DISCUSSION

In total, eight simulations were run in Plaxis 2D and stresses were observed. On comparing the results of simulation in regarding stresses in both cases, unreinforced ballast and geocell confined ballast, improvement in stress distribution was observed. The reason behind the improvement was the inclusion of geocell confinement resulting in a wider distribution of stresses generally over its width. Thus stress distribution along the longitudinal direction was negligible. Figure 4.1 to Figure 4.8 gives subgrade stress distribution contours of 2-D models with unreinforced ballast and geocell confined ballast. For graphical comparison, as shown in Figure 4.9, a plot between subgrade stress at depth 4 m below the subgrade surface and length along with the ballast.

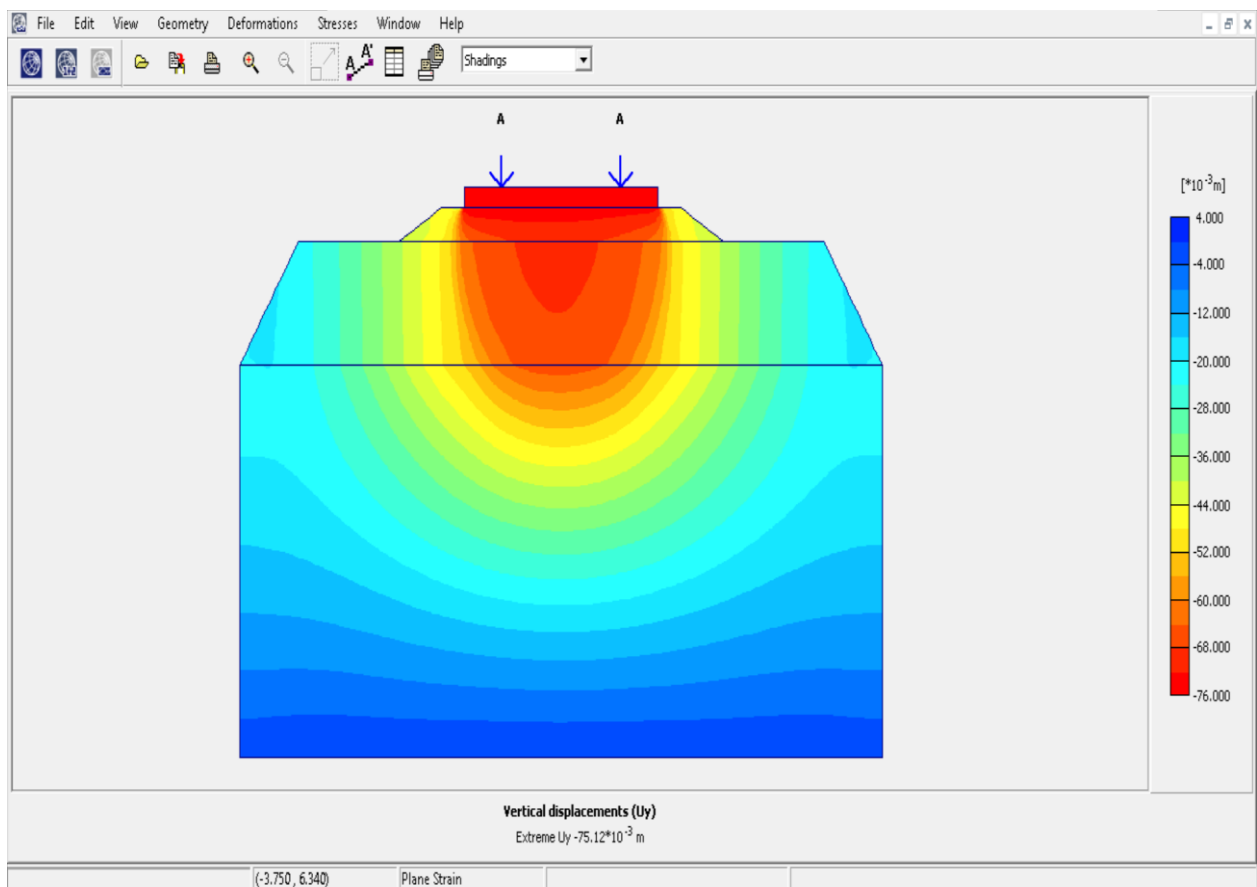


Figure 4.1 Subgrade Vertical Displacement in 2-D Model with Unreinforced Ballast.

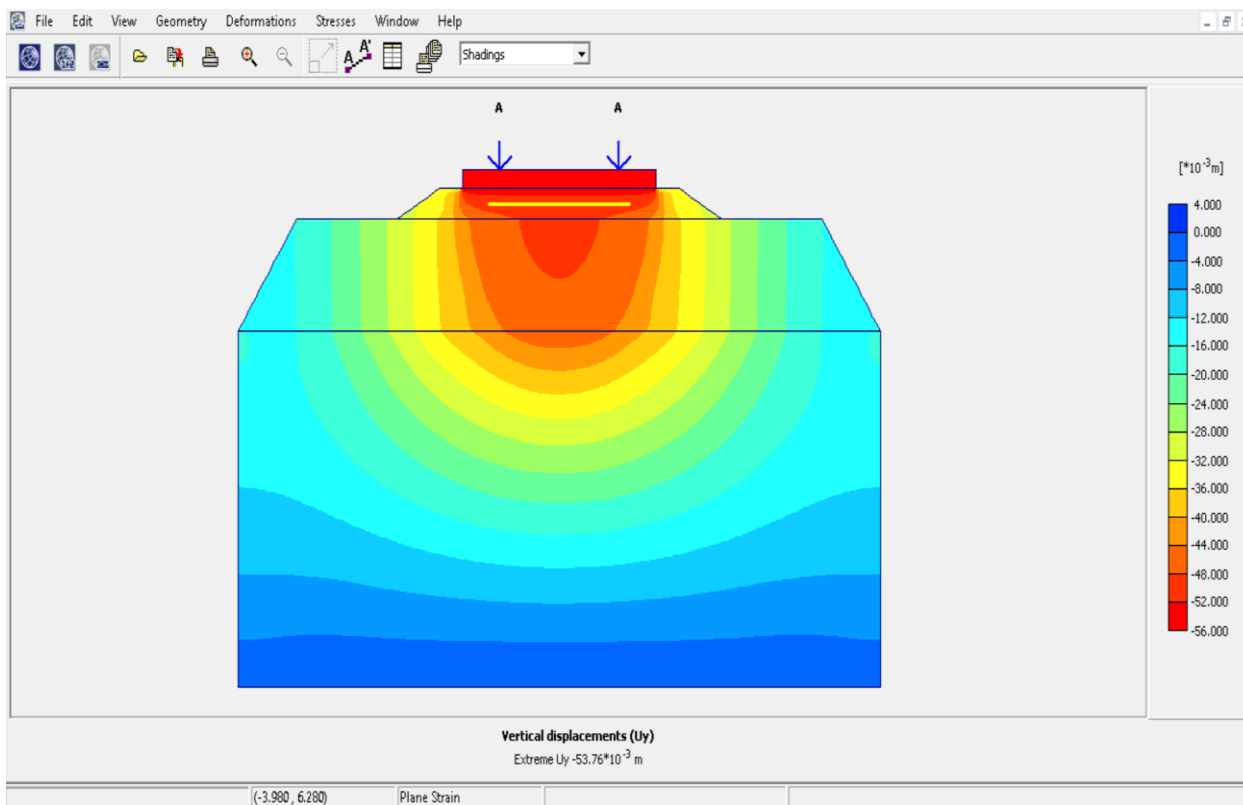


Figure 4.2 Subgrade Vertical Displacement in 2-D Model with Geocell Confinement Width 2.0m.

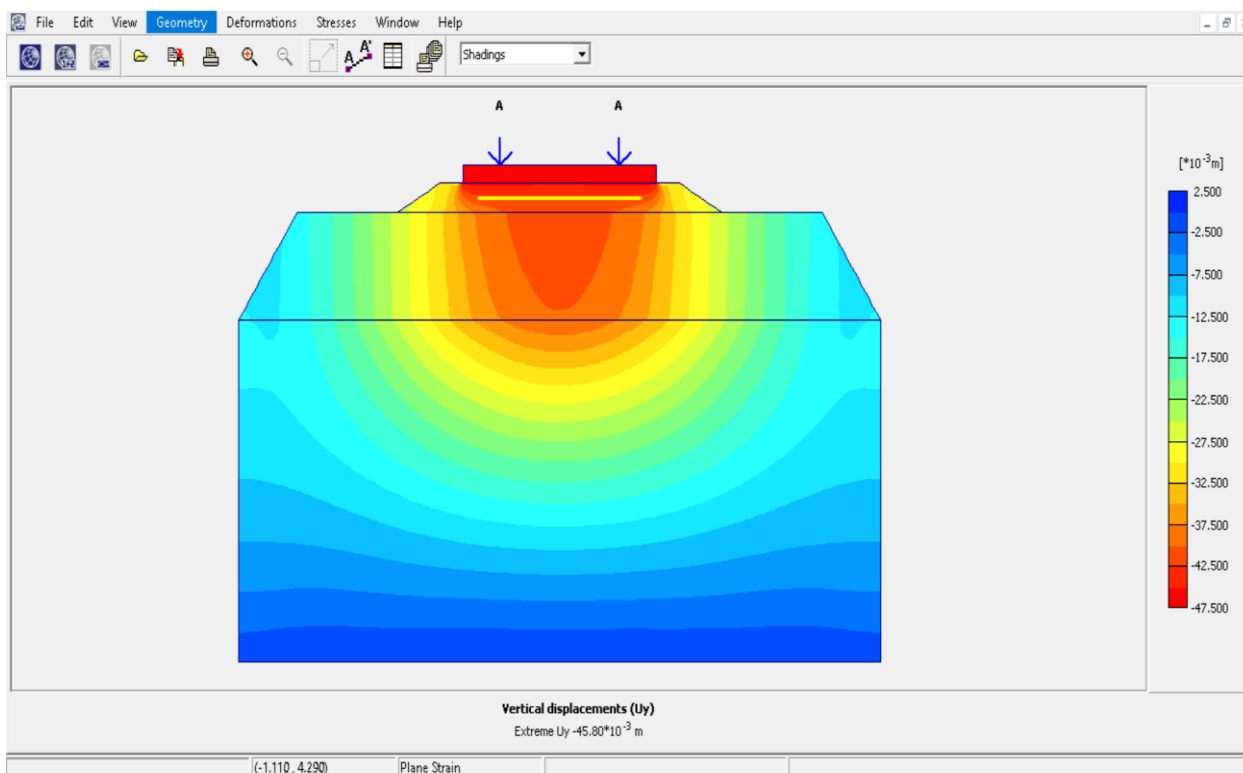


Figure 4.3 Subgrade Vertical Displacement in 2-D Model with Geocell Confinement Width 2.3m.

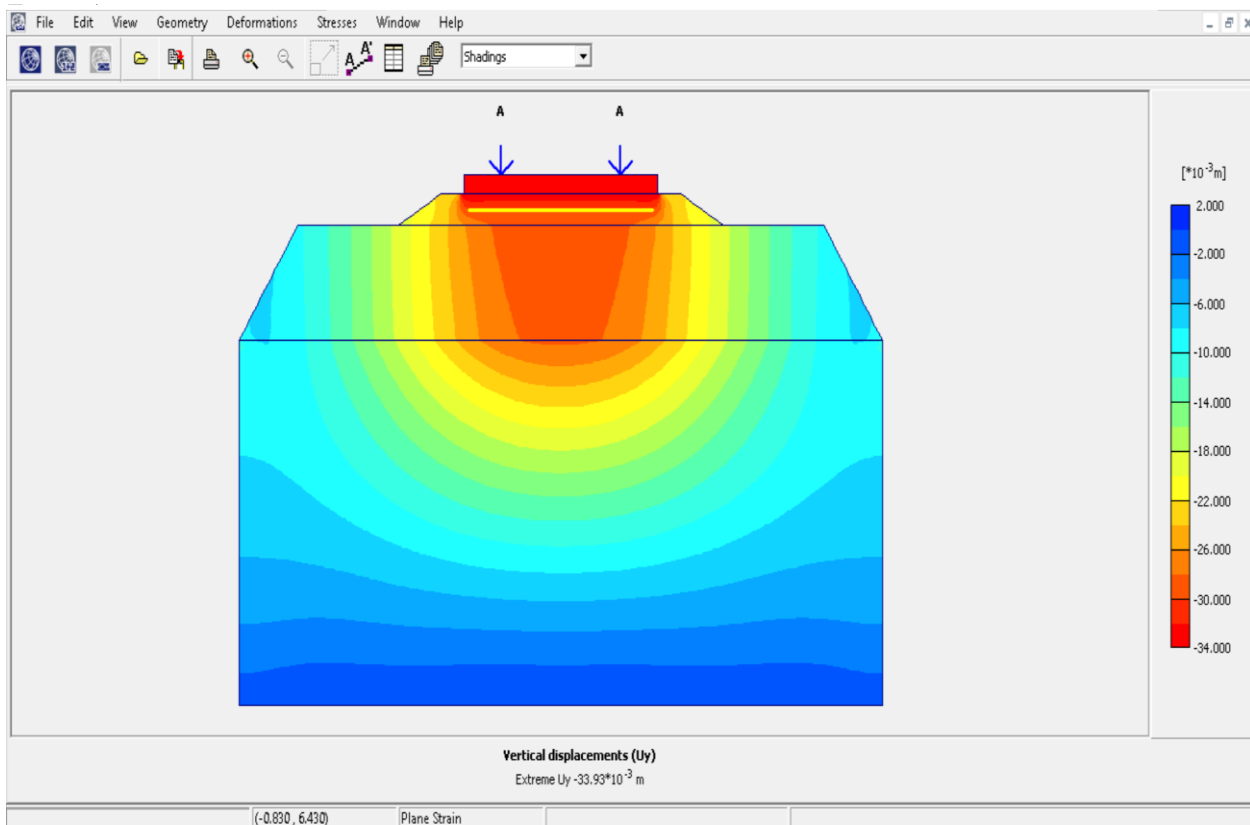


Figure 4.4 Subgrade Vertical Displacement in 2-D Model with Geocell Confinement Width 2.6m.

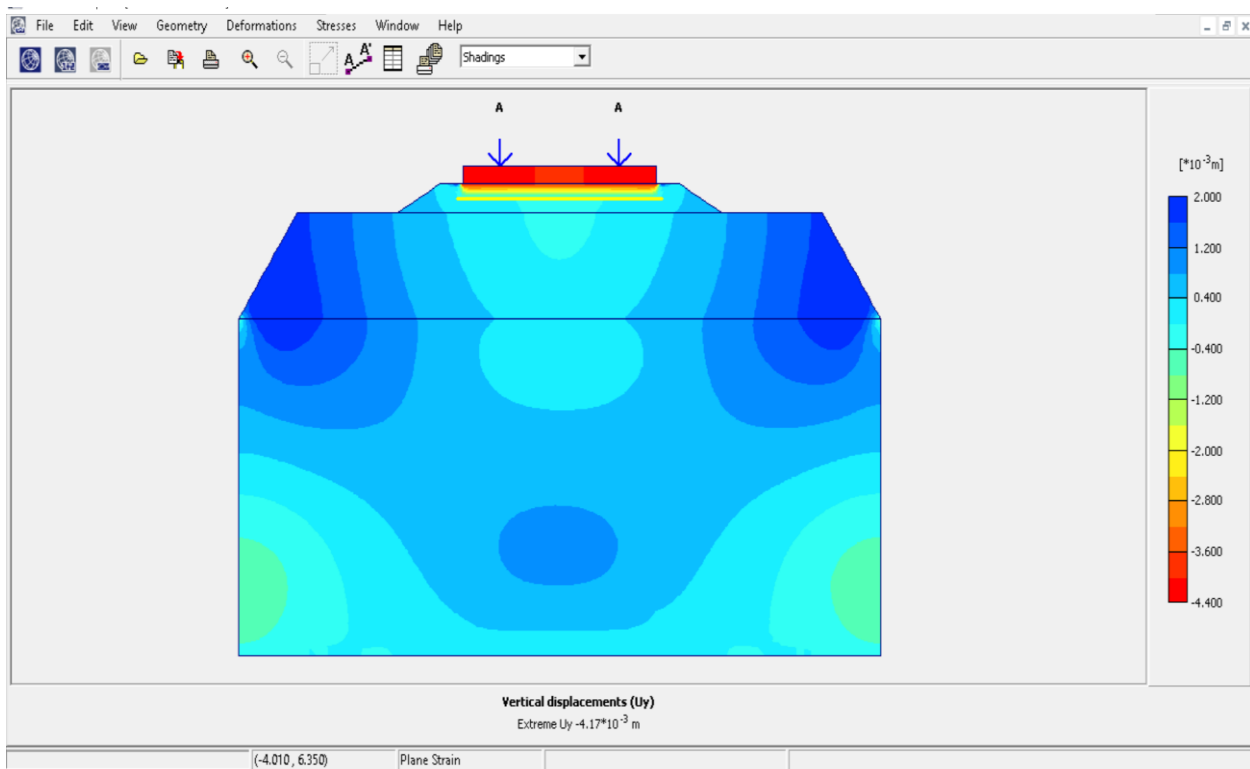


Figure 4.5 Subgrade Vertical Displacement in 2-D Model with Geocell Confinement Width 2.9m.

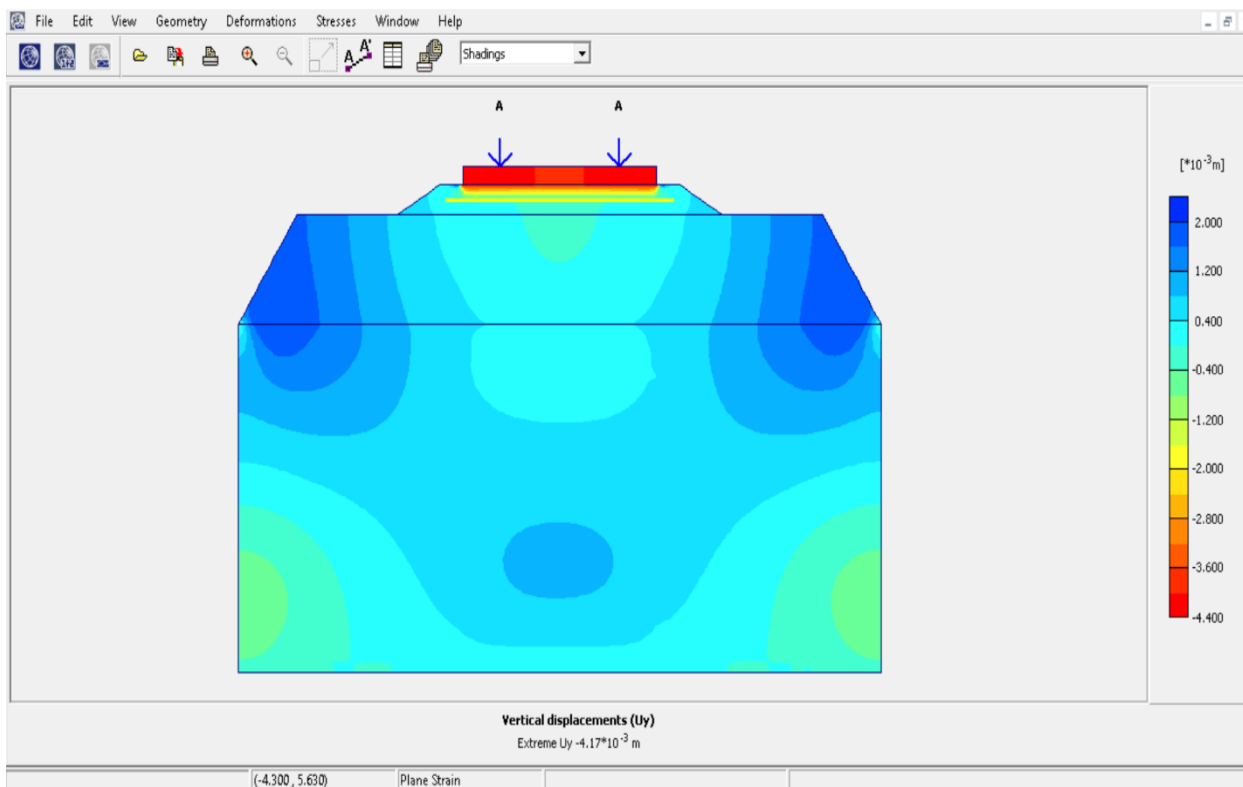


Figure 4.6 Subgrade Vertical Displacement in 2-D Model with Geocell Confinement Width 3.2m.

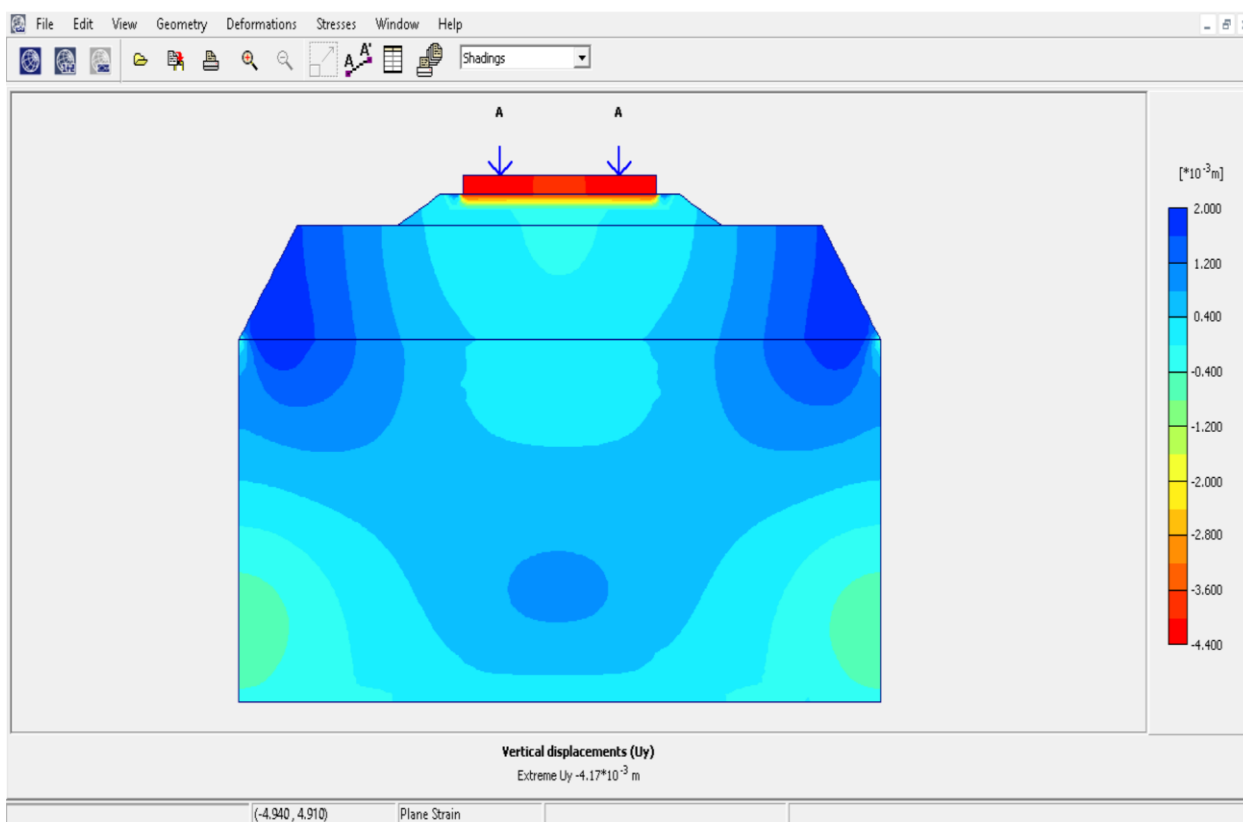


Figure 4.7 Subgrade Vertical Displacement in 2-D Model with Geocell Confinement Width 3.5m.

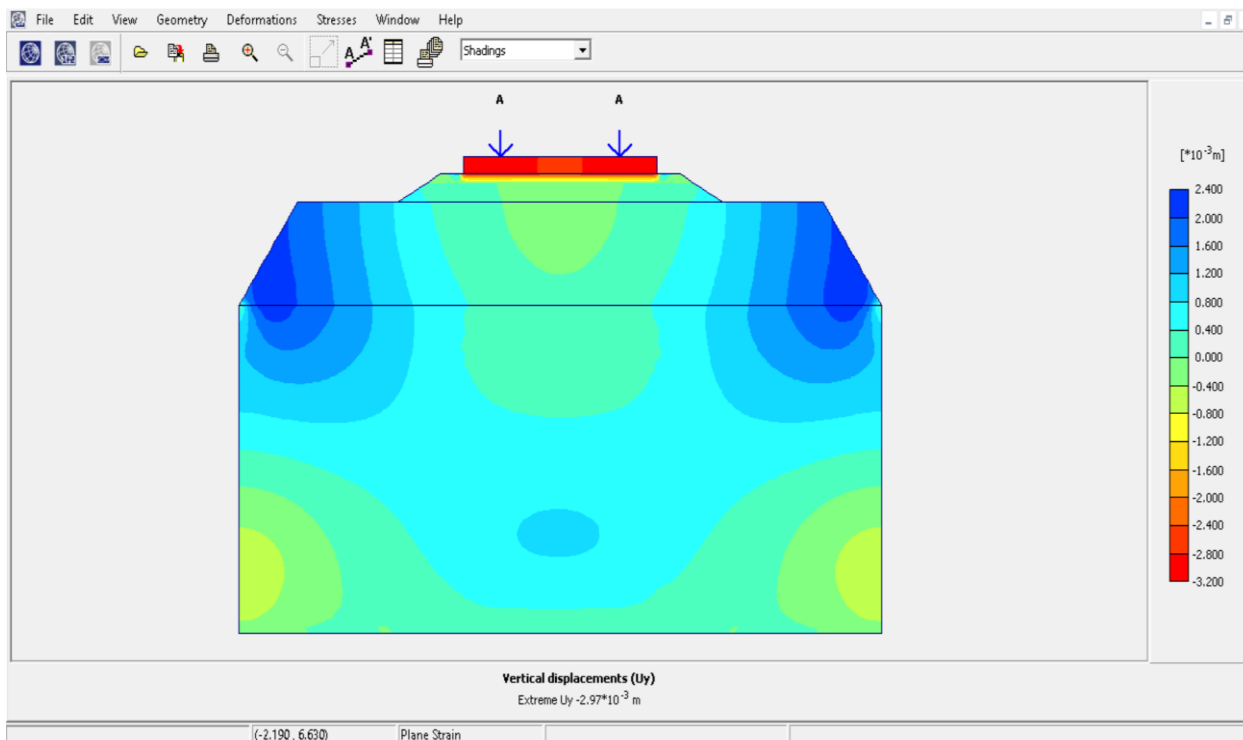


Figure 4.8 Subgrade Vertical Displacement in 2-D Model with Geocell Confinement Width 3.8m.

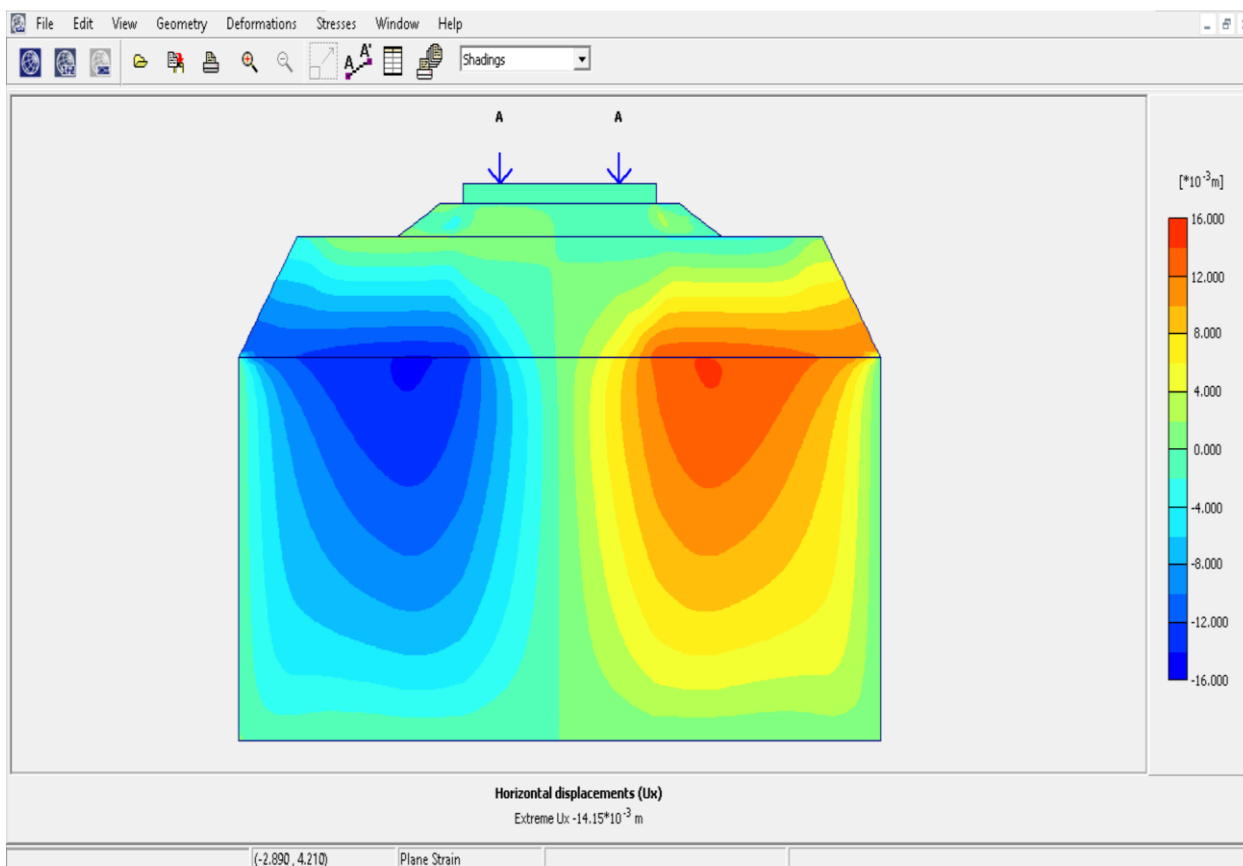


Figure 4.9 Subgrade Horizontal Displacement in 2-D Model with Unreinforced Ballast.

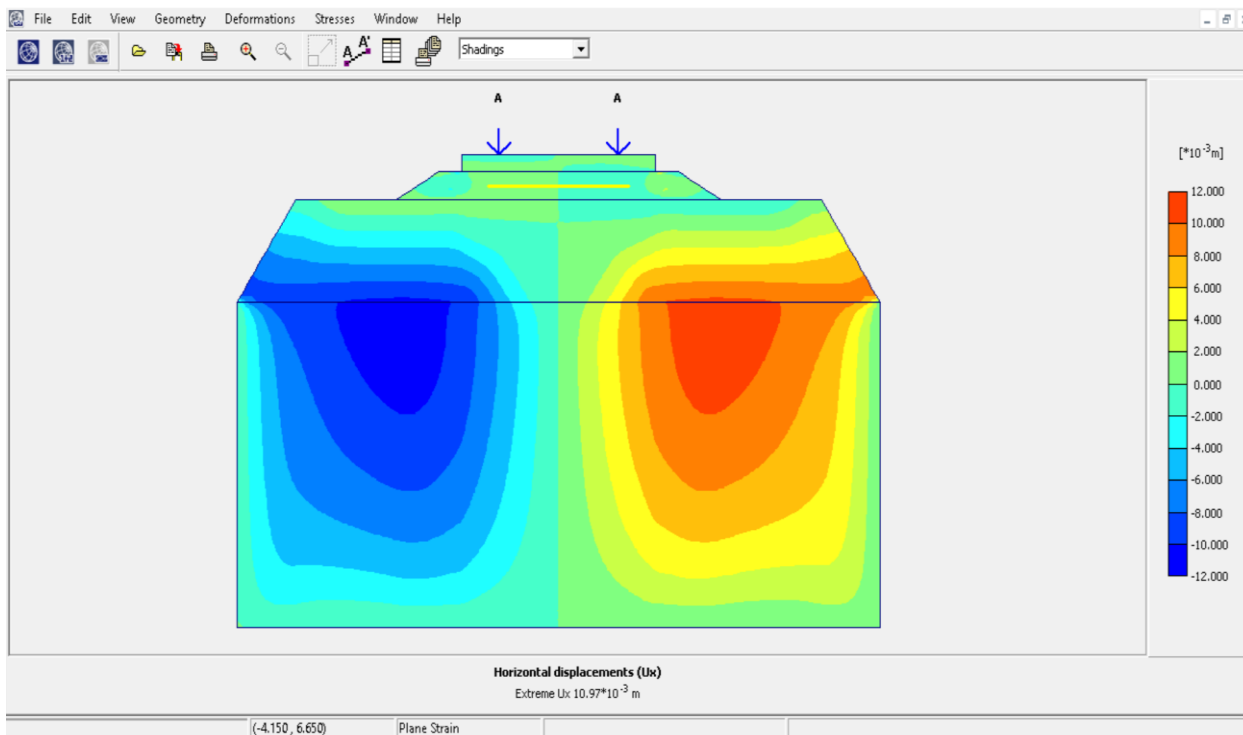


Figure 4.10 Subgrade Horizontal Displacement in 2-D Model with Geocell Confinement Width 2.0m.

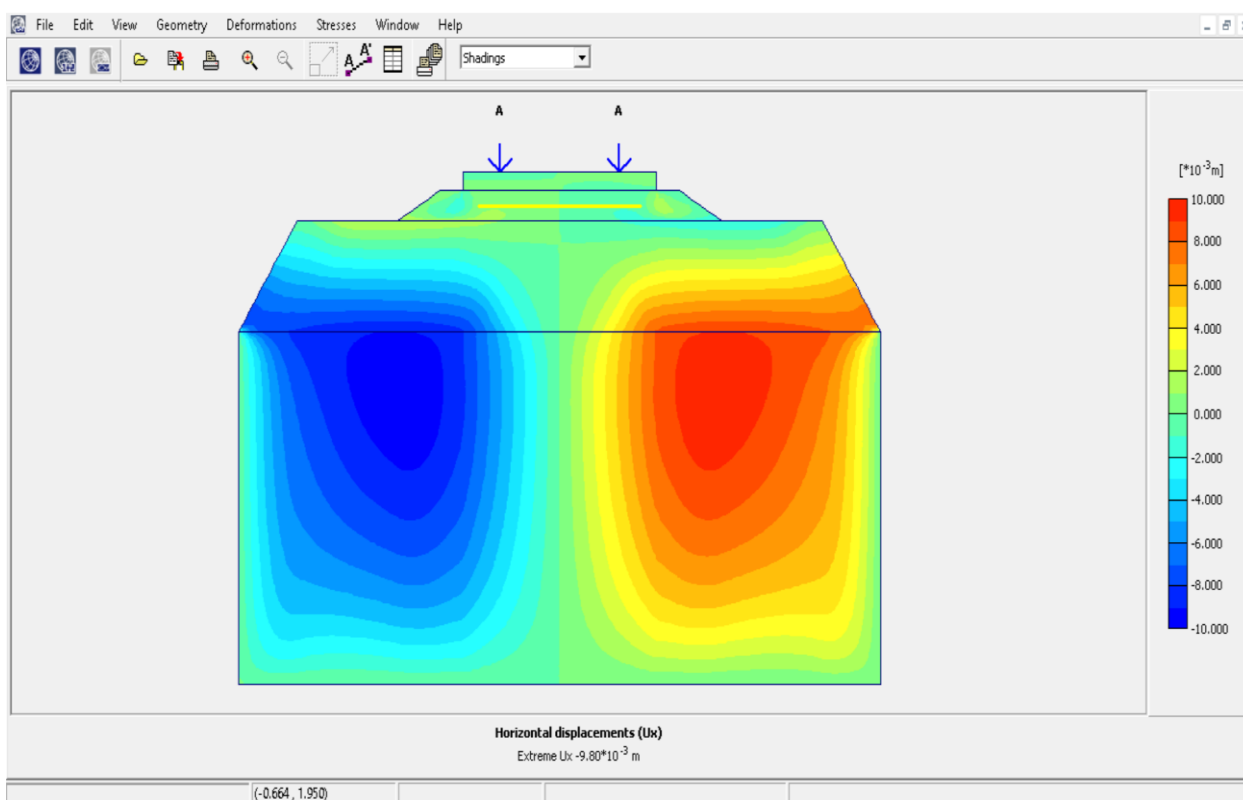


Figure 4.11 Subgrade Horizontal Displacement in 2-D Model with Geocell Confinement Width 2.3m.



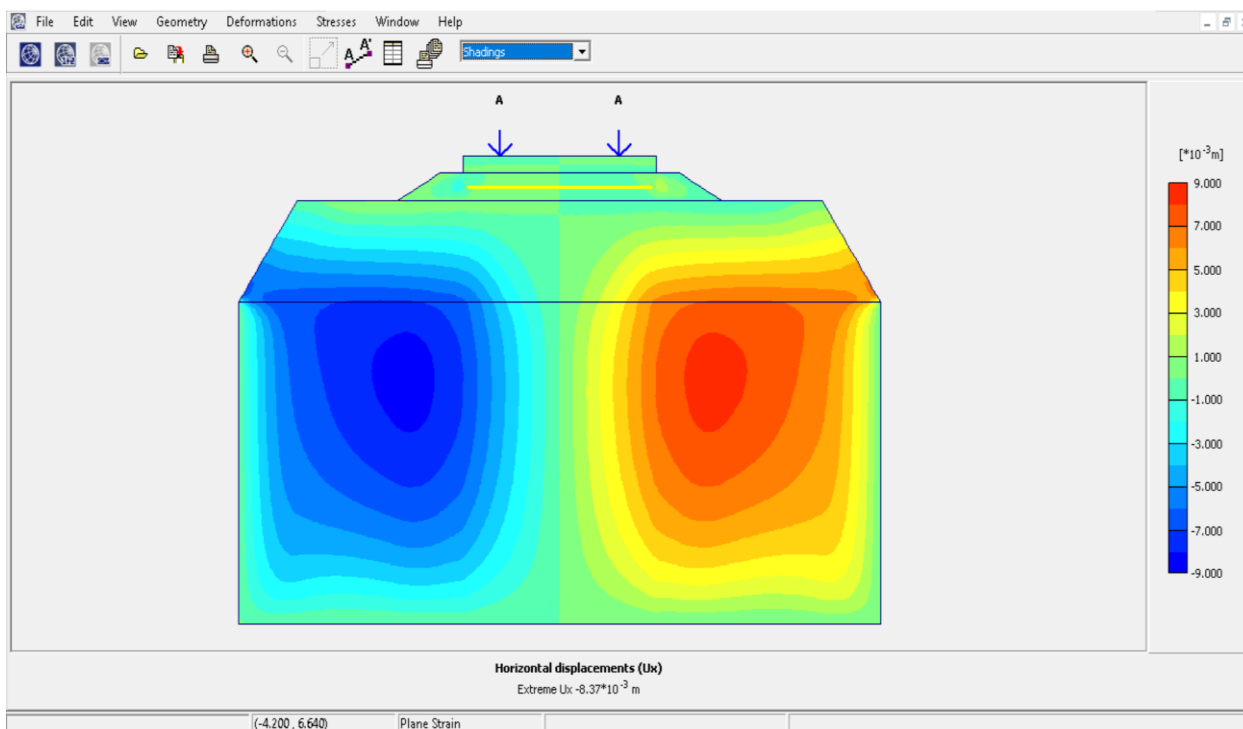


Figure 4.12 Subgrade Horizontal Displacement in 2-D Model with Geocell Confinement Width 2.6m.

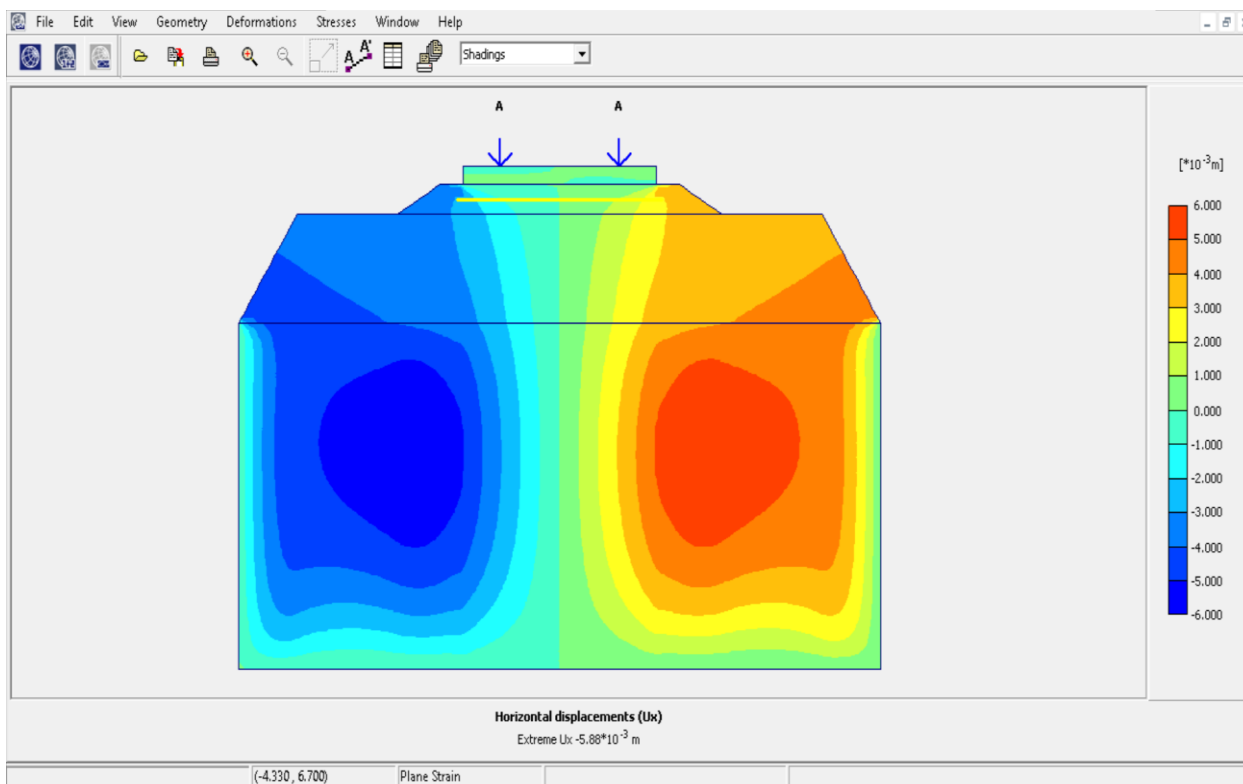


Figure 4.13 Subgrade Horizontal Displacement in 2-D Model with Geocell Confinement Width 2.9m.

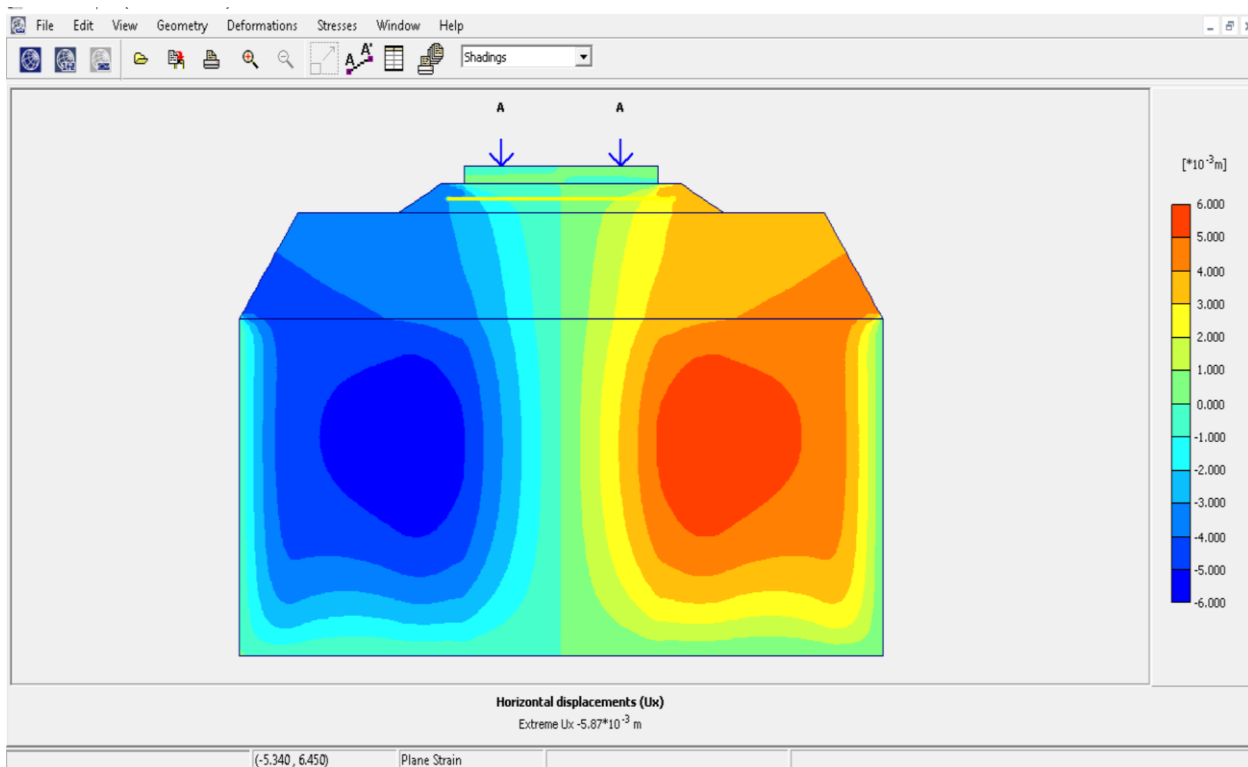


Figure 4.14 Subgrade Horizontal Displacement in 2-D Model with Geocell Confinement Width 3.2m.

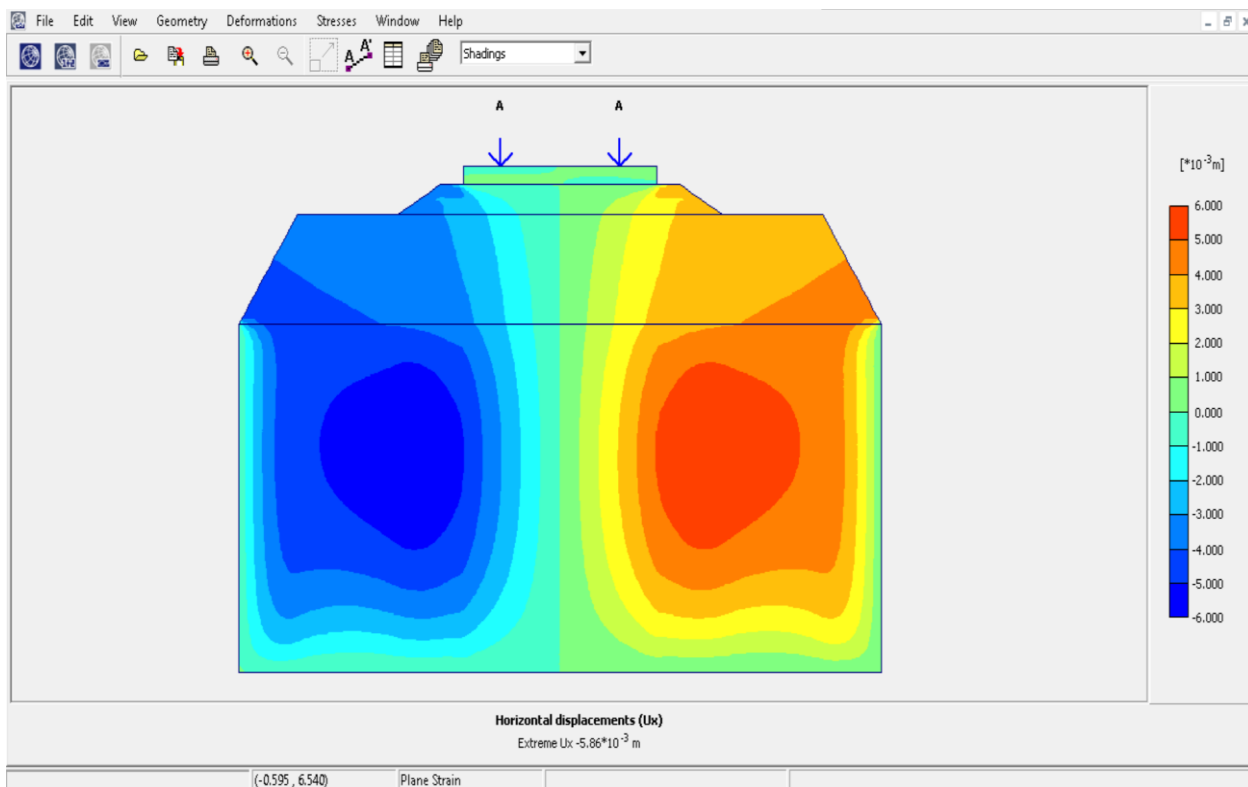


Figure 4.15 Subgrade Horizontal Displacement in 2-D Model with Geocell Confinement Width 3.5m.

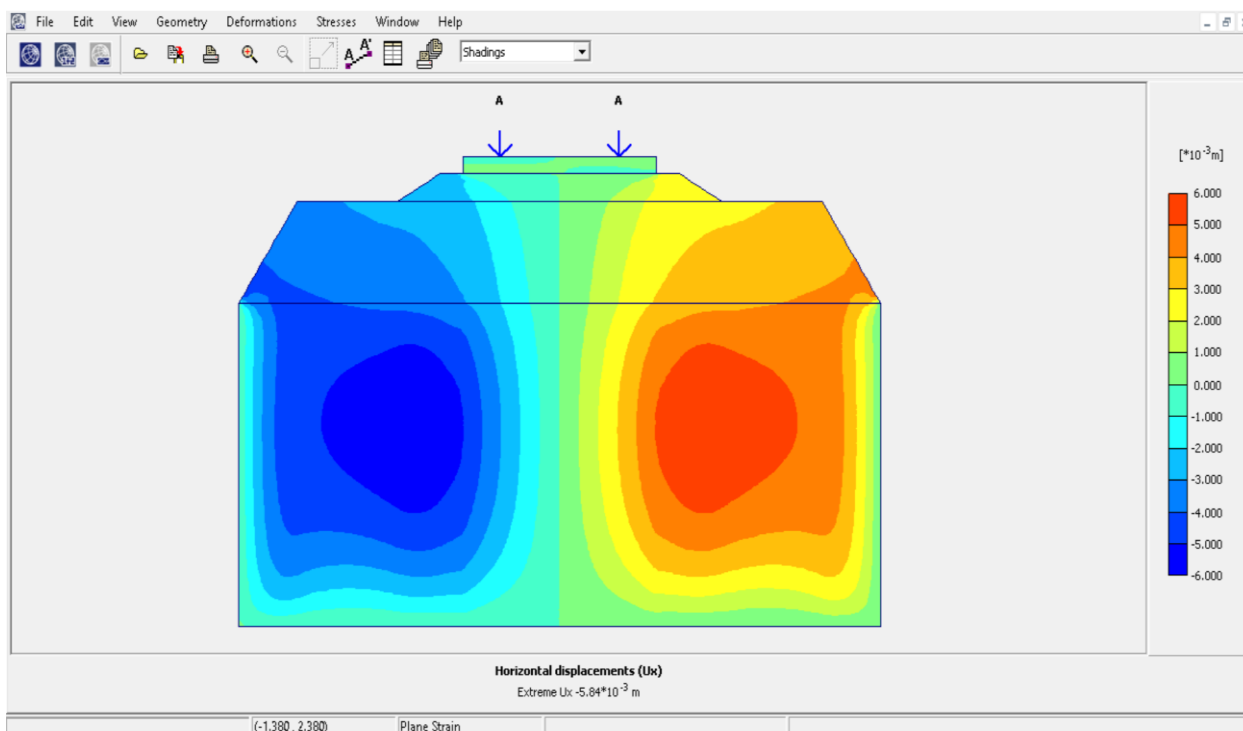


Figure 4.16 Subgrade Horizontal Displacement in 2-D Model with Geocell Confinement Width 3.8m.

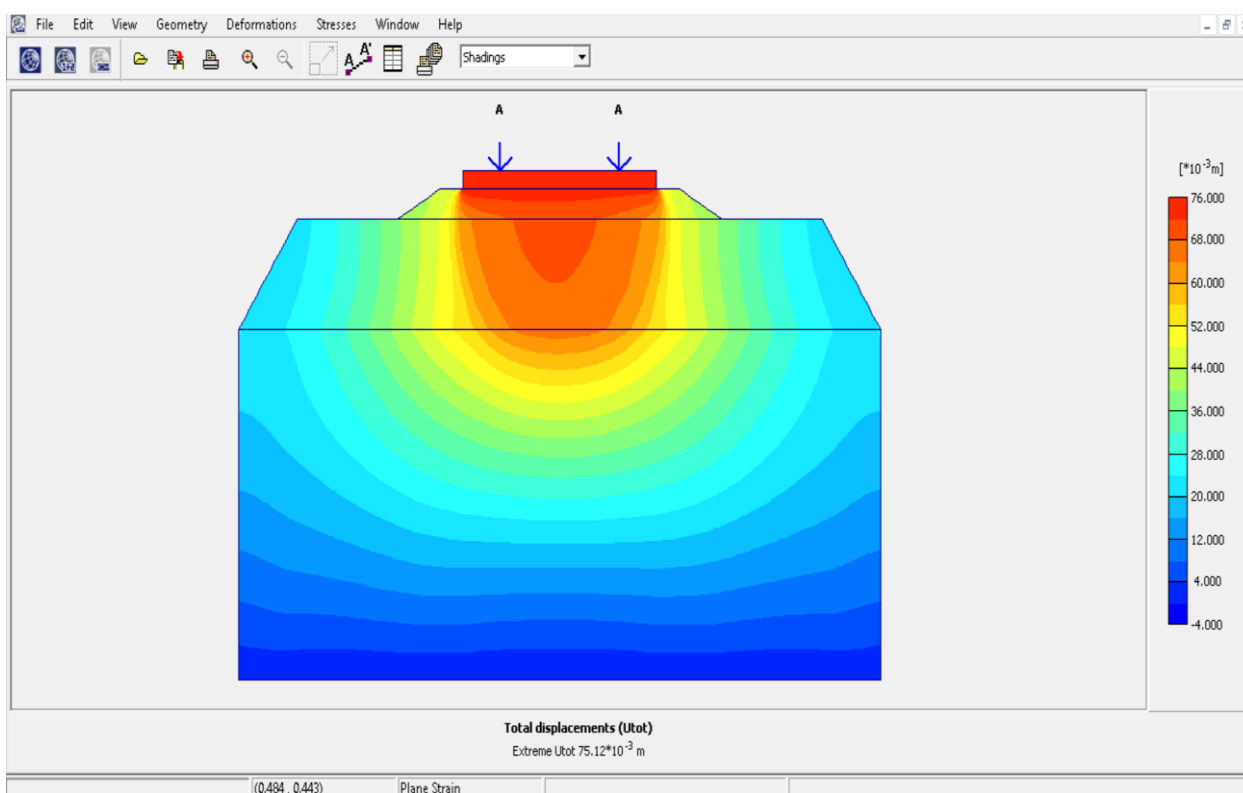


Figure 4.17 Subgrade Total Displacement in 2-D Model with Unreinforced Ballast.

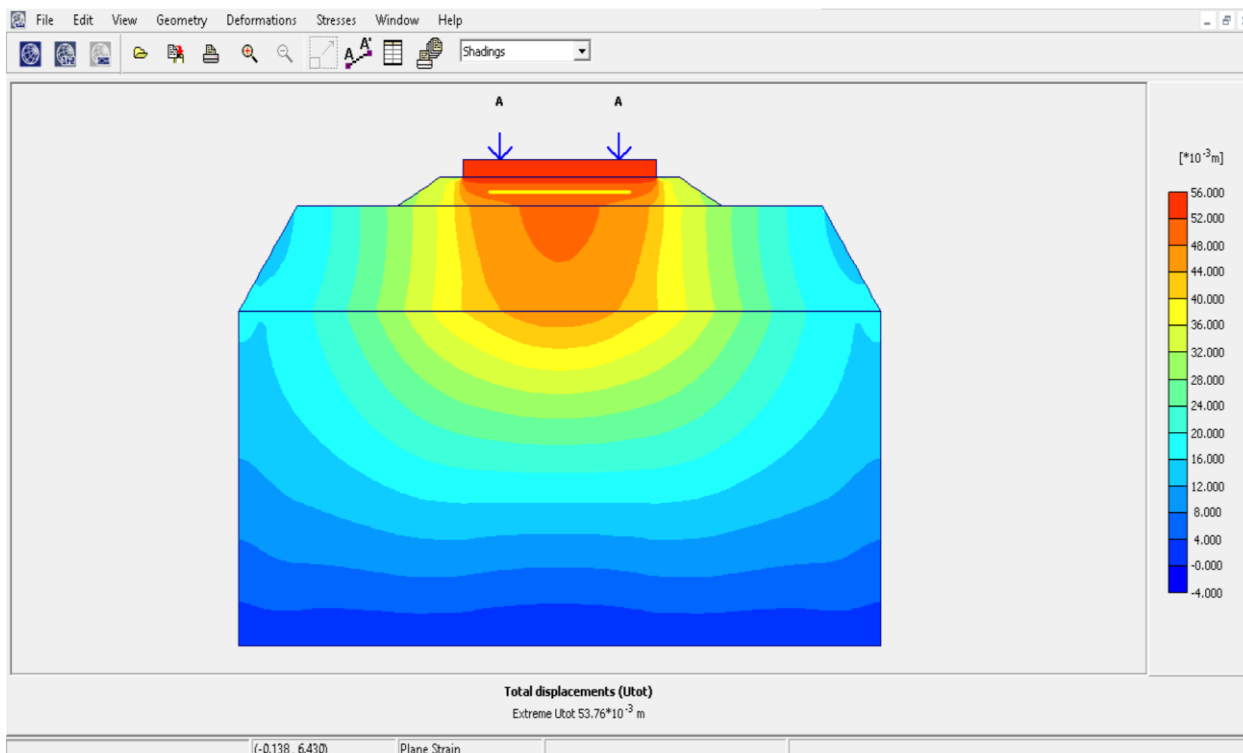


Figure 4.18 Subgrade Total Displacement in 2-D Model with Geocell Confinement Width 2.0m.

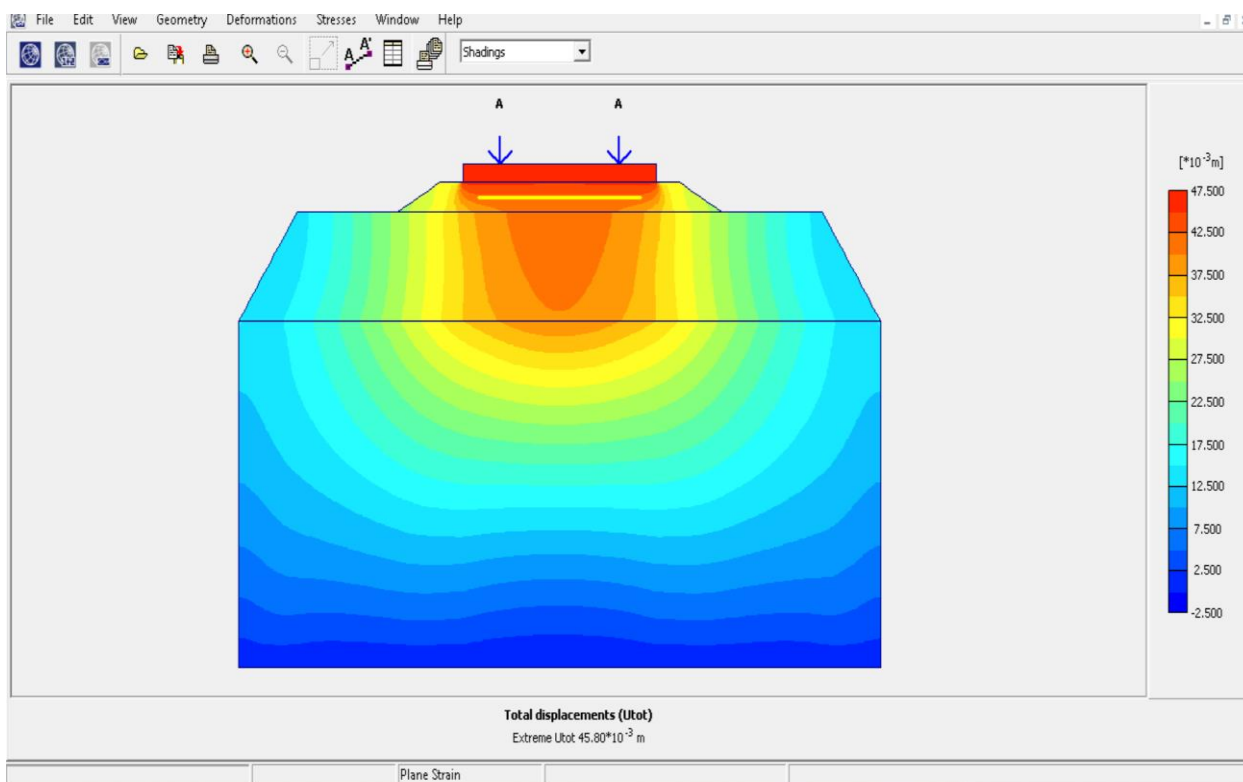


Figure 4.19 Subgrade Total Displacement in 2-D Model with Geocell Confinement Width 2.3m.

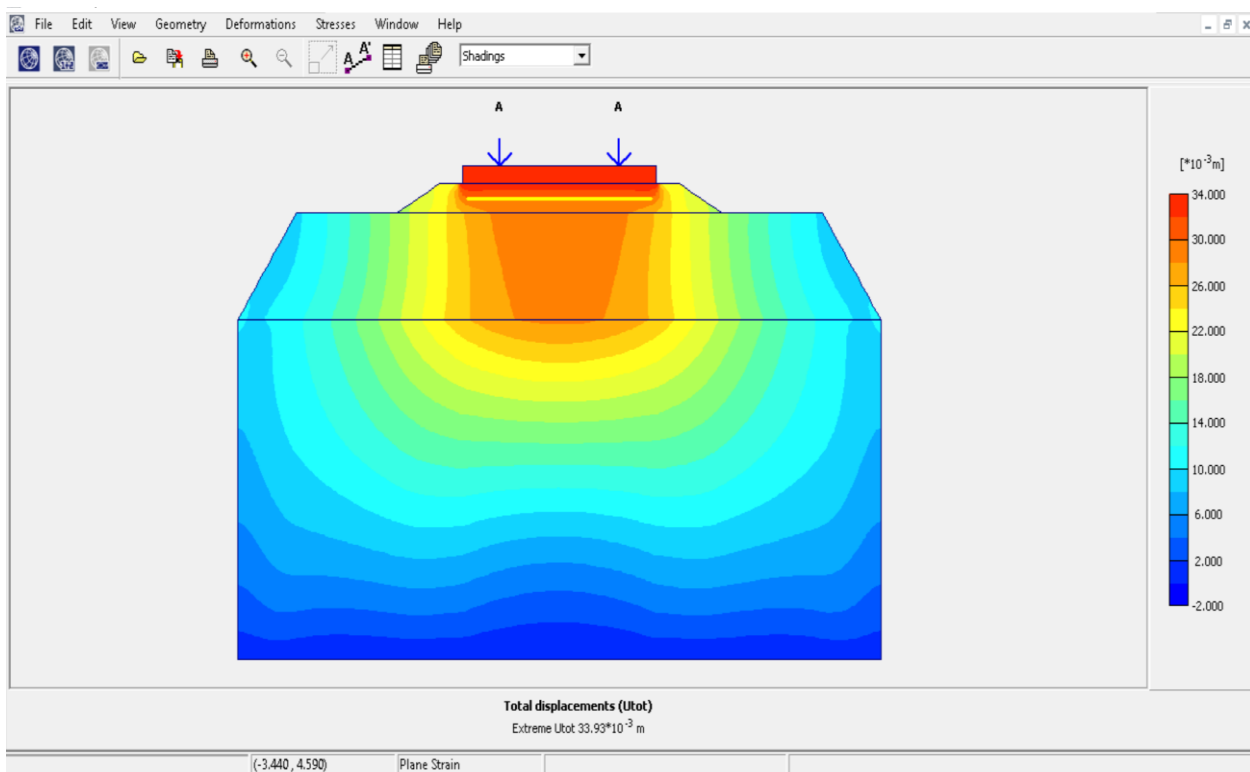


Figure 4.20 Subgrade Total Displacement in 2-D Model with Geocell Confinement Width 2.6m.

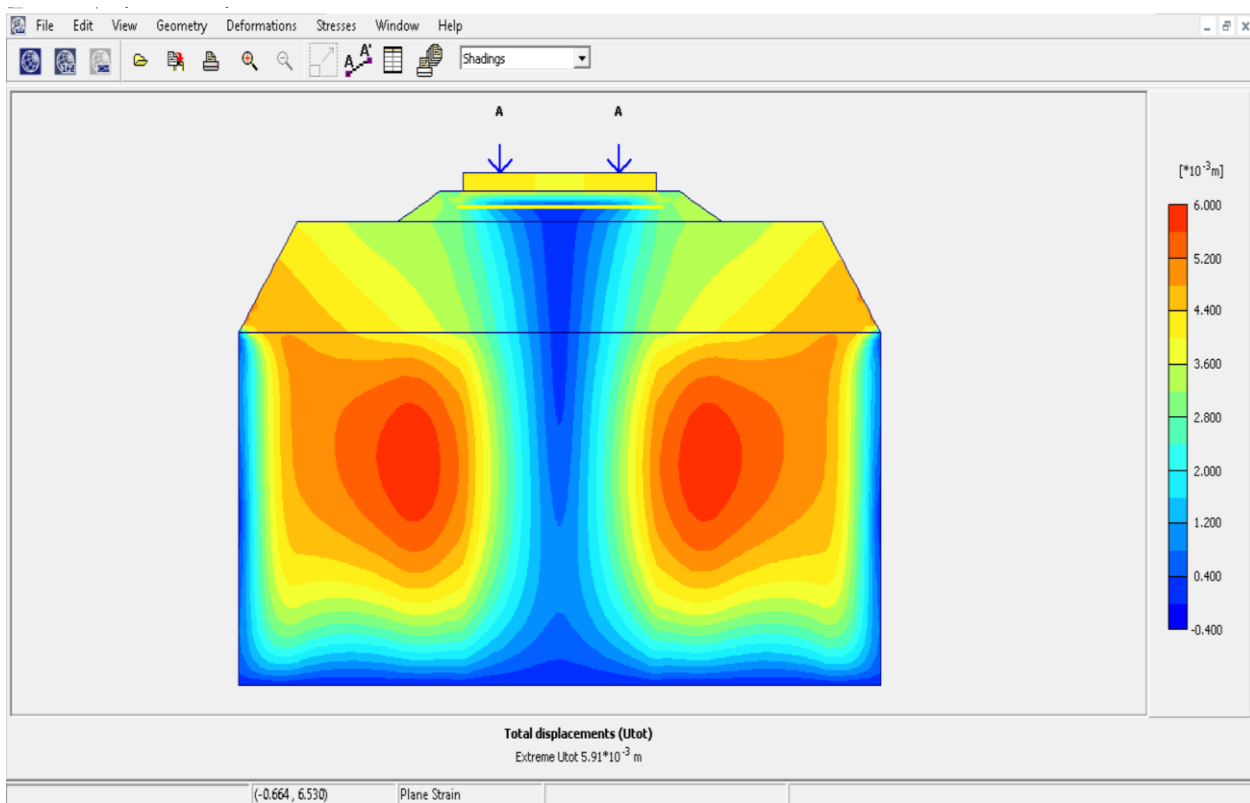


Figure 4.21 Subgrade Total Displacement in 2-D Model with Geocell Confinement Width 2.9m.

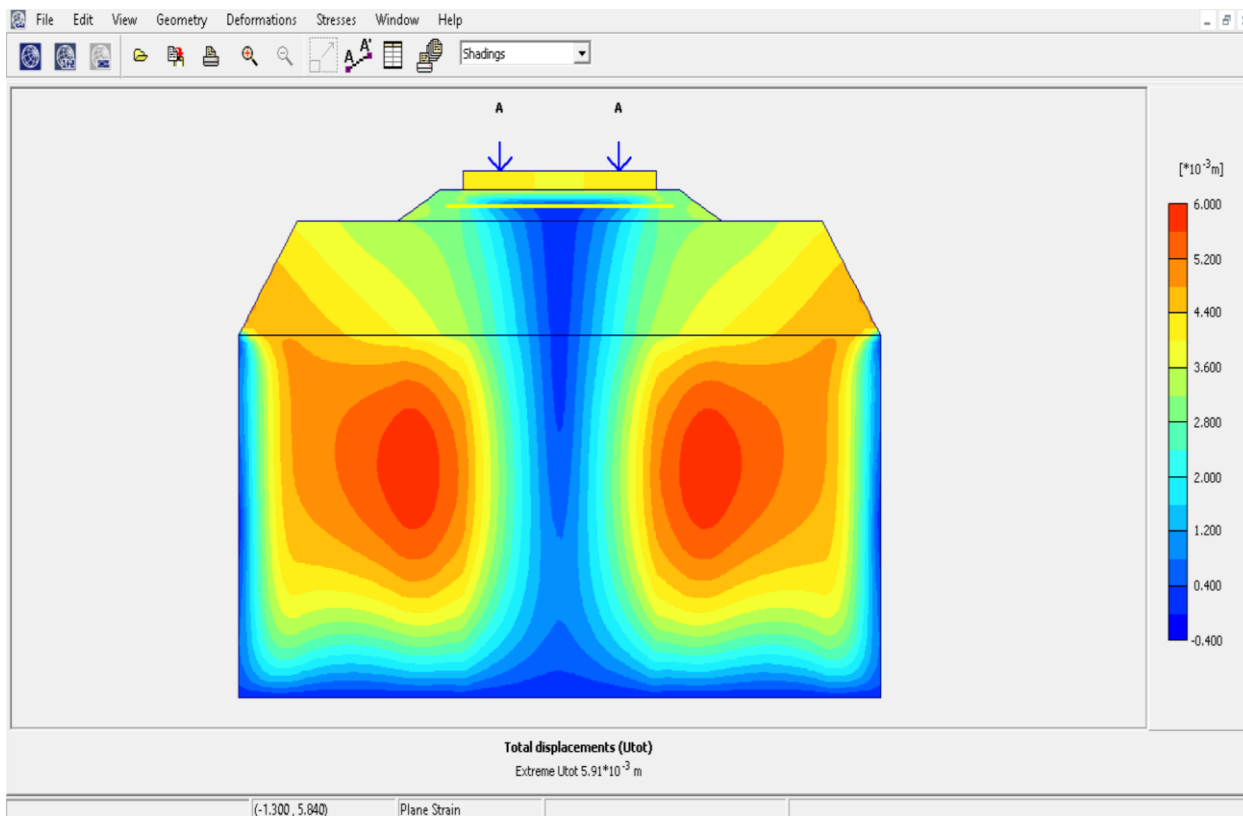


Figure 4.22 Subgrade Total Displacement in 2-D Model with Geocell Confinement Width 3.2m.

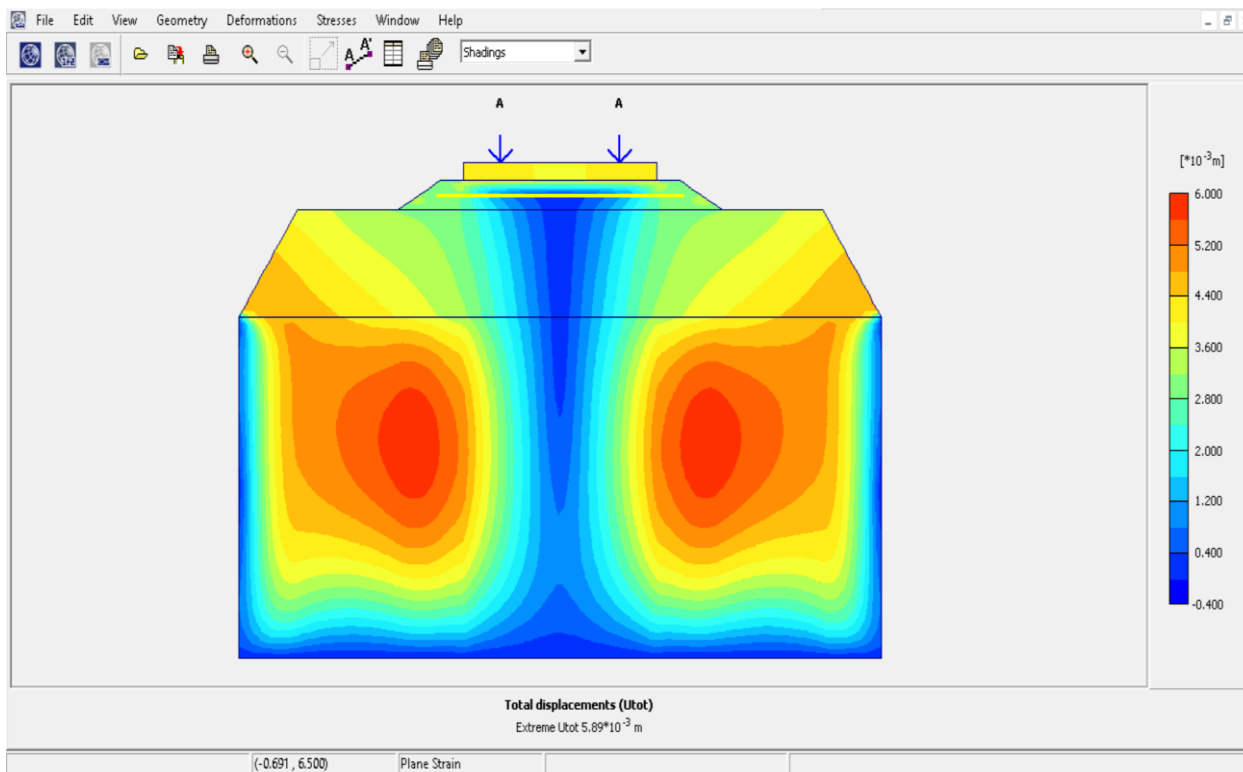


Figure 4.23 Subgrade Total Displacement in 2-D Model with Geocell Confinement Width 3.5m.

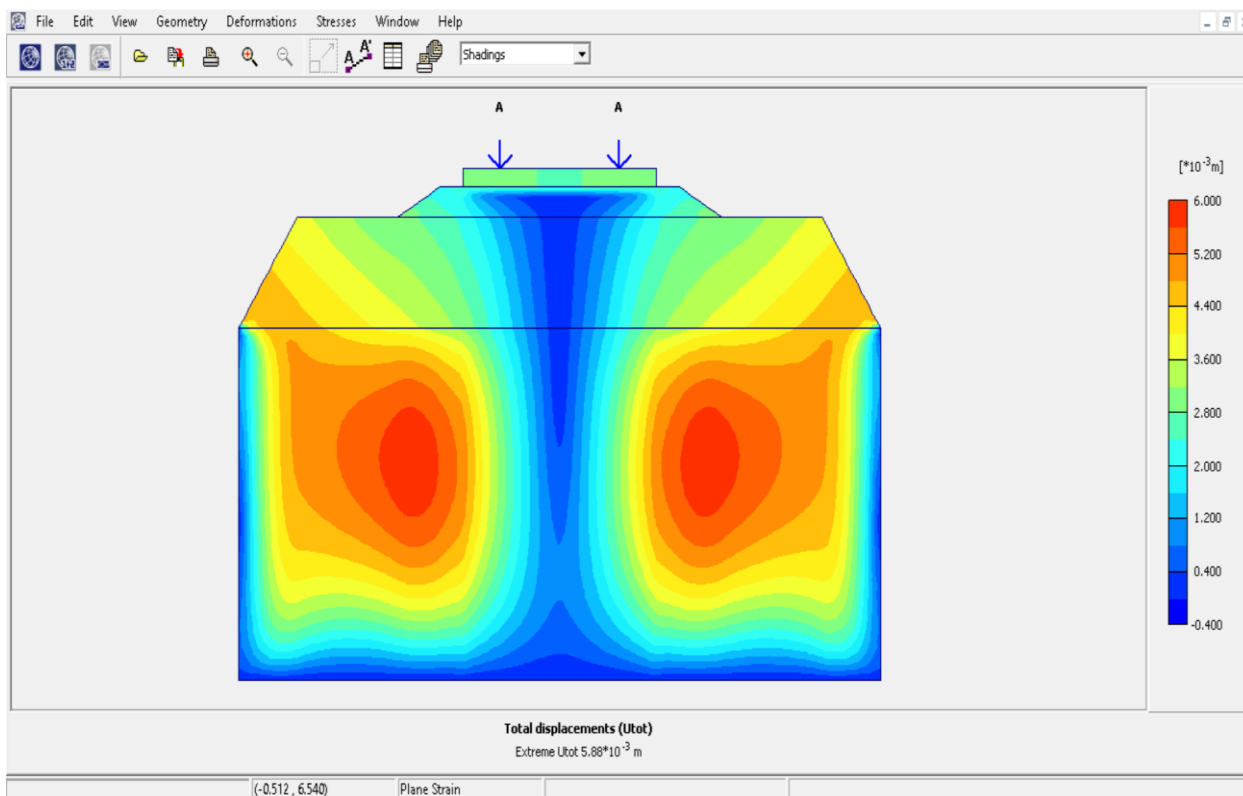


Figure 4.24 Subgrade Total Displacement in 2-D Model with Geocell Confinement Width 3.8m.

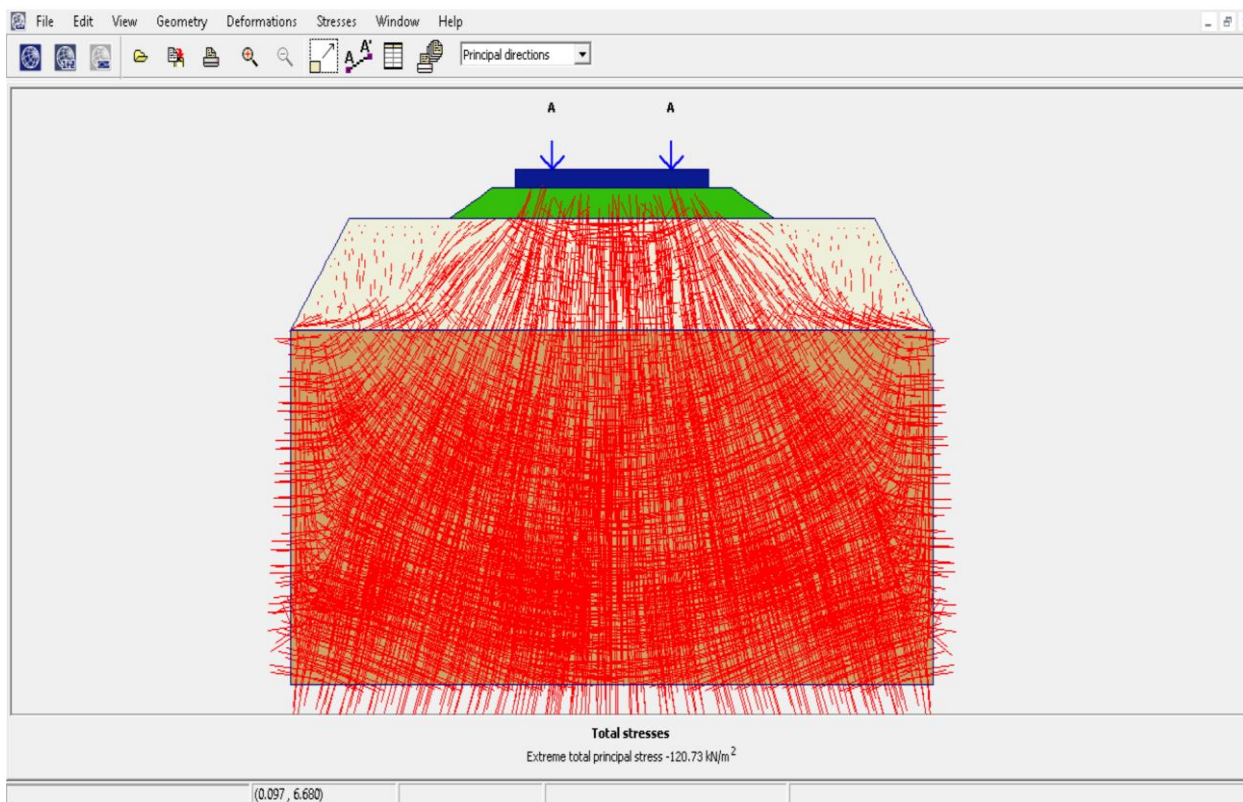


Figure 4.25 Subgrade Mean Stresses in 2-D Model with Unreinforced Ballast.



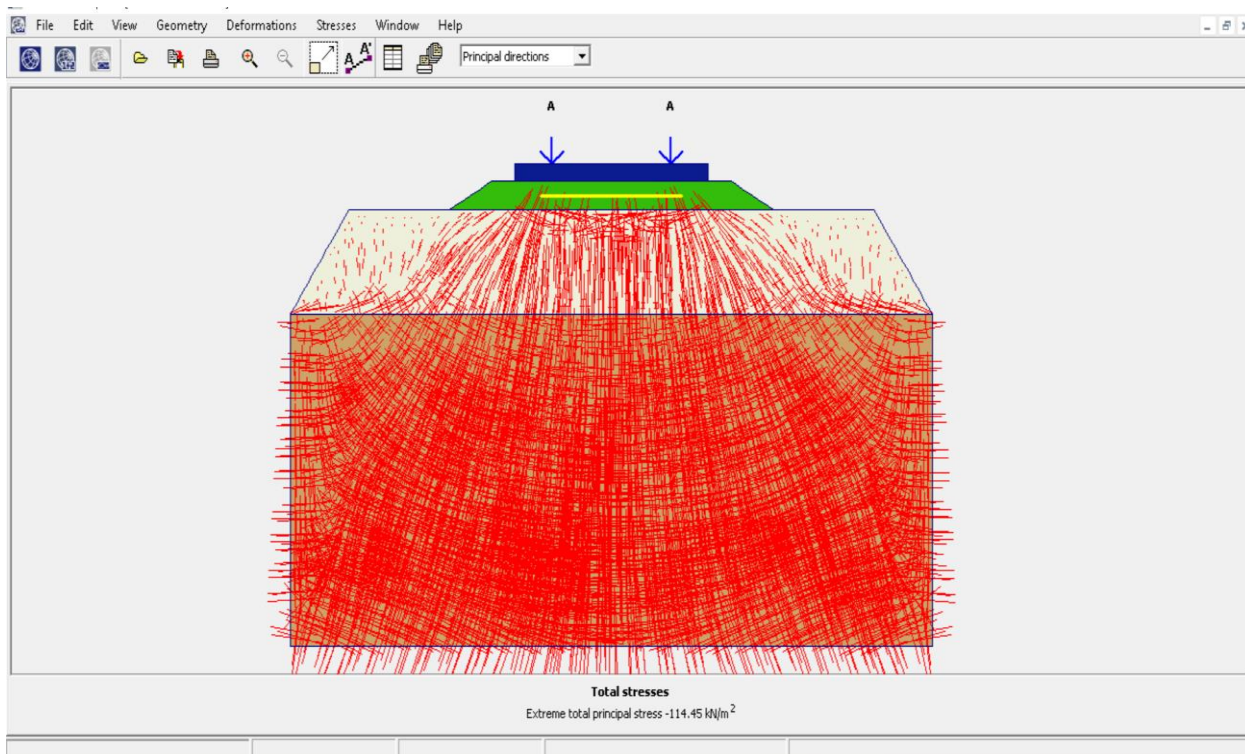


Figure 4.26 Subgrade Mean Stresses in 2-D Model with Geocell Confinement Width 2.0m.

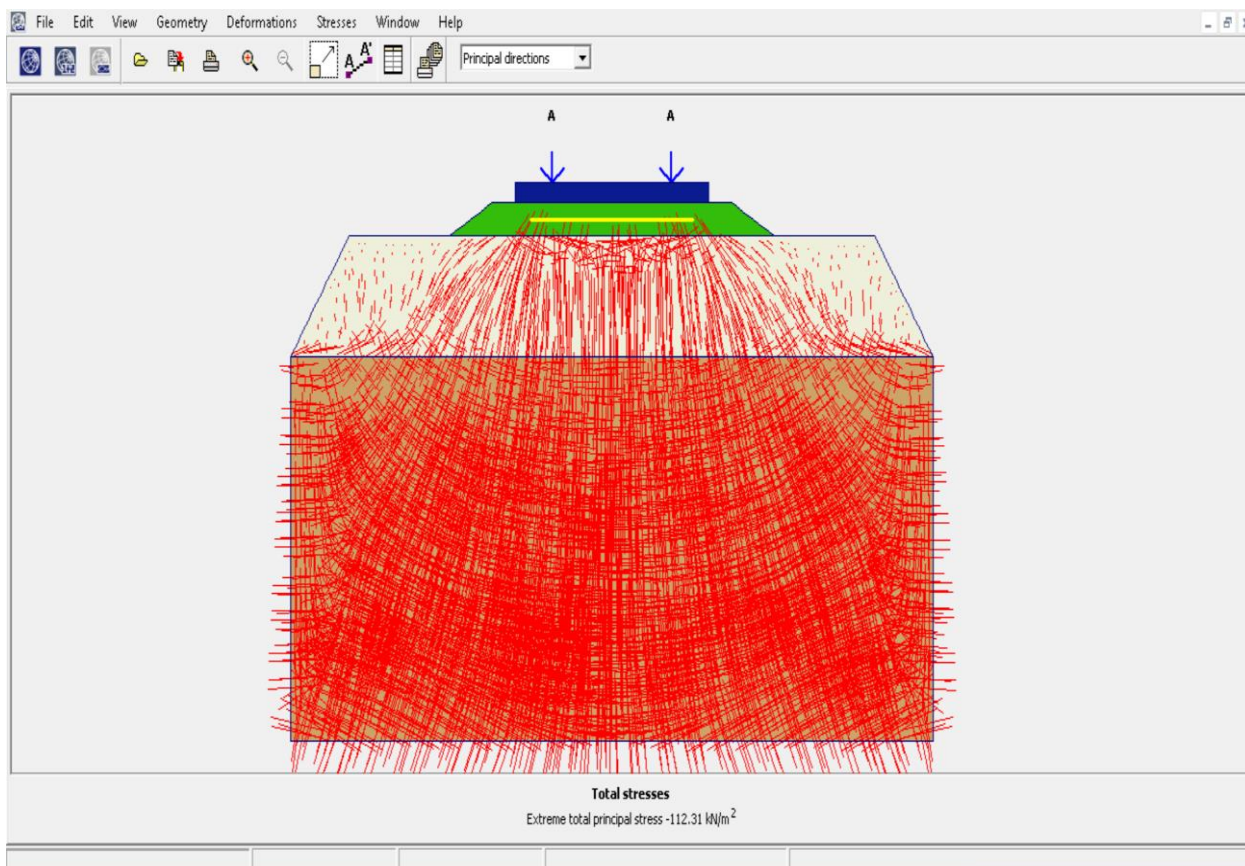


Figure 4.27 Subgrade Mean Stresses in 2-D Model with Geocell Confinement Width 2.3m.



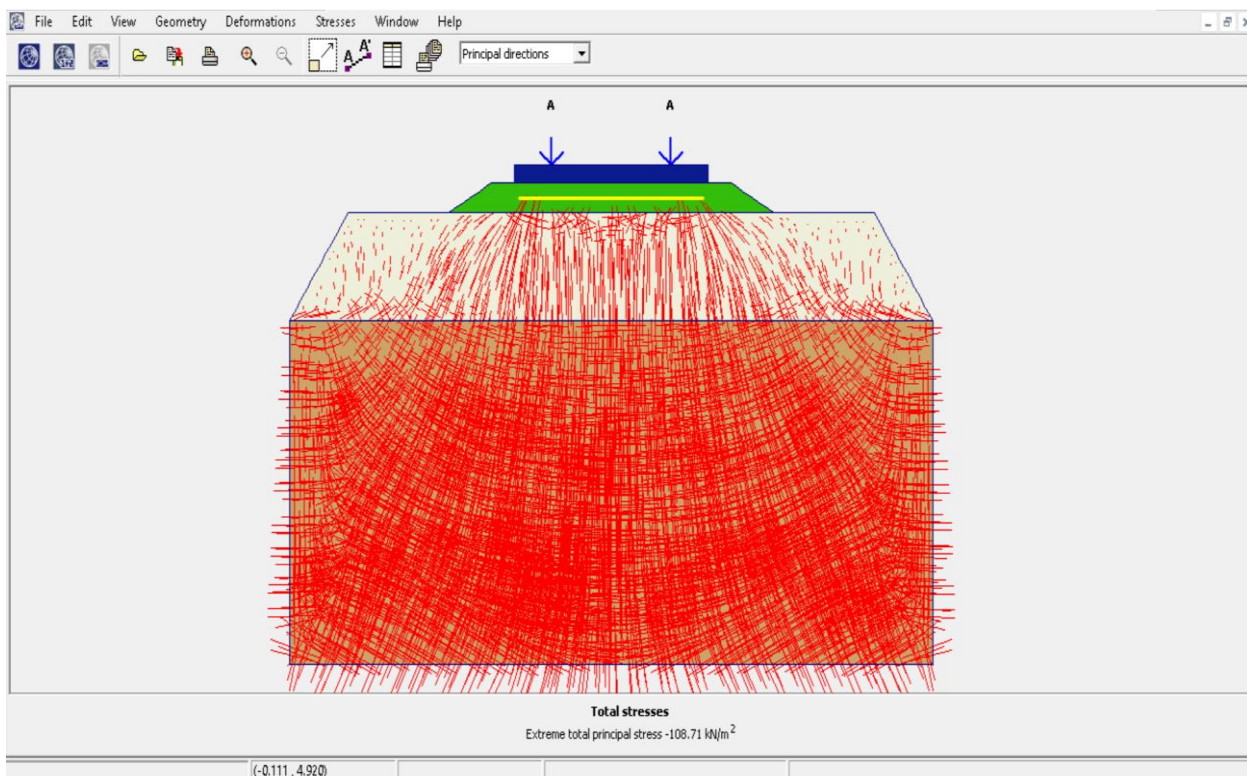


Figure 4.28 Subgrade Mean Stresses in 2-D Model with Geocell Confinement Width 2.6m.

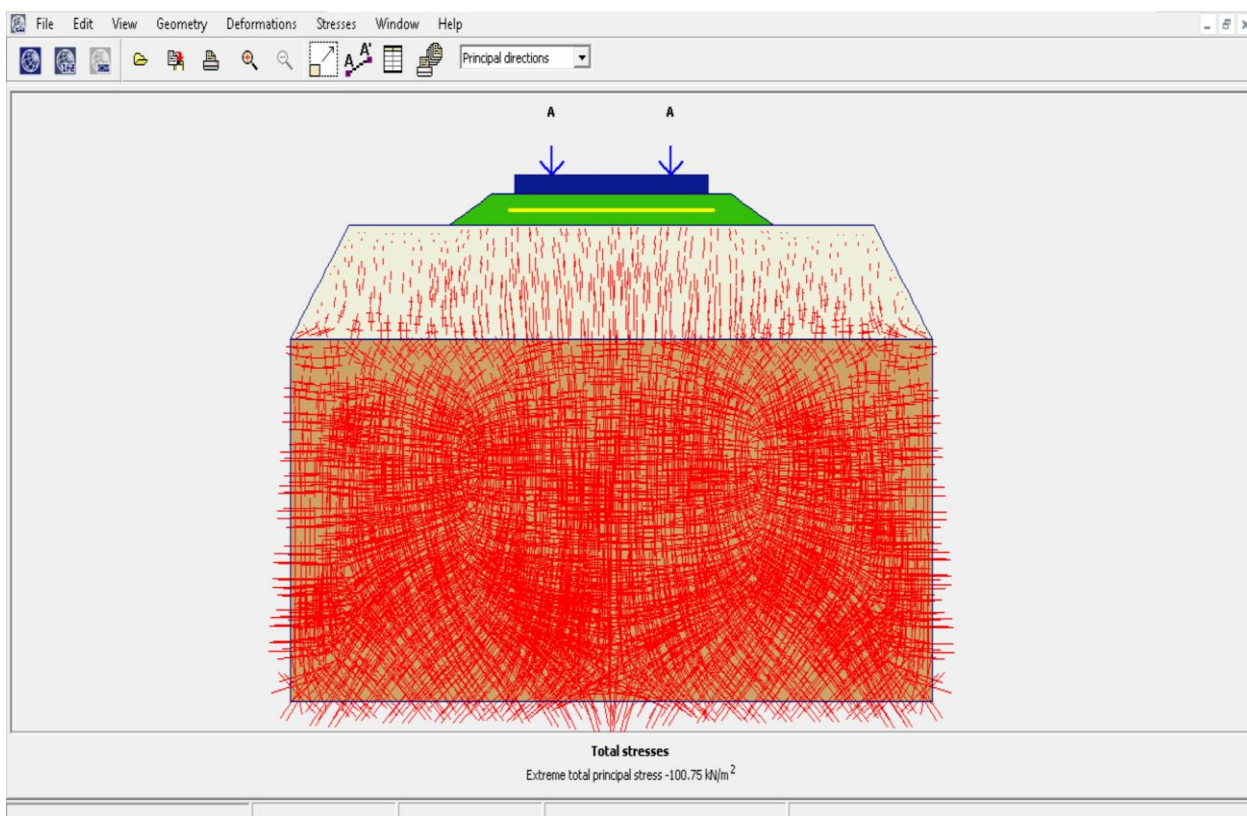


Figure 4.29 Subgrade Mean Stresses in 2-D Model with Geocell Confinement Width 2.9m.

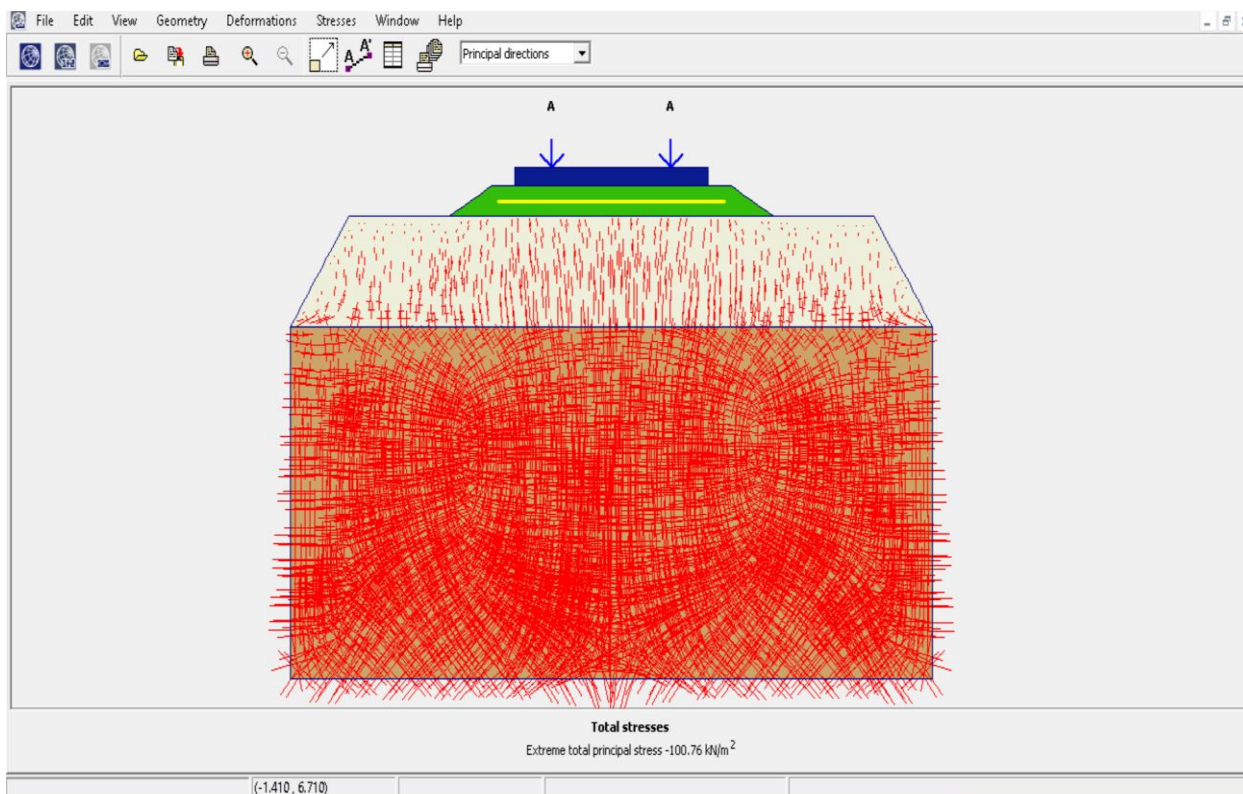


Figure 4.30 Subgrade Mean Stresses in 2-D Model with Geocell Confinement Width 3.2m.

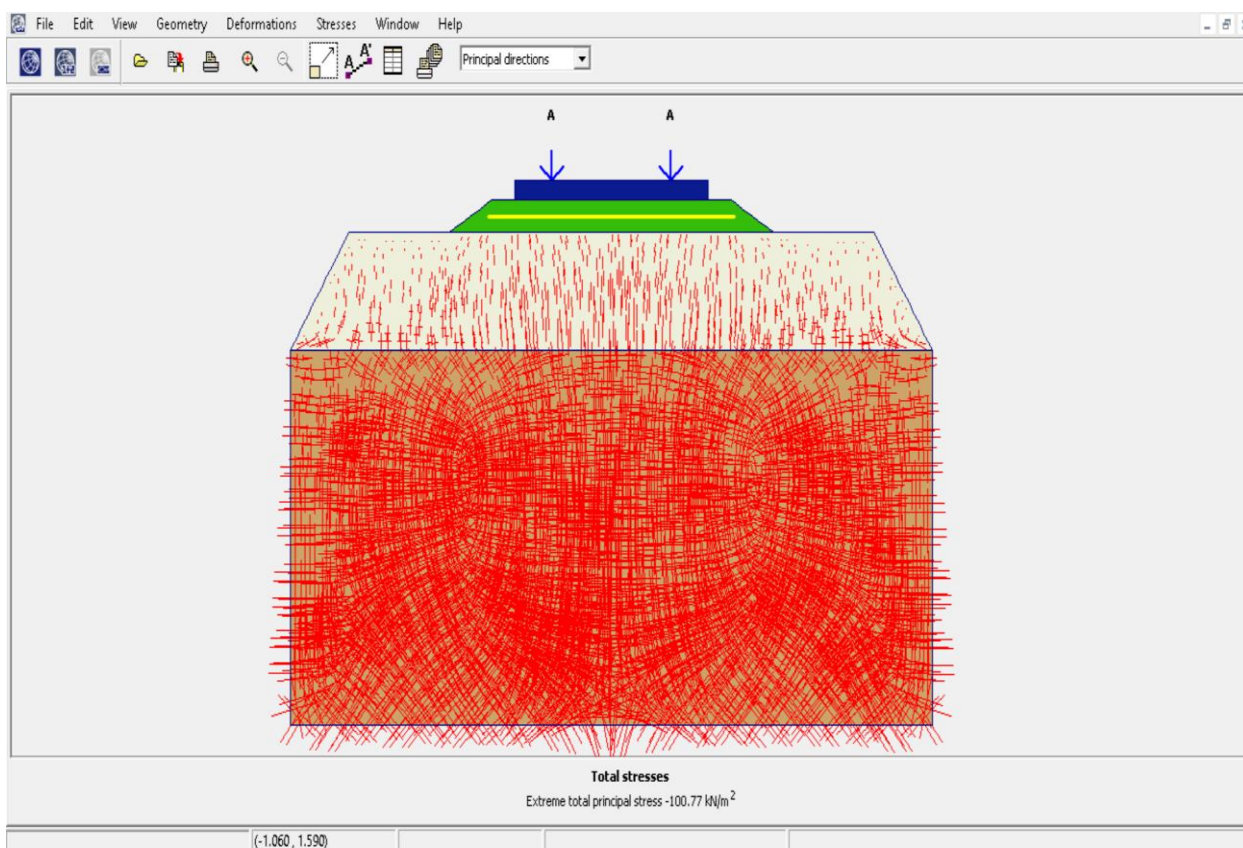


Figure 4.31 Subgrade Mean Stresses in 2-D Model with Geocell Confinement Width 3.5m.



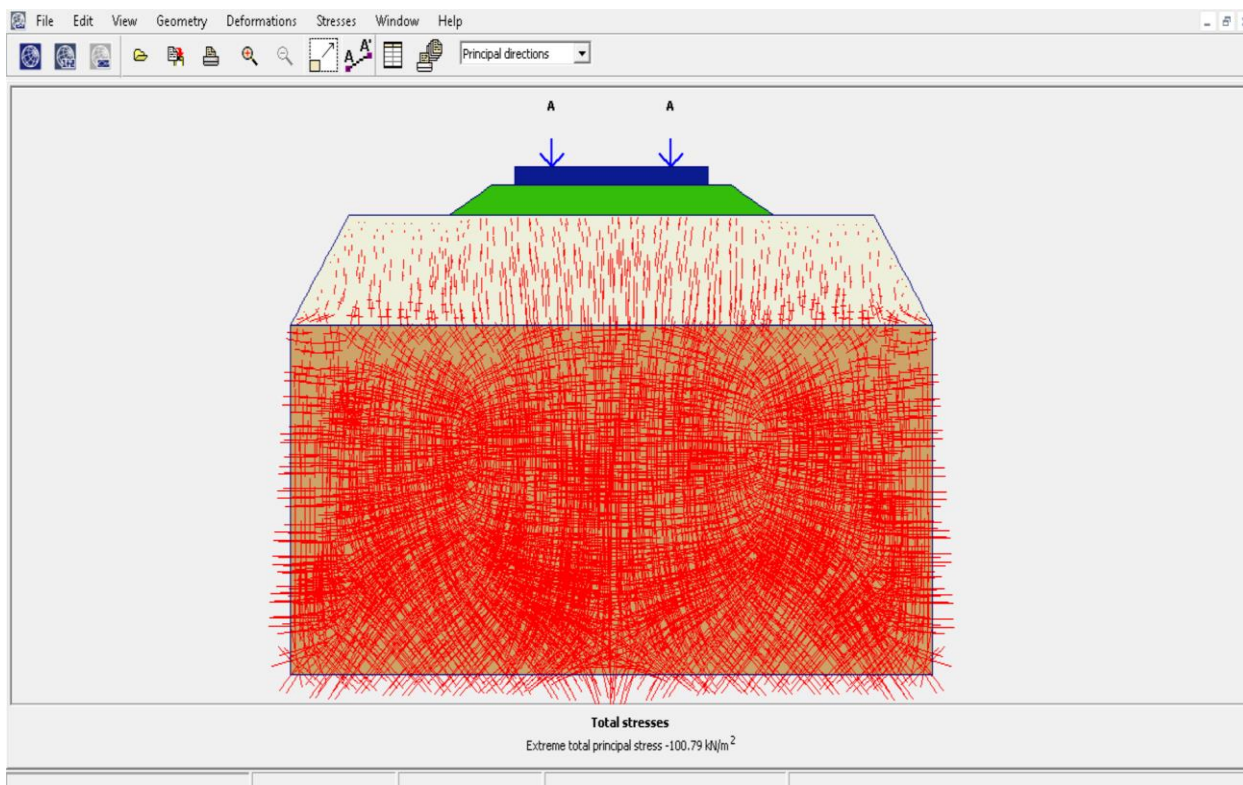


Figure 4.32 Subgrade Mean Stresses in 2-D Model with Geocell Confinement Width 3.8m.

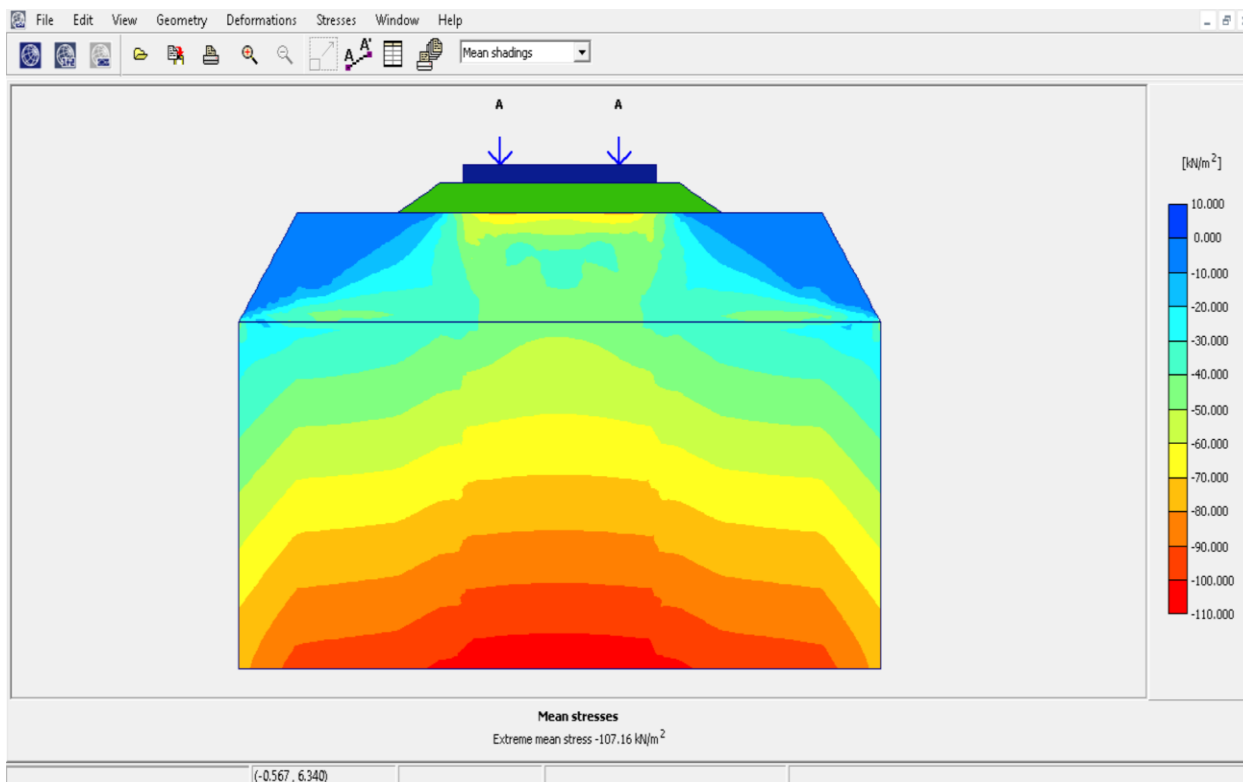


Figure 4.33 Subgrade Total Stresses in 2-D Model with Unreinforced Ballast.

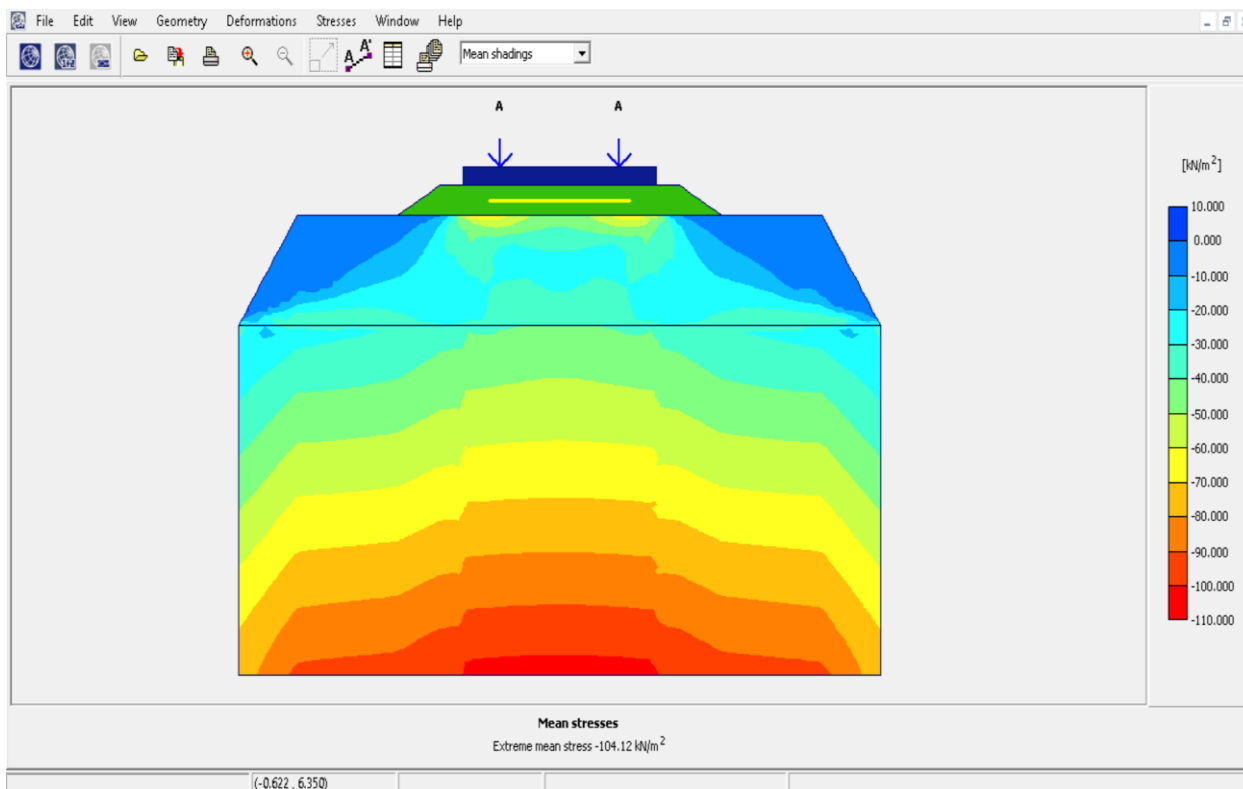


Figure 4.34 Subgrade Total Stresses in 2-D Model with Geocell Confinement Width 2.0m.

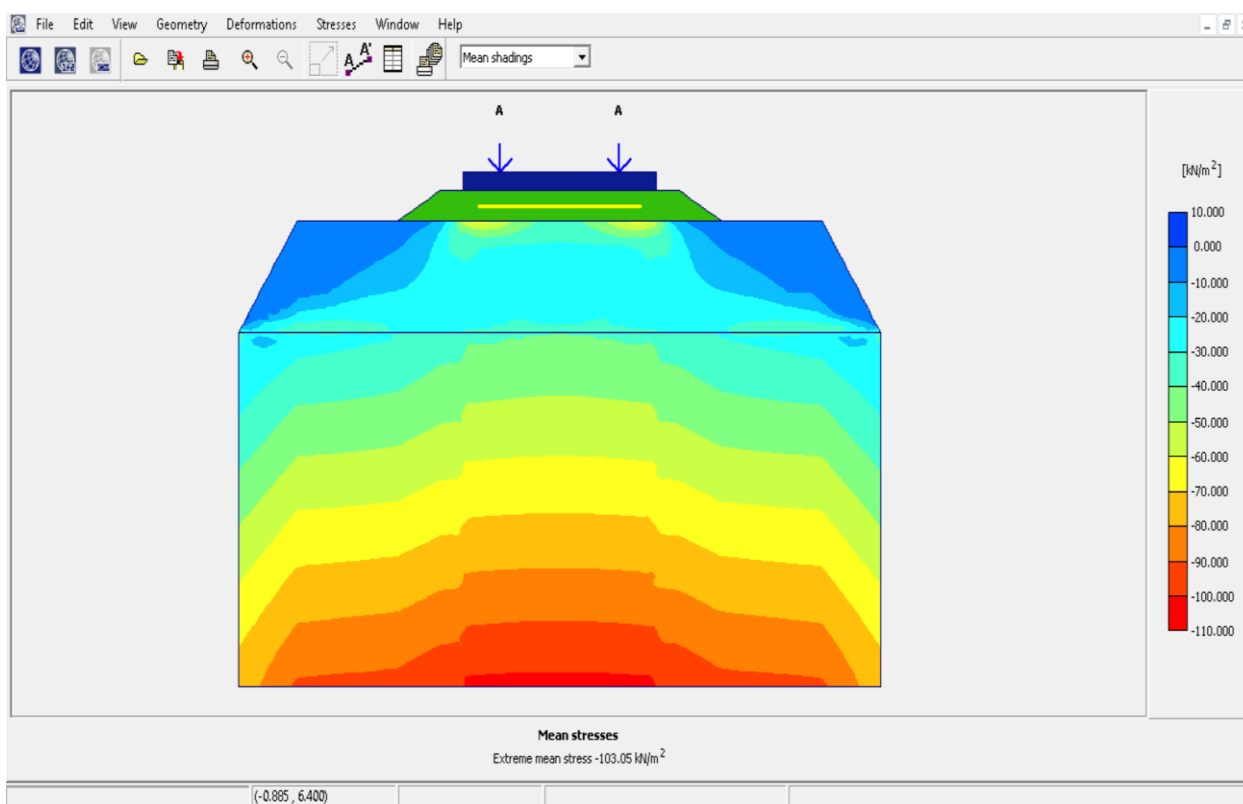


Figure 4.35 Subgrade Total Stresses in 2-D Model with Geocell Confinement Width 2.3m.

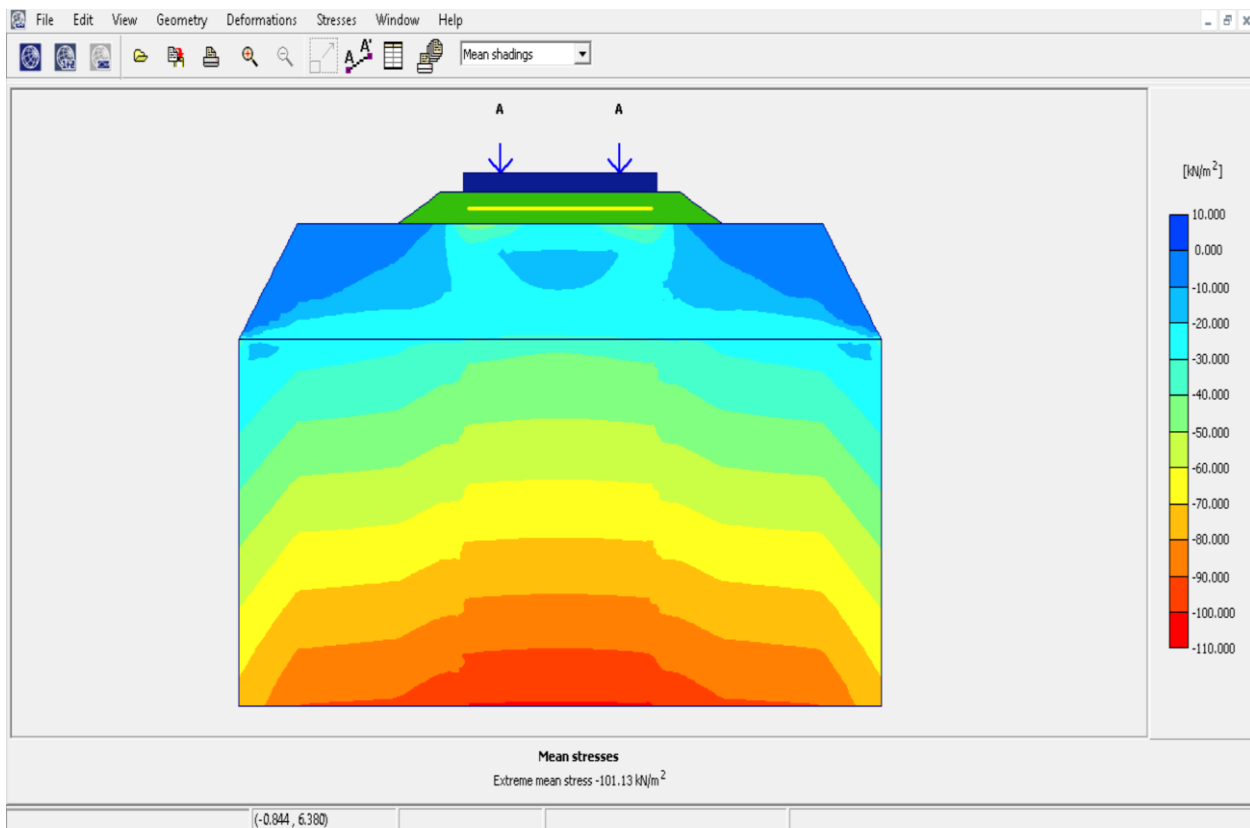


Figure 4.36 Subgrade Total Stresses in 2-D Model with Geocell Confinement Width 2.6m.

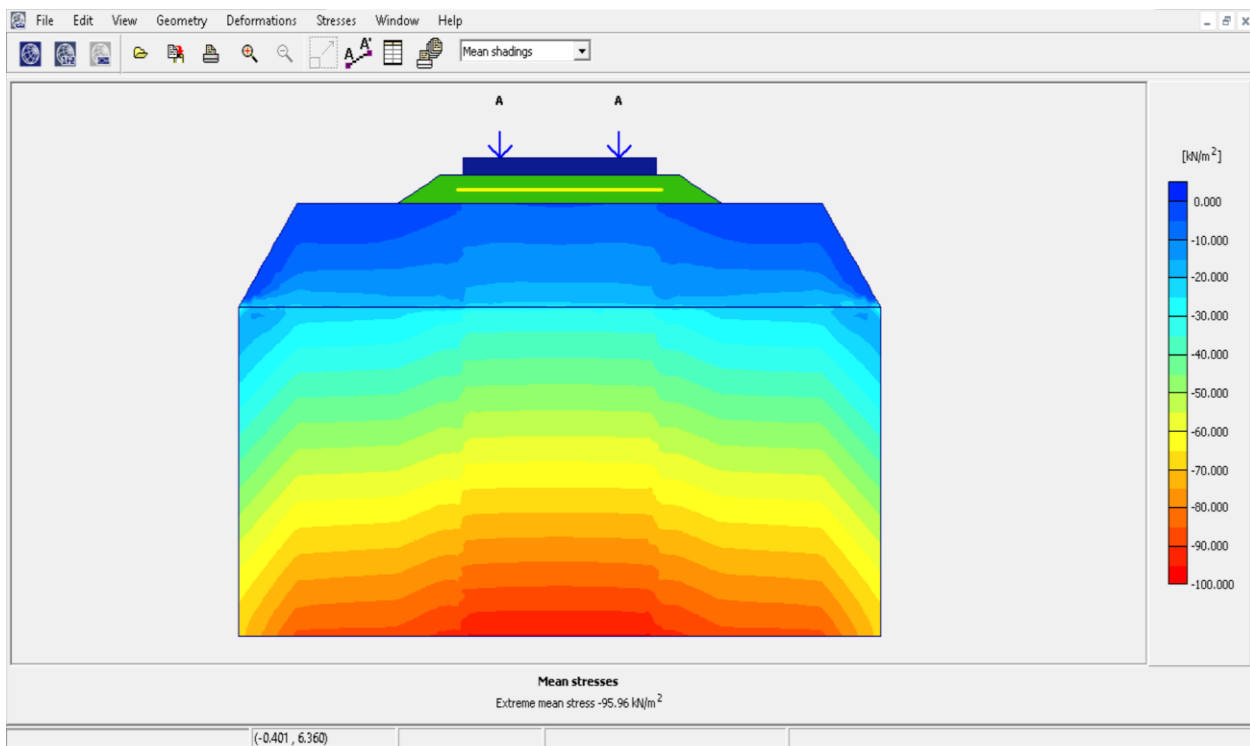


Figure 4.37 Subgrade Total Stresses in 2-D Model with Geocell Confinement Width 2.9m.

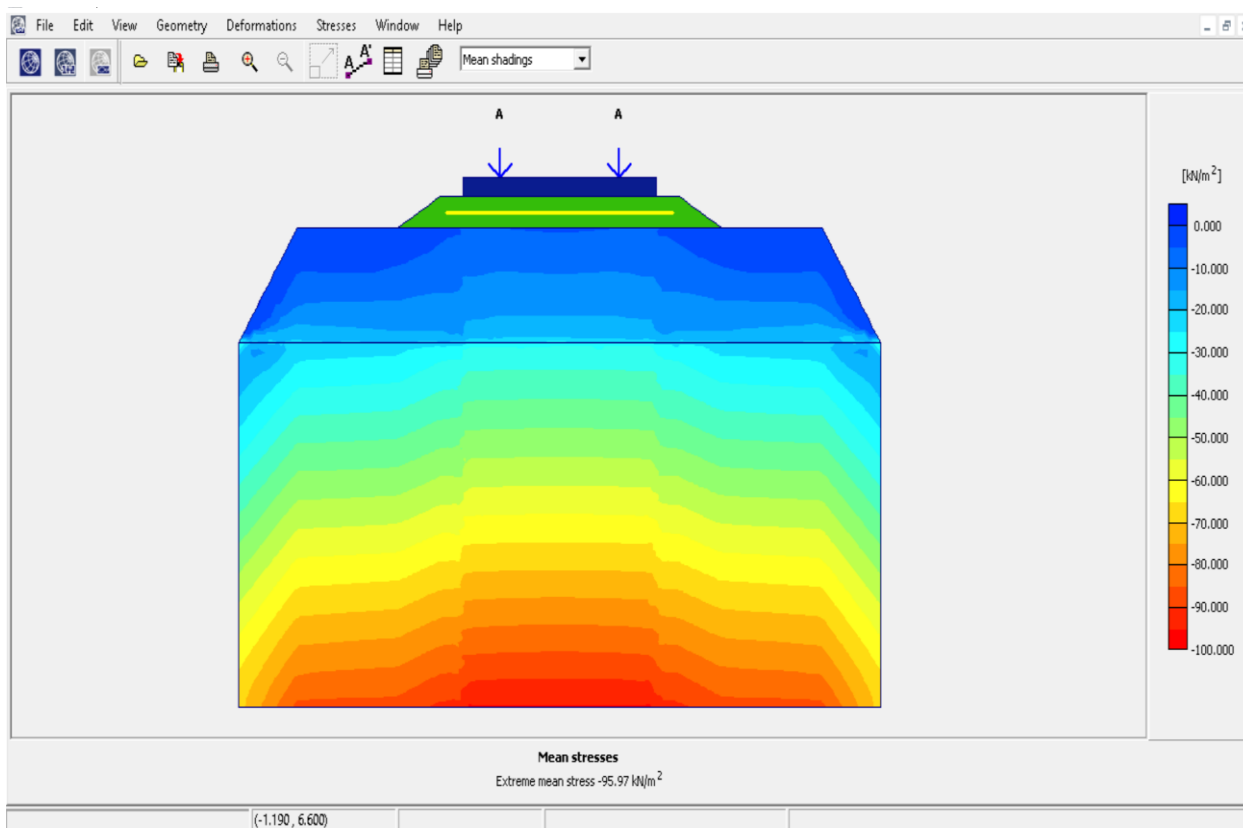


Figure 4.38 Subgrade Total Stresses in 2-D Model with Geocell Confinement Width 3.2m.

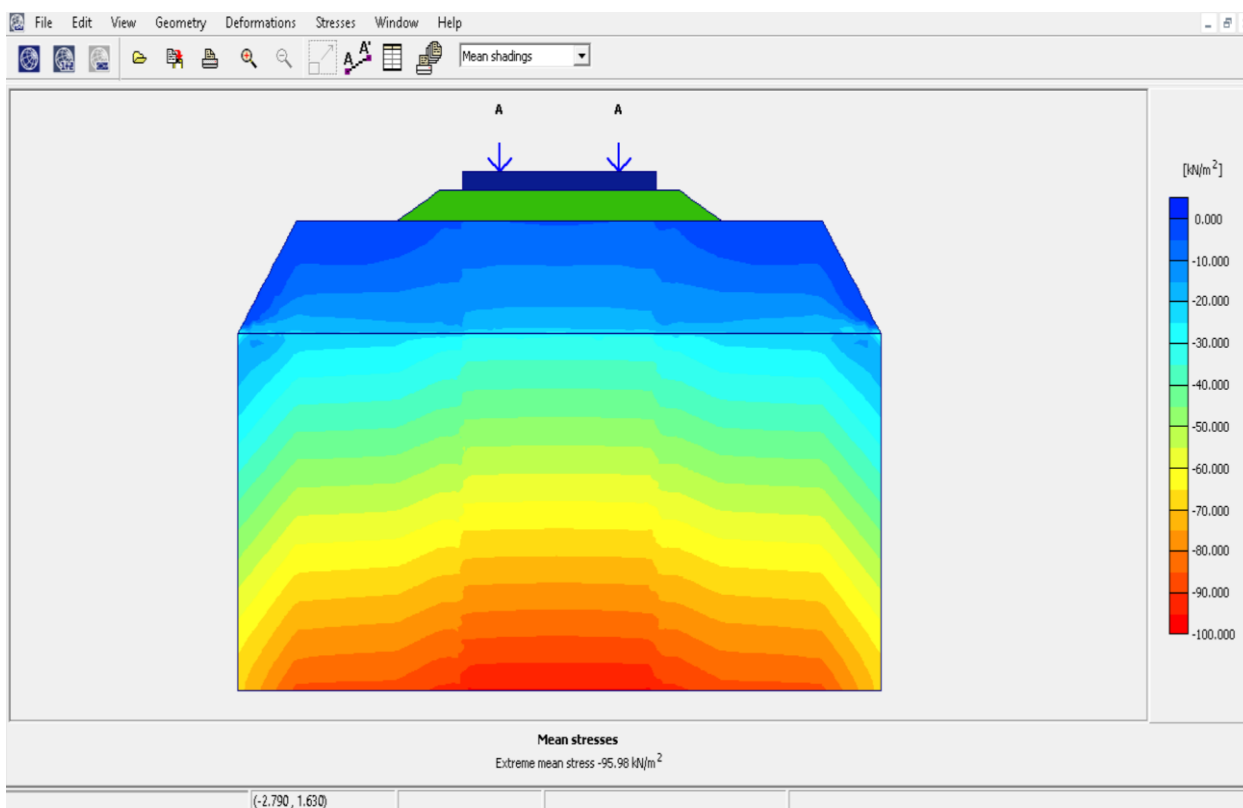


Figure 4.39 Subgrade Total Stresses in 2-D Model with Geocell Confinement Width 3.5m.

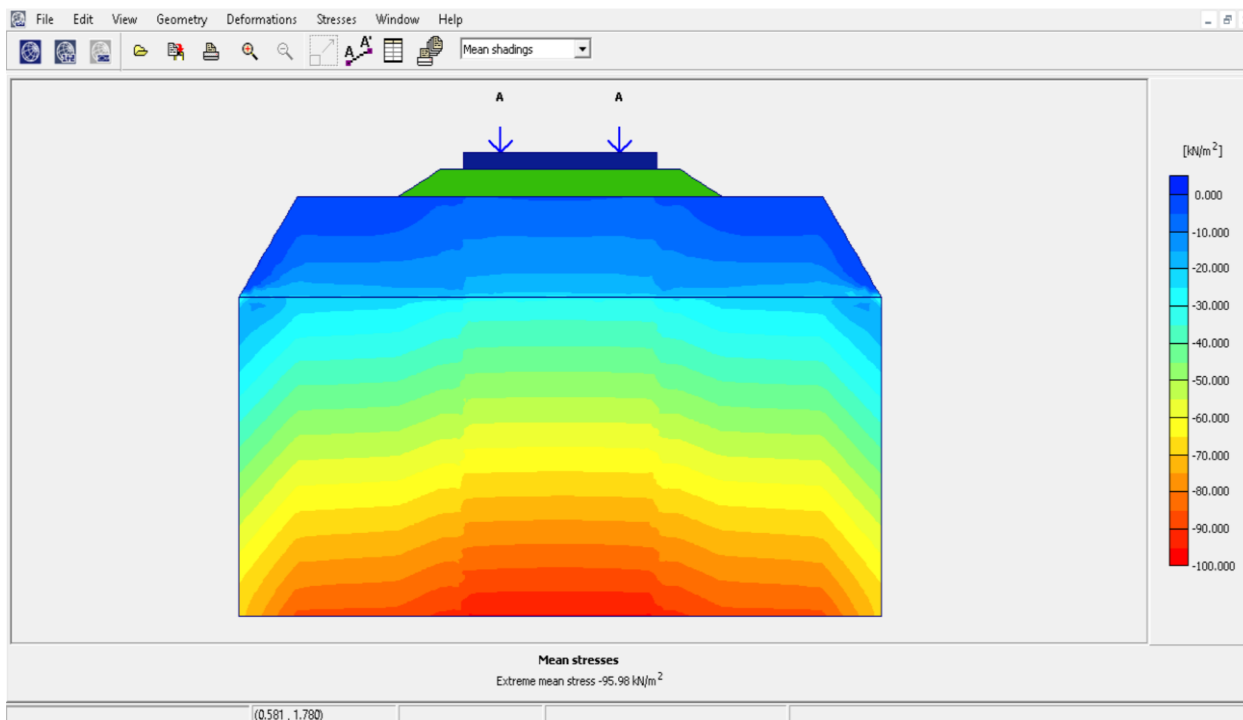


Figure 4.40 Subgrade Total Stresses in 2-D Model with Geocell Confinement Width 3.8m.

On accumulation of stresses can be observed at the end of geocell confinement width whose magnitude is uncertain. In the case of 2-D model analysis, stress accumulation is exaggerated. Also, unreinforced ballast model and model with geocell confinement width 2.0m behaved almost similarly in distributing stresses over the subgrade.

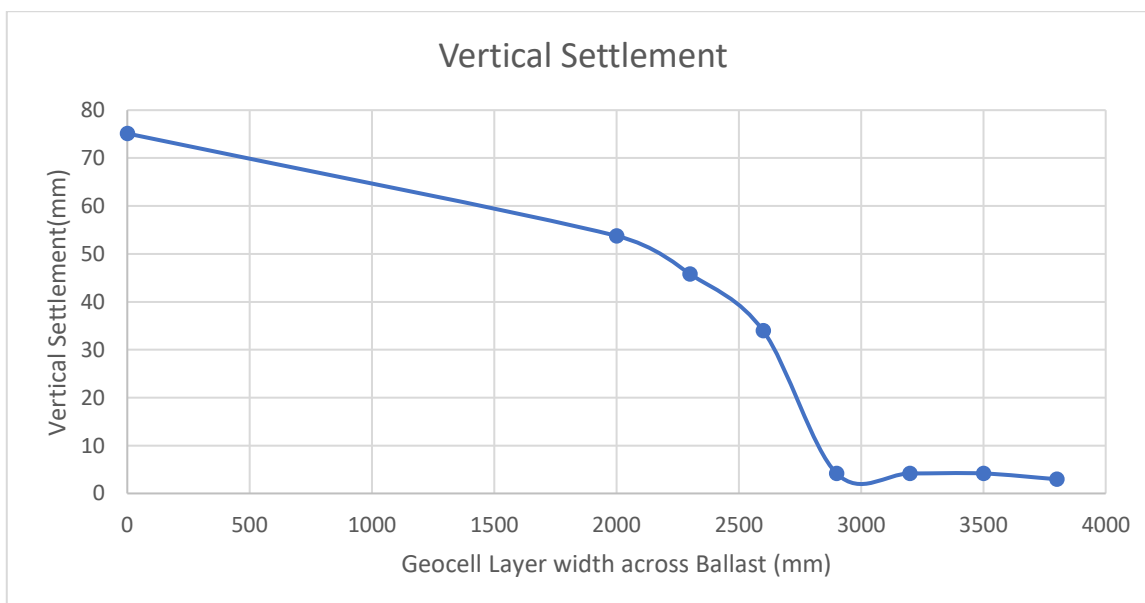


Figure 4.41 Vertical Settlement vs Geocell Layer confinement.

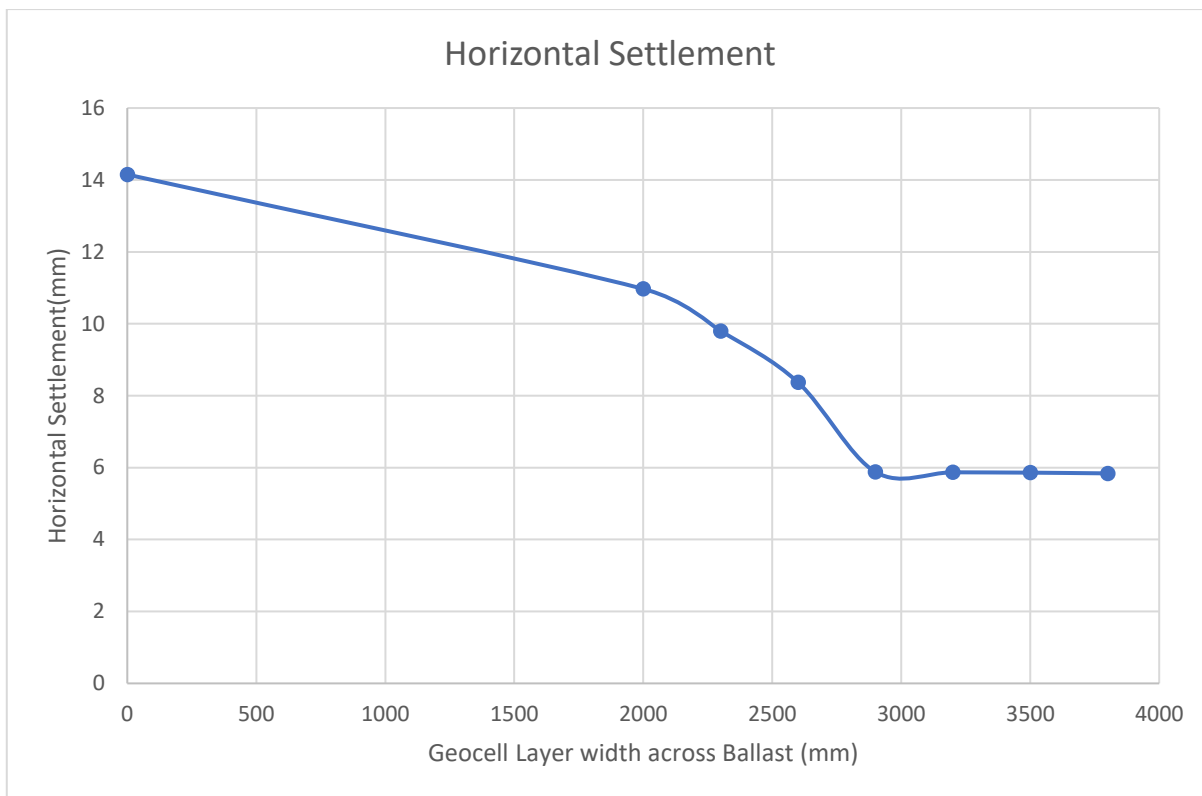


Figure 4.42 Horizontal Settlement vs Geocell Layer confinement.

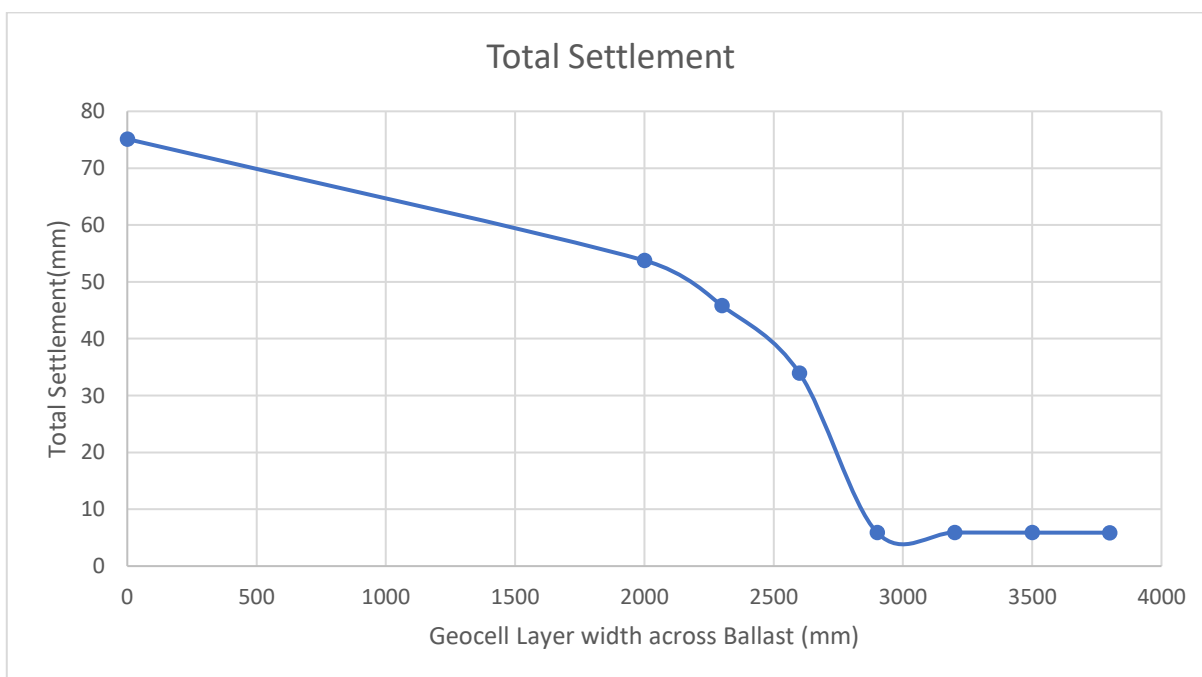


Figure 4.43 Total Settlement vs Geocell Layer confinement.

On comparing all the settlement vs Geocell confinement Layer graphs, we have noted that with increase in confinement of geocell settlement of embankment decreases.



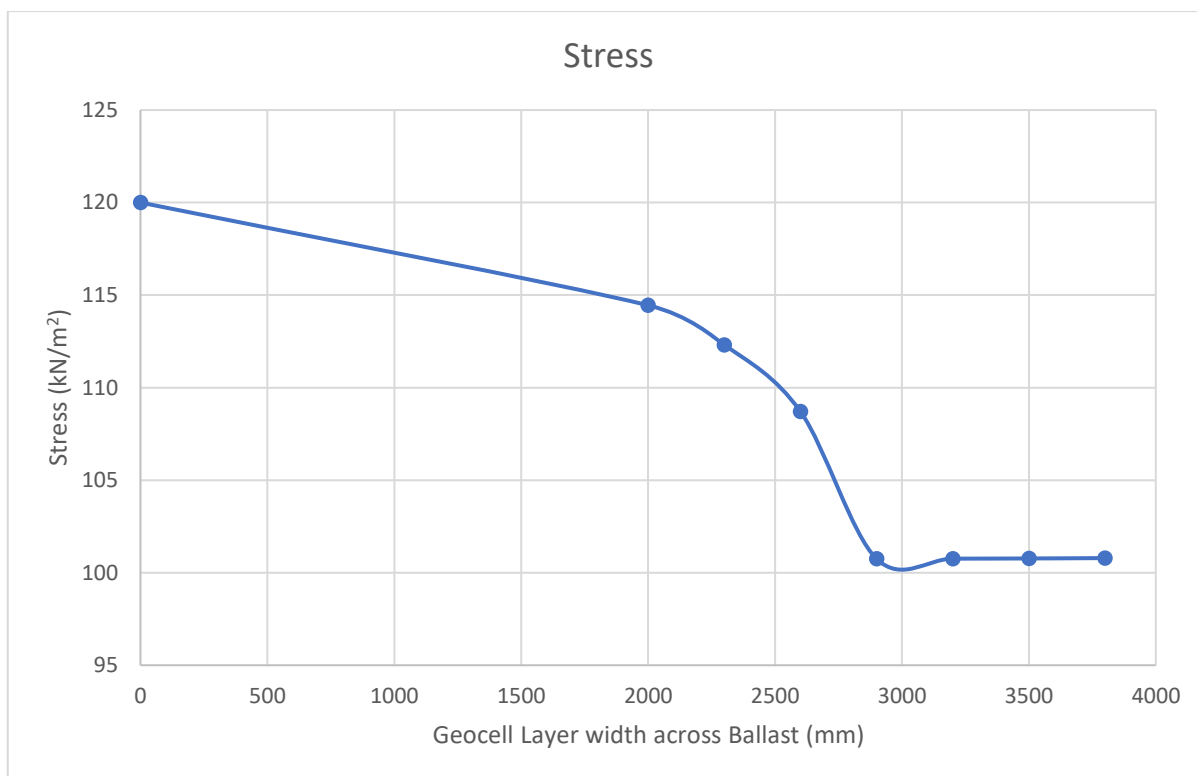


Figure 4.44 Comparison of Subgrade Stresses over the length across the Ballast for varying Geocell Confinement.

Table 4.1 Results Comparison

Embankment Type (Geocell Layer Width)	Meshing Details			Stress kN/m <sup>2</sup>	Vertical Settlement (mm)	Total Settlement (mm)	Decrease in Total Settlement wrt unreinforced (%)
	Elements	Nodes	Stress Points				
Unreinforced	1009	8231	12108	120.00	73.02	75.12	0
2000 mm	1028	8381	12336	114.45	51.56	53.76	28.43
2300 mm	1032	8413	12384	112.31	42.81	45.80	39.03
2600 mm	1030	8397	12360	108.71	31.07	33.93	54.83
2900 mm	1034	8429	12408	100.75	4.17	5.91	92.13
3200 mm	1038	8461	12456	100.76	4.17	5.91	92.13
3500 mm	1040	8477	12480	100.77	4.17	5.89	92.15
3800 mm	1042	8497	12504	100.79	2.97	5.88	92.17

Also, on comparing the results of 2-D models, subgrade stresses were decreased on the inclusion of geocell in ballast layer.

## **CHAPTER 5.**

### **CONCLUSIONS**

#### **5.1 CONCLUSIONS**

After a number of simulations and plots and comparing of results of each simulation, various conclusions were drawn. All the inferences drawn from the whole numerical analysis of all eight models are discussed as follow: -

- 1) Inclusion of geocell confinement in ballast layer improves the stress distribution of the subgrade layer as geocell confined ballast has high-stress tolerance and also distributes the stresses over wider width
- 2) As geocell confinement width increases, while rest conditions remain the same, the magnitude of decrease in subgrade stresses increases.

The optimum width of 2.9m for geocell confinement is suggested on the basis of this numerical analysis.

#### **5.2 FUTURE SCOPE OF THE PROJECT**

Future scope of projects are as follows

- 1) Various Geosynthetic materials can be used for the study.
- 2) The study can be done on two or more track system and effects can be compared.
- 3) The study can be done on PLAXIS 3D.

## REFERENCES

1. Agarwal, M. M. (2017). *Indian Railway Track*, 20th Ed., Standard Publishers Distributors, Delhi.
2. Nayyar, A. S. and Sahu, A.K. (2021). "Numerical analysis of railway substructure with geocell-reinforced ballast" *Geomechanics and Geoengineering*, 1-12.
3. Atalar, C., Shin, E. C., and Das, B. M. (2009). "Elastic modulus of granular soil-geogrid composite from cyclic plate load tests", *Proc., 17th International Conference on Soil Mechanics and Geotechnical Engineering*, Alexandria, Egypt, 2212-2215.
4. Chaney, R., Demars, K., Gabr, M. A., and Hart, J. (2000). "Elastic Modulus of Geogrid-Reinforced Sand Using Plate Load Tests." *Geotechnical Testing Journal*, 23(2), 245-250.
5. Cowland, J. W., and Wong, S. C. K. (1993). "Performance of a road embankment on soft clay supported on a Geocell mattress foundation." *Geotextiles and Geomembranes*, 12(8), 687–705.
6. Das, B. M. (2016). "Use of geogrid in the construction of railroads." *Innovative Infrastructure Solutions*, 1(15), 1-12.
7. Esmaeili, M., Naderi, B., Neyestanaki, H. K., and Khodaverdian, A. (2018). "Investigating the effect of geogrid on stabilization of high railway embankments." *Soils and Foundations*, 58(2), 319–332.
8. Fu, Q., and Zheng, C. (2014). "Three-dimensional dynamic analyses of track-embankment-ground system subjected to high speed train loads." *The Scientific World Journal*, 2014(924592), 1-12.
9. Han, J., and Gabr, M. A. (2002). "Numerical Analysis of Geosynthetic-Reinforced and Pile-Supported Earth Platforms over Soft Soil." *Journal of Geotechnical and Geoenvironmental Engineering*, 128(1), 44–53.
10. Indraratna, B., Khabbaz, H., Salim, W., and Christie, D. (2006). "Geotechnical Properties of Ballast and the Role of Geosynthetics", *Journal of Ground Improvement*, 10(3), 91-102.
11. Indraratna, B., Rujikiatkamjorn, C., Wijeyakulasuriya, V., Shahin, M. A., and Christie, D. (2006). "Soft soil stabilization under railway embankments", *Proc., Indian Geotechnical Conference*, Chennai, India, 41-50.

12. Kumar, K., and Sambasivarao, K. (2014). "Static and Dynamic Analysis of Railway Track Sleeper." *International Journal of Engineering Research and General Science*, 2(6), 662-671.
13. Lackenby, J., Indraratna, B., McDowell, G. R., and Christie, D. (2007). "Effect of confining pressure on ballast degradation and deformation under cyclic triaxial loading." *Geotechnique*, 57(6), 527–536.
14. Lal, R., Singh, R. C., and Singh, D. (2016). "Stress Analysis at Contact Region of Rail-Wheel: Review." *Proc., Vth International Symposium on "Fusion of Science & Technology"*, New Delhi, India, 75-85.
15. Leshchinsky, B., and Ling, H. (2013). "Effects of Geocell Confinement on Strength and Deformation Behavior of Gravel." *Journal of Geotechnical and Geoenvironmental Engineering*, 139(2), 340–352.
16. Leshchinsky, B., Evans, T. M., and Vesper, J. (2016). "Microgrid inclusions to increase the strength and stiffness of sand." *Geotextiles and Geomembranes*, 44(2), 170–177.
17. Li, D., Hyslip, J., Ted Sussmann, T., and Chrismer, S. (2015). *Railway Geotechnics*, 1st Ed., CRC Press, Florida.
18. Mundrey, J. S. (2009). *Railway Track Engineering*, 4th Ed., Tata McGraw Hill Education, New Delhi.
19. Nikraz H, M. A., and H, N. (2015). "Bearing Capacity Evaluation of Footing on a Layered- Soil using ABAQUS. " *Journal of Earth Science & Climatic Change*, 6(3), 1-8.
20. Rajagopal, K., Krishnaswamy, N. R., and Madhavi Latha, G. (1999). "Behaviour of sand confined with single and multiple geocells." *Geotextiles and Geomembranes*, 17(3), 171–184.
21. Smith, M. (2014). *ABAQUS/Standard User's Manual*, Version 6.14, Simulia, Rhode Island.
22. Srinivasan, M. (1969). *Modern permanent way*, 1<sup>st</sup> Ed., Somaiya Publications, Mumbai.
23. Van Dyk, B. J., Edwards, J. R., Dersch, M. S., Ruppert, C. J., and Barkan, C. P. (2017). "Evaluation of dynamic and impact wheel load factors and their application in design processes. " *Proc., Institution of Mechanical Engineers, Journal of Rail and Rapid Transit*, London, England, 231(1), 33–43.

24. Yetimoglu, T., Wu, J. T. H., and Saglamer, A. (1994). "Bearing Capacity of Rectangular Footings on Geogrid- Reinforced Sand." *Journal of Geotechnical Engineering*, 120(12), 2083–2099.
25. Zhou, H., and Wen, X. (2008). "Model studies on geogrid- or geocell-reinforced sand cushion on soft soil." *Geotextiles and Geomembranes*, 26(3), 231–238.
26. Ziaie, R. (2011). "Effect of Utilization of Geosynthetic on reducing the required thickness of sub-base layer of two layered soil", *International Journal of Geological and Environmental Engineering*, 5(1), 27-31.

PAPER NAME

**2K20GTE12 LAV KUSH PRASAD.docx**

AUTHOR

**Luv Kush**

WORD COUNT

**6762 Words**

CHARACTER COUNT

**36137 Characters**

PAGE COUNT

**56 Pages**

FILE SIZE

**10.8MB**

SUBMISSION DATE

**Jun 2, 2022 5:29 PM GMT+5:30**

REPORT DATE

**Jun 2, 2022 5:31 PM GMT+5:30**

### ● 4% Overall Similarity

The combined total of all matches, including overlapping sources, for each database.

- 1% Internet database
- 4% Publications database
- Crossref database
- Crossref Posted Content database
- 0% Submitted Works database

### ● Excluded from Similarity Report

- Small Matches (Less than 14 words)